Republic of Iraq
Ministry of Higher Education and Scientific Research
Al-Nahrain University
College of Science

Satellite Image Analysis and Quality Estimation

A Thesis
Submitted to the College of Science, Al-Nahrain University
In Partial Fulfillment of the Requirements for
The Degree of Master of Science in Computer Science

By

Esraa Hussain Ali
(B.Sc. 2005)

Supervised By

Dr. Ali Abid Dawood Al-Zuky

May 2009   **Jamady Al-Awal 1430**

بسم الله الرحمن الرحيم

وَيَسْأَلُونَكَ عَنِ الرُّوحِ قُلِ الرُّوحُ مِنْ أَمْرِ رَبِّي وَمَا أُوتِيتُم مِّنَ الْعِلْمِ إِلاَّ قَلِيلاً

صدق الله العظيم

سورة الاسراء

Supervisor Certification

I certify that this thesis was prepared under my supervision at the Department of Computer Science/College of Science/Al-Nahrain University, by **Esraa Hussain Ali** as partial fulfillment of the requirements for the degree of Master of Science in Computer Science.

Supervisor

Signature:

Name   : **Dr. Ali Abid Dawood Al-Zuky**

Title   : **Assist. Prof.**

Date   :   /   / **2009**

The Head of the Department Certification

In view of the available recommendations, I forward this thesis for debate by the examination committee.

Signature:

Name   : **Dr. Taha S. Bashaga**

Title   : **Head of the Department of Computer Science,**

                   Al-Nahrain University.

Date   :   /   / **2009**

Examining Committee Certification

We certify that we have read this thesis and as an examining committee, examined the student in its content and what is related to it and that in our opinion it meets the standard of a thesis for the degree of Master of Science in Computer Science.

Examining Committee Certification

Signature:
Name   : **Dr. Loay E. George**

Title   : **Assis. Prof. (Chairman)**
Date   :   /   / **2009**

Signature: Signature:

Name   : **Dr. Ban Nadeem Thannoon**   Name   : **Dr. Haitham A. Omar**

Title   : **Assis. Prof. (Member)**   Title   : **Lecturer (Member)**
Date   :   /   / **2009**   Date   :   /   / **2009**

Supervisor Certification

Signature:
Name   : **Dr. Ali Abid Dawood Al-Zuky**

Title   : **Assis. Prof.**

Date   :   /   / **2009**

The Dean of the College Certification

Approved by the Council of the College of Science

Signature:

Name   : **Dr. Laith Abdul Aziz Al-Ani**

Title   : The Dean of College of Science, **Al-Nahrain University.**

Date   :   /   / **2009**

Dedication

    To the two candles of my life my father and mother, who put books in my hands at an early age, and raised me into the person I am today, with all my love . . . .

    Special thanks to my brother and sisters for their assistance and encouragement . . . .

    To everyone

            Taught me a letter . . . .

                    Esraa

Acknowledgement

First of all, my thanks to God who helped me and gave me the ability to perform this work.

I would like to express my sincere appreciation and gratitude to my supervisor, **Dr. Ali Abid Dawood Al-Zuky**, for giving me the major steps, the valuable advices, and the constant help throughout this work.

Also, I wish to give my thanks to all the members of Computer Science Department in Al-Nahrain University for their help and encouragement, especially the Head of Department of Computer Science **Dr. Taha S. Bashaga**.

Special thanks to my faithful friends in Al-Nahrain and Al-Mustansiriyah Universities for supporting and giving me advices.

I would like to thank my family for their love and patience during my project time.

Abstract

The image quality analysis techniques of TV-Satellite images come from the significant processing of high importance of image information in the multimedia world. In this research, the quality of TV-Satellite images on the three satellites (Arabsat, Hotbird and Nilesat) was studied to estimate the best quality image. A number of image quality metrics have been introduced. The introduced image quality metrics consist of two methods. The first method is called the contrast of image edges and the second method is called the cross correlation.

In the contrast of image edges method, the edges have been extracted from the image by applying Sobel edge detector on the R, G, B and L components using different threshold values. The amount, the SNR, the mean and the standard deviation of image edges were calculated for all R, G, B and L components. The contrast of image edges metric had been determined for different threshold values using Michelson formula. The Michelson contrast equation was modified in different ways to present number of contrast approaches that applied on the edges of the image.

In the cross correlation method the correlation of selected homogenous regions in different locations of the image has been computed for all R, G, B and L components. The regions' selection was made manually and automatically from the image. The results for the quality metrics used in this research indicated that TV-Satellite images from Nilesat hold better quality from Arabsat and Hotbird images. The quality of the images on the Arabsat came in the second place and the Hotbird became last.

Abbreviations

A/D	Analog/Digital
CMY	Cyan, Magenta, Yellow
CSF	Contrast Sensitivity Function
DIC	Digital Image Correlation
GCF	Global Contrast Factor
HSI	Hue, Saturation, Intensity
HVS	Human Visual System
LNB	Low Noise Block
MPEG	Motion Picture Expert Group
MSE	Mean Square Error
NTSC	National Television System Committee
PAL	Phase Alternating Line
PDF	Probability Density Function
PSNR	Peak Signal to Noise Ratio
RF	Radio Frequency
RGBL	Red, Green, Blue, Luminance
RMS	Root Mean Square
SNR	Signal to Noise Ratio
STD	Standard Deviation
TV	Television

Table of Contents

Chapter Four: Results and Discussions

Chapter Five: Conclusions and Future Works

Chapter One
General Introduction

Chapter One
General Introduction

1.1 Introduction

The technology has an important role in people's life, and the way of dealing with this technology has become one of the essential needs of our daily life, so that there is no choice but accepting its developed role in present and future. During the last three decades, the satellite telecommunication technology has developed significantly. Since 15 years ago the home receivers was counted in thousands but today it has become in millions, and the cable TV has invaded the world markets in the last two decades more than the previous decades [Wah00].

Cable television is a system of providing television to consumers via radio frequency signals transmitted to televisions through fixed optical fibers or coaxial cables as opposed to the over-the-air method used in traditional television broadcasting (via radio waves) in which a television antenna is required. Signals captured from the physical world via a special type of antenna called satellite dish which designed to capture a particular type of broadcasted signals, are transmitted into digital form by digitizing using a satellite home receiver [Wah00].

Cable television systems are utilized for providing general access and extra services of enormous number of customers. General-accessible services include satellite radio and TV programs. In this case the signals are transmitted from one provider to many subscribers [Val06].

1.2 Artificial Satellites

An artificial satellite is a manufactured object that continuously orbits Earth or some other body in space. Most artificial satellites orbit Earth. People use them to study the universe, help forecast the weather, transfer telephone calls over the oceans, assist in the navigation of ships and aircraft, monitor crops and other resources, and support military activities. Piloted spacecraft in orbit, such as space capsules, space shuttle orbiters, and space stations, are also considered artificial satellites [Dun07].

1.3 Types of Artificial Satellites

Artificial satellites are classified according to their missions. There are six main types of artificial satellites: (1) Scientific research, (2) Weather, (3) Communications, (4) Navigation, (5) Earth observing, (6) Military. Communication satellites serve as relay stations, receiving radio signals from one location and transmitting them to another. A communications satellite can relay several television programs or many thousands of telephone calls at once. Communications satellites are usually put in a high altitude, geosynchronous orbit over a ground station. Aground station has a large dish antenna for transmitting and receiving radio signals. Countries and commercial organizations, such as televisions broadcasters and telephone companies use these satellites continuously [Dun07].

1.4 Transmission and Reception Systems of TV Satellite Broadcasting

Every communication satellite in its simplest form involves the transmission of information from an originating ground station to the

satellite (the uplink), followed by a retransmission of the information from the satellite back to23 the ground (the downlink). The downlink may either be to a select number of ground stations or it may be broadcast to everyone in a large area. Hence the satellite must have a receiver and a receive antenna, a transmitter and a transmit antenna, some method for connecting the uplink to the down link for retransmission, and prime electrical power to run all the electronics. Figure (1.1) shows the basic communication satellite components [Leo07].
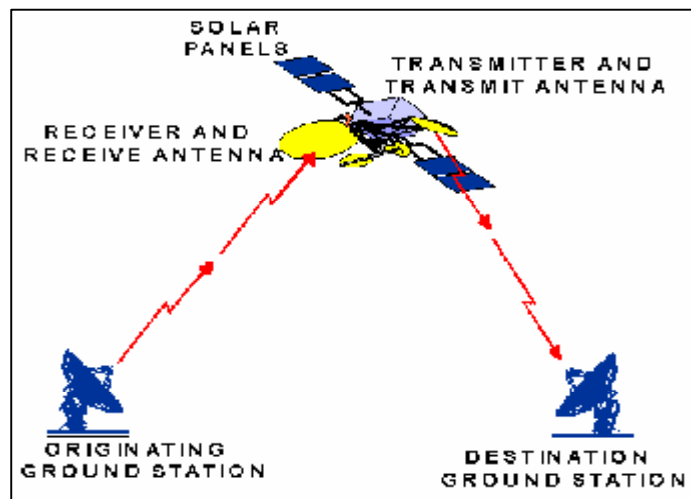
Figure (1.1): The basic communication satellite components [Leo07]

1.4.1 Transmitters

The amount of power which a satellite transmitter needs to send out mainly depends on whether it is in low Earth orbit or in geosynchronous orbit. This is a result of the fact that the geosynchronous satellite is at an altitude of 22,300 miles, while the low Earth satellite is only a few hundred miles. The geosynchronous satellite is nearly 100 times as far away as the low earth satellite. We can show fairly easily that this means the higher satellite would need almost 10,000 times as much power as the low-orbiting one, if everything else were the same [Leo07].

1.4.2 Antennas

Virtually all antennas in use today radiate energy preferentially in some direction. An antenna used by a commercial terrestrial radio station, for example, is trying to reach people to the north, south, east, and west. However, the commercial station will use an antenna that radiates very little power straight up or straight down. Since they have very few listeners in those directions (except maybe for coal miners and passing airplanes) power sent out in those directions would be totally wasted. The communications satellite carries this principle even further. All of its listeners are located in an even smaller area, and a properly designed antenna will concentrate most of the transmitter power within that area, wasting none in directions where there are no listeners. The easiest way to do this is simply to make the antenna larger. Doubling the diameter of a reflector antenna (a big "dish") will reduce the area of the beam spot to one fourth of what it would be with a smaller reflector [Leo07]**.**

1.4.3 Engine Power

There is no line from the power company to the satellite. The satellite must generate all of its own power. For a communications satellite, that power usually is generated by large solar panels covered with solars cells - just like the ones in solar-powered calculator. These convert sunlight into electricity. Since there is a practical limit to the how big a solar panel can be, there is also a practical limit to the amount of power which can generated [Leo07].

1.5 Satellite Television Receiver Components

The satellite television receiver consists of number of important components; these components are illustrated in the following sections:

1.5.1 Dish Antenna

Dish antenna has an elliptical round shape rounded around the axis of symmetry that illustrated in figure (1.2). It gathers and focuses the spot beams on the parabolic reflector just like how the light spherical mirrors. The surface of the antenna dishes has to be made from a metal to reflect the receptor radio signals. In spite of that there are some dishes are made from plastic or fiber, but they contain a hidden metal mesh that helps to reflect the recipient signals from the artificial satellites [Wah00].

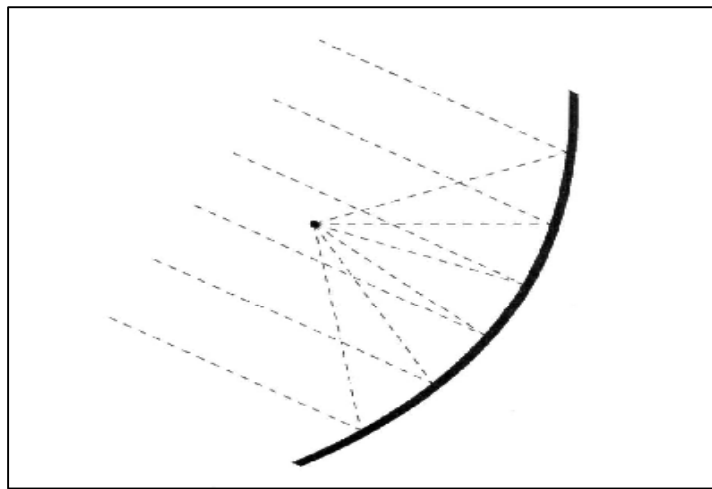Figure (1.2): The dish antenna aimed at the satellite [Loo04]

The purpose of the satellite antenna is to collect and concentrate signals coming from a targeted satellite, while ignoring extraneous signals and noise. These seemingly simple design objectives, the subject of unique scientific and engineering discipline for many years, must be mated with economic considerations. Therefore, a technically

excellent antenna must also be moderately priced, aesthetically pleasing, durable, easy to install and virtually maintenance- free [Bay97].

As the frequency goes up, the size of the antenna will decrease for a given gain and beam width. For a fixed antenna size, this will significantly reduce the interference from adjacent satellite systems [Loo04].

1.5.2 Low Noise Block Downconverters (LNB)

The low noise block downconverter, known as an LNB, has the crucial function of detecting the signal relayed via the dish and feed and converting it to an electrical signal amplifying the extremely weak signal and downconverting or lowering its frequency. In effect, it accomplishes the remarkable feat of 'pulling' the signal out from the noise. The downconverted signal is then relayed along coaxial cable to an indoor satellite receiver [Bay97].

LNB is the first electrical part of the satellite dish components which deals with satellite receiver system. It is used for as a signal amplifiers which reduce the noise to amplify the weak received signals, that come from transmitter of about 100 000 times of reducing the noise level [Ald08].

1.5.3 Coaxial Cable

Cable television systems provide analog broadcast signals on a coaxial cable, instead of through the air, with the attendant freedom to use additional frequencies and thus provide a greater number of channels than over-the-air broadcast [Fly98].

Coaxial cable used to transmit the high frequency signals RF which can be amplified using LNB which connected to the reception unit [Ald08].

Coaxial cable is composed of two concentric conductors separated by an insulating material called a dielectric as illustrated in figure (1.3). The whole assembly of the cable is sheathed in a non-conducting jacket for protection against the elements. The signal travels along the central wire. Using this configuration greatly reduces radiative losses at high frequencies by confining the electromagnetic field to within the coaxial structure. It is interesting to note that with increasing frequencies the signal travels progressively closer to the surface of the center conductor [Bay97].

Figure (1.3) The coaxial cable [Cat01]

1.5.4 Satellite Home Receivers

It is a device which received the waves that come from the LNB and convert it to a signal that can be displayed on the television. The home receiver is an essential part of a receiving system [Ald08].

Receivers designed to process MPEG digital compressed broadcast are in many respects similar to the analog components. In general an analog satellite receiver has to perform the following functions:

1. Provide power to the LNB.

2. Control polarization switching at the feed.

3. Power and, when required, control the actuator.

4. Downconvert and select one channel from those available on any particular satellite.

5. Amplify the signal.

6. Extract the original information.

A digital satellite receiver is similar to its analog counterpart in the requirement to power and control both LNB and actuators as well as to tune and filter the signal. However its operation corrects errors in the bit stream. It decrypts, and then MPEG decodes the audio, video and data signals. Finally the audio and video signals are converted from digital into analog forms [Bay97].

1.6 Literature Survey

There is a lot of previous work performed on studying and estimating the quality of the images, and some relevant work is described below:

1. ***Eli Peli, 1990*** [Pel90].

In this paper a definition of local band-limited contrast measure in images is proposed that assigns a contrast value to every point in the image as a function of the spatial frequency band. For each frequency band, the contrast is defined as the ratio of the bandpass-filtered image at that frequency to the low-pass image filtered to an octave below the same frequency (local luminance mean). This definition raises important implications regarding the perception of contrast in complex images and is helpful in understanding the effects of image-processing algorithm on the perceived contrast. The purpose

of this definition is better to link measured physical contrast with visual contrast perception.

2. ***Eli Peli, Lawrence Arend, Angela T. Labiance, 1996*** [Pel96].

The interaction of the effects of luminance and spatial frequency on perception of suprathreshold contrast was studied with use of a contrast-matching paradigm. Contrast sensitivity was demonstrated across the entire luminance range tested for all highest frequencies. As at threshold, reduction in luminance across the levels commonly available on a CRT display has only minimal effects on low frequency suprathreshold contrast perception. They determined these effects as important implications for visual models used in image quality analysis.

3. ***Ismail Avacibas, 2001*** [Ava01].

Categorized a comprehensively image quality measures, extend measures defined for gray scale images to their multispectral case, and propose a novel image quality measure. The statistical behavior of the measures and their sensitivity to various kinds of distortion, data hiding and coding artifacts are investigated via Analysis of Variance techniques.

4. ***Peter J. Bex and Walter Makous, 2001*** [Bex01].

Examined contrast sensitivity and suprathreshold apparent contrast with natural images. The spatial frequency components within single octaves of the images were removed (notch filtered), their phases were randomized, or the polarity of the image was inverted. Of Michelson contrast, root-mean-square (RMS) contrast and band-limited contrast, they discovered that RMS contrast was the best index

of detectability. They use contrast detection thresholds and suprathreshold matching function which showed the elevation and loss of spatial frequency dependant contrast for both notch filtering and phase randomize.

5. **Amy L. Rachenmacher and Nidal Abi Saab, 2002** [Rac02].

They used Digital Image Correlation (DIC) to measure local deformation in dense sands to evaluate deformation patterns associated with shear band formation and the uniformity of deformation within persistent shear bands. The matching of pixel intensity values, and thus the measured displacement of a subset, is accomplished mathematically through minimizing of a normalized cross-correlation coefficient.

6. **K. Matkovic, L. Neumann and N. Neumann, 2005** [Mat05]**.**

They introduced different contrast definition. The newly introduce Global Contrast Factor (GCF) corresponds closer to the human perception of contrast. GCF uses contrast at various resolution levels in order to compute ovelall contrast. Experiments were conducted in order to find weight factors needed to calculate GCF. GCF measures richness of detail as perceived by a human observer and such can be used in various application areas like rendering tone mapping volume visualization, and lighting design.

7. **V. Srinivasan, S. Radhakrishan and Y.Zhang, 2005** [Sri05].

They demonstrated a simple, full field displacement characterization technique based on digital image correlation (DIC). They developed a robust correlation measure implemented in a code

and use it to characterize materials at high spatial and displacement resolution.

8. ***Radhi Sh. Al Taweel, 2006*** [Alt06]**.**

He analyzed the associated noise of the TV-satellite images in digital receiver system statistically and then he enhanced these images using different digital filters, and applied these filters on different color spaces such as RGB, HLS and YIQ. Also, he made an assessment to the attributes of noise in TV-Satellite images; also he studied the noise as a function of a signal transfer wire resistance.

9. ***Abdulah H. Al Jiboori, 2006*** [Alj06]**.**

This research studied and analyzed the associated noise of TV images and the ways of reducing the noise, and he studied the type of the noise and the relationship between the rotating angle of the antenna and the statistical measures which include mean, standard derivation and variance for three bands RGB and Luminance of the TV-colored images.

10. ***Nabeel M. Al Dalawy, 2008*** [Alda08]**.**

He studied the noise associated with TV images and determined the type of the noise and the relationship between the mean and the standard deviation for regions illumination components of small rotating angles of the antenna. Also, he studied the relationship between the rotating angle of the antenna and the statistical measures which include mean, standard deviation, variance and mean square error (MSE) for three bands RGB and Luminance.

11.***Ali J. Al Dalawy, 2008*** [Ald08].

He studied the TV-Satellite images of "Al-Hurra" channel broadcasts on Arabsat, Hotbird and Nilesat. Analyzing these images done statistically by finding the statistical distribution and studying the relations between the mean and the standard deviation of the RGB-bands and L- components for the image as whole and for the extracted homogeneous regions. Also he studied the contrast of image edges depending on Sobel operator for different threshold values. The results indicated that the image on Hotbird has the best quality among the three satellites.

1.7 Aim of the Research

The aim of this research is to study the colored TV-satellite images and estimate their quality. The quality of the TV-Satellite images on the three satellites (Arabsat, Hotbird and Nilesat) has been evaluated to determine the best quality image. Determining the quality of the TV-Satellite images based on two methods. One to compute the contrast of image edges using different suggested contrast approaches. The other to compute the correlation of the selected homogenous regions from the image using cross correlation. The amount, the Signal to Noise Ratio (SNR), the mean and the standard deviation of image edges have been considered as well to determine the quality of the TV-satellite images.

1.8 Thesis Outline

This thesis consists of five chapters. The contributions of this thesis are presented through chapters three, four and five; these chapters are organized as follows:

1. Chapter two introduces the classification of image quality metrics and also this chapter explains some basic facts about color and image types.

2. Chapter three presents the TV-Satellite image analysis system, where it shows the procedures of calculating the quality measurement methods.

3. Chapter Four shows the results and discussions of the most important results obtained after the implementation method.

4. Chapter Five introduces the conclusions and some suggestions for future works.

Chapter Two
Image Quality
Measurement

Chapter Two
Image Quality Measurement

2.1 Introduction

There has been an explosive growth in multimedia technology and application in the past several years. Efficient representation of a good image and good image estimation are some of challenges faces. Estimating the quality of digital image can play a variety of roles in image processing applications. It can be used to optimize algorithms and parameter setting of image processing systems [Ava01].

There are some of quality metrics that are categorized according to the type of information they are using. The categories used are [Ava01]:

- Statistical image measurement such as image histograms, mean and Standard deviation.
- Pixel difference-based measures such as mean square distortion.
- Human visual system-based measures.

2.2 Image Representation

The Human Visual System (HVS) receives an input image as a collection of spatially distributed light energy; this form is called an optical image. Optical images are the types that people deal with everyday-camera capture them, monitors display them, and people see them. These optical images are represented as video information in the form of analog electrical signals and these are sampled to generate the digital image. The digital image is represented as a two dimensional array of data, where each pixel value corresponds to the brightness of the image. The monochrome images data are those who have one color, what

are normally referred to as black and white. The multiband images can be modeled by different functions, each one corresponds to one separate band of brightness information [Umb98].

2.2.1 Binary Images

The pixels in a binary image can assume only two values, 0 or ;1 a gray image may be quantized to a number of intensity levels, depending on the application, while a color image may be quantized in different color bands. As the number of intensity levels increases, the image is represented to a better approximation, although the storage requirements also grow proportionately. The binary images are thus least expensive, since the storage and also processing requirement is the least in case of binary images. Examples of binary images are line drawings, printed text on a white page. These images contain enough information about the objects in the image and we can recognize them easily. There are a number of applications in computer vision where binary images are used for object recognition, tracking, and so on [Ach05].

2.2.2 Gray-Scale Images

Gray-Scale images are referred to as monochrome, or one color images. They contain brightness information only, no color information. The number of bits used for each pixel determines the number of different brightness levels available. The typical image contains 8 bits/pixel data, which allows us to have 256 (0-255) different brightness (gray) levels. This representation provides more than adequate brightness resolution, in terms of the human visual system's requirements. Additionally, the 8-bit representation is typical due to the fact that the *byte*, which corresponds

to 8-bits of data, is the standard small unit in the world of digital computers [Umb98].

2.2.3 Color Images

Color images can be modeled as three-band monochrome images data, where each band of data corresponds to a different color. The actual information stored in the digital image data is the brightness information in each spectral band. When the image is displayed, the corresponding brightness information is displayed on the screen by picture elements that emit light energy corresponding to that particular color [Umb98].

a) RGB Color Space

The red, green, and blue (RGB) color space is widely used throughout computer graphics. Red, green, and blue are three primary additive colors (individual components are added together to form a desired color) and are represented by a three- dimensional, Cartesian coordinate system (Figure 2.1). The diagonal of the cube, with equal amounts of each primary component, represents various gray levels. The RGB color space is the most prevalent choice for computer graphics because color displays use red, green, and blue to create the desired color. Therefore, the choice of RGB color space simplifies the architecture and design of the system. Also, a system that is designed using the RGB color space can take advantage of a large number of existing software routines, since this color space has been around for a number of years. To convert an image from RBG color to gray scale, use the following equation [Cra97]:

$$Y = 0.299R + 0.587G + 0.114B \qquad\qquad … (2.1)$$

This equation comes from the NTSC standard for luminance.

To further reduce the color to black and white, you can set normalized values less than 0.5 to black and all others to white. This is simple but doesn't produce the best quality. Most people are not familiar with additive primary mixing used in the RGB color space. Children are taught that mixing red and green yields brown. In the RGB color space, red plus green produces yellow. Those who are artistically inclined are quite proficient at creating a desired color from the combination of subtractive [Cra97].
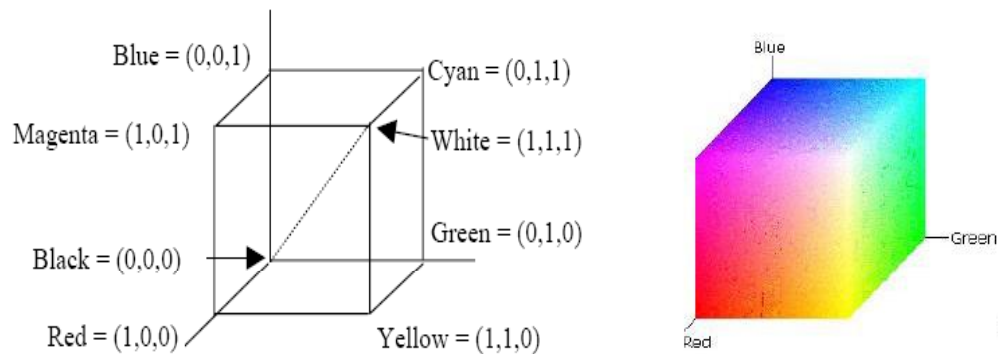
Figure (2.1): The RGB Color Space Cube
[Umb98]

Cyan, Magenta, and yellow are the secondary colors of light or, alternatively, the primary colors of pigment. For example when a surface coated with cyan pigments is illuminated with white light, no red light is reflected from the surface. That is cyan subtracts red light from reflected white, which itself is composed of equal amounts of red, green, and blue light [Gon02].

Most devices that deposit colored pigments on paper, such as color printer and copiers, require CMY data input or perform on RGB to CMY conversion internally. This conversion is performed using the simple

operation where again, the assumption is that all color values have been normalized to the range [0,1].

$$\begin{bmatrix} C \\ M \\ Y \end{bmatrix} = \begin{bmatrix} 1 \\ 1 \\ 1 \end{bmatrix} - \begin{bmatrix} R \\ G \\ B \end{bmatrix} \qquad \dots (2.2)$$

Equation (2.2) demonstrates that light reflected from a surface coated with pure cyan does not contain red (that is, C=1-R in the equation). Similarly, pure magenta does not reflect green, and pure yellow does not reflect blue [Gon02].

b) YUV/YIQ Color Spaces

In this space Y refers to the perceived intensity component from the chromatic components allow us to broadcast video images with each pixel encoded as three numbers, the YUV coordinates. A black and white TV, for example, just decodes the Y component and produces a picture. A psychophysical measurement of the perceived intensity of colors has led to many proposals for the perceived intensity of colors (which is also very variable between humans) the formula used is (2.1) mentioned in the previous section [For03].

Green has a higher weight than red, and almost five time higher than blue. The human eye contains just 2% of blue cones, but they are more sensitive than the green cones, so that final weighting must be obtained from actual experiments the U and V components are obtained from the following expressions [For03]:

U=C1(B-Y)= -0.169R − 0.332G + 0.500B +128   … (2.3)

and

V=C2(R-Y)= - 0.500R − 0.419G − 0.0813B +128   … (2.4)

Where C1 and C2 are normalizations constants adjusted to obtain the coefficient 0.5 in front of the blue component (in the first equation), and

of the red component (in the second equation), and where the variables R, G, and B run from 0 to 255. The constant 128 is add to avoid negative U and V values [For03].

YIQ the NTSC Transmission color coordinate system. In the development of the color television system in the United States, NTSC formulated a color coordinate system for transmission composed of three values. Y values called luma, is proportional to the gamma-corrected luminance of a color. The other two components, I and Q called chroma, jointly desired the hue and saturation attributes of an image [For03].

c) HSI Color Space

The Hue, Saturation, and Intensity (HSI) color transform allows us to describe colors in terms that we can more readily understand (see figure (2.2) [Umb98].
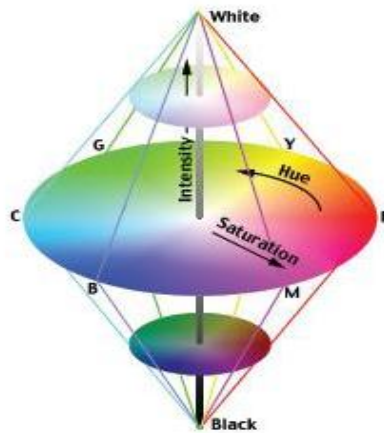

Figure (2.2): HIS Color Space
[Umb98]

The lightness is the brightness of the color, and the hue is what we normally think of as "color" (for example green, blue, or orange). The saturation is a measure of how much white is in the color (for example, pink is red with more white, so it is less saturated than a pure red). Most

people can relate to this method of describing color. For example, "a deep, bright orange" would have a large intensity "bright", a hue of "orange" and a high value of saturation "deep". We can picture in our minds, but if we defined this color in terms of its RGB components, R=245, G=110, and B=20, most people would have no idea how this color appears. Because the HIS color space was developed based on heuristics relating to human perception, various methods are available to transform RGB pixel values into the HIS color space. Most of these are algorithmic in nature and are geometric approximations to mapping the RGB color cube into some HIS-type color space [Umb98].

2.3 Edge Detection

Edge detection algorithms usually detect sharp transitions of intensity and/or color within an image. These transitions are characteristic of object edges. Once edges of an object are detected other processing such as region segmentation, text finding, and object recognition can take place. However, the edges and regions thus generated will probably not only outline material boundaries, but also shadows, and intensity changes across the object [Wes99].

2.3.1 Edge Detection in Gray-Scale Images

Edge detection can be used to find complex object boundaries by making potential edge points corresponding to pla8uces in an image where rapid changes in brightness occur. After these points have been marked, they can be merged to form lines and object outlines [Umb98].

Edge detection operators are based on the idea that edge information in an image is found by looking at the relationship a pixel has with its neighbors. If a pixel's grey-level value is similar to those around it, there

is probably not an edge at that point. However, if a pixel has neighbors with widely varying grey levels, it may represent an edge point. In other words, an edge is defined by a discontinuity in grey-level values [Umb98].

2.3.2 Edge Detection in Color Images

Color is a key feature describing the contents within an image scene, and it is found to be a highly reliable attribute that should be employed in the edge detection. The primary assumption used in color edge detection is that there is a change in chromaticity or intensity of pixels at the boundaries of objects. Hence, boundary detection can be accomplished by searching for abrupt discontinuities of the color features [Luk07].

In many cases, edge detection based only on the intensity of the image may not be sufficient, because no edges will be detected when neighboring objects have different chromaticity but the same luminance (see figure 2.3).
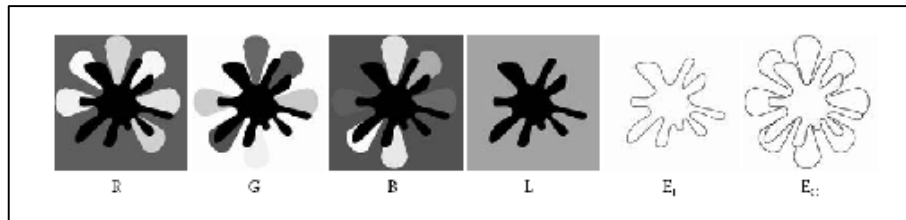
Figure (2.3): Test image with its *R*, *G*, *B* channels and the luminance *L*. *EL* depicts the edges found utilizing only the luminance, and *EC* shows the detected edges when the color information is also considered [Luk07]

Because the capability of distinguishing between different objects is crucial for applications such as object recognition and image segmentation, the additional boundary information provided by color is of great importance. Therefore, there is a strong motivation to develop

efficient color edge detectors that provide high-quality edge maps [Luk07].

2.3.3 Edge Detectors in Color Images

The major performance issues concerning edge detectors are their ability to precisely extract edges. An optimal edge detector should address the following issues [Luk07]:

- § *Detection* — none of the image edges should be missed, and nonexisting edges should not be detected
- § *Localization*—the edges should be well localized, which means that the distance between real and detected edges should be minimized
- § *Response* —an optimal edge detector should have only one response to a single edge

There are many types of filters could be used as edge detectors (such as Sobel, Preweit, Gradient, and Laplacian filter). The sobel operator is a very well known edge detector. It has been shown to be a good edge detector. In its expanded form, it will deal better with the information contained in color images where the operator is applied to each color plane independently [Wes99].

The sobel edge detection masks look for edges in both the horizontal and vertical directions and then combine this information into a single metric. The masks are as follows [Umb98]:

-1	-2	-1
0	0	0
1	2	1

-1	0	1
-2	0	2
-1	0	1

Row Mask   Column Mask

Figure (2.4): The sobel edge detector's two masks

These masks are each convolved with the image. At each pixel location we know have two numbers: (s_1), corresponding to the result from the row mask, and (s_2), from the column mask. We use these numbers to compute two metrics, the edge magnitude (G) and the edge direction (θ), which are defined as follows [Umb98]:

Edge Magnitude

$$G = \sqrt{s_1^2 + s_2^2} \qquad \text{Or} \qquad G = Max\left[\left[|s_1|, |s_2|\right]\right] \quad \dots (2.5)$$

Edge Direction

$$\theta = \tan^{-1}\left[\frac{s_1}{s_2}\right] \qquad \dots (2.6)$$

The edge direction is perpendicular to the edge itself because the direction specified is the direction is gradient, along which the grey levels are changing [Umb98].

2.4 Image Quality Measures

An image is a visual representation of an object or group of objects. Probably most people are familiar with photographic images; however, photographic images do not lend themselves to computer analysis because computers work with numerical rather than pictorial information. Image processing manipulates information within an image to make it more useful. In order to process an image with a computer, the image must be converted into numeric form. This process is known as Image Digitization [Pan02].

A computer image is a matrix (a two-dimensional array) of *pixels*. The value of each pixel is proportional to the *brightness* of the corresponding point in the scene; its value is often derived from the output of an A/D converter. The matrix of pixels, the image, is usually square and we shall describe an image as *NXN m*-bit pixels where *N* is the number of points along the axes and *m* controls the number of brightness values. Using *m* bits gives a range of 2^m values, ranging from 0 to 2^m- 1. If *m* is 8 this gives brightness levels ranging between 0 and 255, which are usually displayed as black and white, respectively, with shades of grey in between. Smaller values of *m* give fewer available levels reducing the available contrast in an image [Nix02].

There are number of image quality metrics used to analyze the quality of the image, these are:

2.4.1 Statistical Image Measures

Imagine an experimental setup in which we are imaging a certain object. The measured quantity at a certain point in the image plane (a pixel) is the irradiance. Because of the statistical nature of the observed process, each measurement gives different value. This means that the observed signal is not characterized by a single value but rather a *probability density function* (*PDF*) *P(g)* [Jah05].

Undoubtedly the most important probability distribution used to describe a random variable is the normal probability distribution. The normal probability distribution has been applied in a wide variety of practical applications in which the random variables involve scientific measurements. The following are the number of statistical image measures [Pan02]:

a) Histogram

The histogram method is perhaps the oldest method of density estimation. It is the classical method by which a probability density is constructed from a set of samples [Web02].

A histogram of an image is a list (vector) that contains one element for each quantization level. Each element contains the number of pixels whose value corresponds to the index of the element. Histograms can be calculated easily for data of any dimension [Jah05]. Given the probability density function p(i) of size N, where 0≤p(i)≤1 and the relationship between p(i) and i are called histogram. This can be defined as follow [Web02]:

$$p(i) = \frac{1}{N} \sum_{j=1}^{N} \delta(i - v_j) \qquad \qquad ...\,(2.7)$$

Where
$$\delta(w) = \begin{cases} 1 & if \quad w = 0 \\ 0 & Otherwise \end{cases}$$

Where i is the scale (0 … 255), v_j is the intensity which its rank is j in the data set of size N. Where the data set presents a digital colored image or a part of a digital image.

In the equation above, δ is the unitary impulse function. The *p(i)* values are normalized in order to sum to one. A histogram can be determined for each color component, resulting in three different color histograms for every single image. Another possible method is to have a single color histogram for all of the color channels. In the latter approach, the color histogram is simply a compact combination of three histograms [Kon02].

b) Mean

The **mean**, indicated by **μ** (a lower case Greek *mu*), is the statistician's jargon for the average value of a signal. It is found just as you would expect: add all of the samples together, and divide by the number of samples (N) in the signal [See02].

The *image mean* is the average pixel value of an image. For a gray scale image this is equal to the average brightness or intensity. The mean of N pixels in the region (R) is given by the following equation [You98]:

$$\mu = \frac{1}{N} \sum_{(i,j) \in R} I[i, j] \qquad \qquad ... \quad (2.8)$$

Where μ is the mean of pixels of size N, R is the region of the image, and i, j are the region indices.

c) Standard Deviation

The unbiased estimate of the standard deviation (σ) of the brightness within a region (R) with N pixels is called the sample standard deviation that can be computed from the equation bellow [You98]:

$$\mu_s = \frac{1}{N} \sum_{(i,j) \in R} (I(i,j))^2 \qquad \qquad … \quad (2.9)$$

$$\sigma = \sqrt{\mu_s - \mu^2} \qquad \qquad … \quad (2.10)$$

Where μ_s represents the mean square of N-pixels.

2.4.2 Pixel Difference-based Measures

These measures calculate the distortion between two images In This section a number of pixel measures is given. These measures are organized as follows:

a) Mean Square Error (MSE)

The computation of distortion involves some measure of the distance between the original distorted or processed images. A common measure of distortion between images is the mean squared error (MSE). The (MSE) is calculated according to the following equation [Sha03]:

$$MSE = \frac{1}{N} \sum_{(i,j)\in R}^{N} [I_1(i,j) - I_2(i,j)]^2 \qquad \dots (2.11)$$

Where I_1 is the original image, I_2 is the image whose MSE counted for, and N is the number of images pixels. In practice, the MSE is often presented in another form: the peak signal-to-noise ratio (PSNR). PSNR is by far the most commonly used distortion measure for images and is defined for eight bits per pixel. While PSNR is easy to compute, it provides a poor approximation of the perceived difference between images, except when the PSNR values are relatively high. In general, MSE-like measures do not anticipate human visual characteristics. For example, if one compares an image with a version of itself spatially shifted by a couple of pixels, the resulting MSE number will be high, even though the images are almost indistinguishable [Sha03].

b) Signal-to-Noise Ratio (SNR)

The usual description of the magnitude of image noise is a signal-to-noise ratio expressed in decibels. This is defined in terms of the standard deviation values in the blurred (σ_I) and the noisy (σ_N) images (which of course may not be known), as shown in the equation bellow [Rus07]:

$$SNR = 10.\log_{10}\left(\frac{\sigma_I}{\sigma_N}\right) \qquad \text{dB} \qquad \dots (2.12)$$

When the signal-to-noise ratio is greater than 50 dB, the noise is, practically speaking, invisible in the image and has a minimal effect on deconvolution. On the other hand, a low signal-to-noise ratio of 10 to 20 dB makes the noise so prominent that deconvolution becomes quite impractical [Rus07].

2.4.3 Human Visual System (HVS)-based Measures

Human beings are intensely visual creatures. Most of the information we acquire comes through our eyes (and the related circuitry in our brains), rather than through touch, smell, hearing, or taste [Rus07].

Humans are especially poor at judging color or brightness of features within images unless they can be exactly compared by making them adjacent. Gradual changes in brightness with position or over time are generally ignored as representing variations in illumination, for which the human visual system compensates automatically. This means that only abrupt changes in brightness are easily seen. It is believed that only these discontinuities, which usually correspond to physical boundaries or other important structures in the scene being viewed, are extracted from the raw image falling on the retina and sent up to the higher-level processing centers in the cortex [Rus07].

In human visual system the eye and the retina are the transmission channel, the optic nerve and the processing engine, are the visual cortex. In the retina there are three kinds of photoreceptors responsible for daily vision, called L-, M-, and S- cones or more simply red, green, and blue cones. They reach their maximum sensitivity at the wavelength corresponding to these basic colors. In recent models of color vision, the color information issued from the cones are combined and transformed into three channels, one achromatic and others chromatic. Achromatic

channel or luminance is treated more or less separately from chrominance channels by the HVS [Del98].

a) Spatial Frequency Resolution

In order to understand the concept of spatial frequency, it has been first need to define exactly what resolution is. Resolution has to do with the ability to separate two adjacent pixels – if two adjacent pixels have been seen as being separate, then the two have been resolved. The spatial frequency concept must include the distance from the viewer to the object as a part of the definition. With a typical television image, human can not resolve the individual pixels unless it get very close, so the distance from the object is important when defining the spatial frequency. The necessity can be eliminated to include distance by defining spatial frequency in terms of cycle per degree, which provides us with a relative measure [Umb98].

In a bright region, the black pixels are widely spaced in a low spatial frequency pattern. In darker regions, the black pixels are closer together generating a higher spatial frequency pattern [Sha03].

In general, we have the ability to perceive higher spatial frequencies at higher levels but overall the cutoff frequency is about 50 cycle per degree, peaking at around 4 cycles per degree [Umb98].

b) Brightness Adaptation

Brightness is one of the most significant pixel characteristics. It is involved in many image-editing such as contrast or shadow/highlight. Brightness defined as an attribute of a visual sensation according to which a given visual stimulus appears to be more or less intense; or, according to which the area in which the

visual stimulus is presented appears to emit more or less light, and range variation in Brightness from "bright" to "dim". Not so long ago, **Luminance** was used as a synonym of Brightness. Thus, a value Photoshop employs for Brightness in color – to – Grayscale transformation well correlates with Luminance definition. Another popular brightness substitution is **Luma**. Luma is widely used in image processing algorithm imitating performance of corresponding color TV adjusting knobs. The gray Scale intensity or brightness is calculated from equation (2.1) [Ser08].

The attribute of brightness and lightness are very often interchanged, despite the fact that they have very different definitions. Brightness: Attribute of a visual sensation according to which an area appears to emit more or less light. Lightness: The brightness of an area judged relative to the brightness of similarity illuminated area that appears to be white or highly transmitting. Brightness refers to the absolute perception of the amount of light of stimuli, while lightness can be thought of as the relative brightness. The human visual system generally behaves as a lightness detector [Sha03].

A very simple example can be seen with a typical newspaper. This paper, when read indoors, would have a certain brightness and lightness. When viewed side by side with standard office paper, the newspaper often looks slightly gray, while the office paper appears white. When the newspaper and office paper are brought outdoors on a sunny summer day, they would then have much higher brightnesses. Yet the newspaper still appears darker than the office paper, as it has a lower lightness. The physical amount of light reflected from the newspaper might be more than a hundred times greater than the office paper was indoors, yet the relative amount of light reflected has not

changed. Thus, the relative appearance between the two papers has not changed [Sha03].

c) Contrast and Contrast Sensitivity Function

Contrast of an image is its distribution of light and dark pixel, or is the range from the darkest regions of the image to the lightest regions [Cra97]. Contrast is relative measure of intensity of a stimulus, as compared to its surroundings (It is dimensionless). In psychophysical studies, the typical measure of contrast between two intensities I_{Max} and I_{Min} (I_{Max} being brighter) is the Michelson contrast [Cra97]:

$$Ct = \frac{I_{Max} - I_{Min}}{I_{Max} + I_{Min}} \qquad \qquad \text{... (2.14)}$$

High contrast images have large regions of dark and light regions. Images with good contrast have a good representation of all luminance intensities. As the contrast of an image increase, the viewer perceives an increase in detail. This is purely a perception as the amount of information in the image does not increase. Human perception is sensitive to luminance contrast rather than absolute luminance intensities, Figure (2.5) shows this [Cra97]:
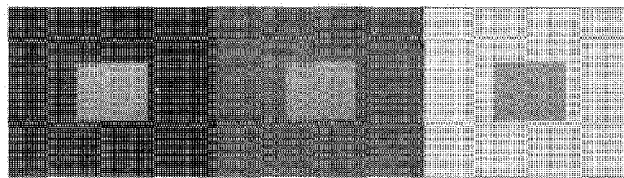

Figure (2.5): Example of simultaneous Contrast [Cra97]

Although the small squares in the middle of the larger squares have the same luminance, they are not perceived to be equally bright because of their surroundings. This phenomenon is the product of linear spatial frequency filtering. Apparent brightness depends strongly on the local background intensity [Cra97].

Contrast sensitivity, which is simply the reciprocal of the contrast, is the typical measure used by psychophysical gauge human visual performance [Dou02]. The Contrast Sensitivity Function (CSF) describes the pattern sensitivity of the Human Visual System (HVS) as a function of contrast and spatial frequencies. Psychophysical experiments have shown the high sensitivity of the (HVS) for low frequencies and low sensitivity for high frequencies. The CSF is probably the most important stage in any HVS model [Bri05].

Less contrast is needed between the light and dark locations to detect them when the features are larger. Brightness variations about 1-mm wide represent a spatial frequency of about nine cycles per degree, and under ideal viewing conditions can be resolved with a contrast of a few percent, although this assumes the absence of any noise in the image and a very bright image. Acuity drops significantly in dark images or in ones with superimposed random variations, and is much poorer at detecting color differences than brightness variations [Rus07].

At a normal viewing distance of about 50 cm, 1 mm on the image is about the optimum size for detecting the presence of detail. As the spatial frequency drops (features become larger), the required contrast increases, so that when the distance over which the brightness varies from minimum to maximum is about 1 cm, the required contrast is about ten times greater. The variation of spatial resolution ("acuity")

with contrast is called the modulation transfer function (Figure 2.6) [Rus07].
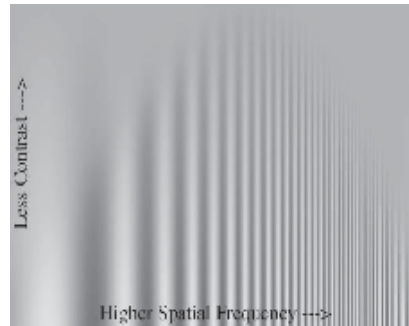
Figure (2.6): Illustration of the modulation transfer function for human vision, showing that the greatest ability to resolve low-contrast details occurs at an intermediate spatial frequency and becomes poorer for both smaller and larger details [Rus07].

Graphical representation of variation in contrast sensitivity over a range of spatial frequencies describes the contrast sensitivity function (CSF). In general, the human visual system is most sensitive to spatial frequencies in the range 2-6 cycles per degree (cpd), and more contrast is needed for detection of lower and higher spatial frequencies, figure (2.7) shows the typical shape of the contrast sensitivity function [Bri05].
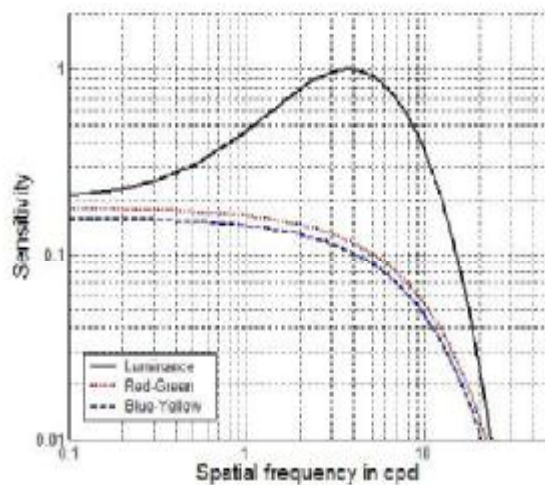
Figure (2.7): Typical shape of contrast sensitivity function [Bri05].

d) Contrast Stretching

One of the simplest processing linear functions is a contrast stretching transform [Gon02]. Low contrast images are mostly dark, mostly light or mostly gray [Cra97]. The idea behind contrast stretching is to increase the dynamic range of the gray levels in the image being processed. An image with low contrast has a histogram is either concentrated on the right, left, or in the middle of the gray scale [Gon02].

The components of the histogram in the high contrast image cover a board range of the gray scale and, further that the distribution of pixel is not too far from uniform, with very few vertical lines being much higher than the others. Intuitively, it is reasonable to conclude that an image whose pixels tend to occupy the entire range of possible gray levels and, in addition, tend to be distributed uniformly, will have an appearance of high contrast and will exhibit a large variety of graytones, figure (2.8) shows the histograms of high and low contrast [Gon02].

Figure (2.8): Two images of low and high contrast and their corresponding histograms [Gon02]

2.2.4 Correlation-based Measures

The closeness between two digital images can also be quantified in terms of correlation function. These measures measure the similarity

between two images, hence in this sense they are complementary to the difference-based measures: Some correlation based measures are as follows [Gon02]:
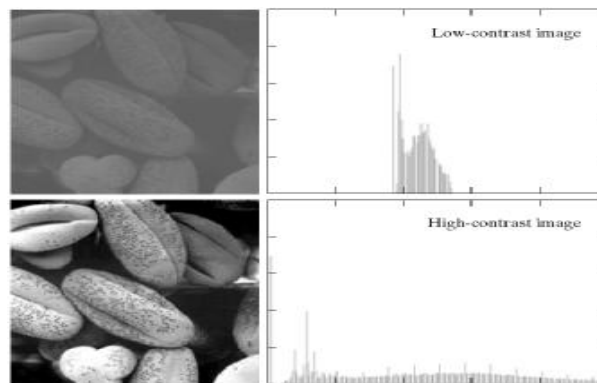
$$Cor = \frac{\left(\sum\limits_{i=1}^{m} \sum\limits_{j=1}^{n} (I_1(i,j) - \mu_{I_1})(I_2(i,j+1) - \mu_{I_2}) \right)}{\sqrt{\sum\limits_{i=1}^{m} \sum\limits_{j=1}^{n} \left(I_1(i,j) - \mu_{I_1}\right)^2 \sum\limits_{i=1}^{m} \sum\limits_{j=1}^{n} \left(I_2(i,j+1) - \mu_{I_2}\right)^2}} \qquad \text{... (2.15)}$$

In eq. (2.15), μ_{I_1} and μ_{I_2} denote the arithmetic mean gray level in the reference image and the part of the search image covered by the reference image, respectively. All sums are to be taken over all pixels of the reference image [Ava01].
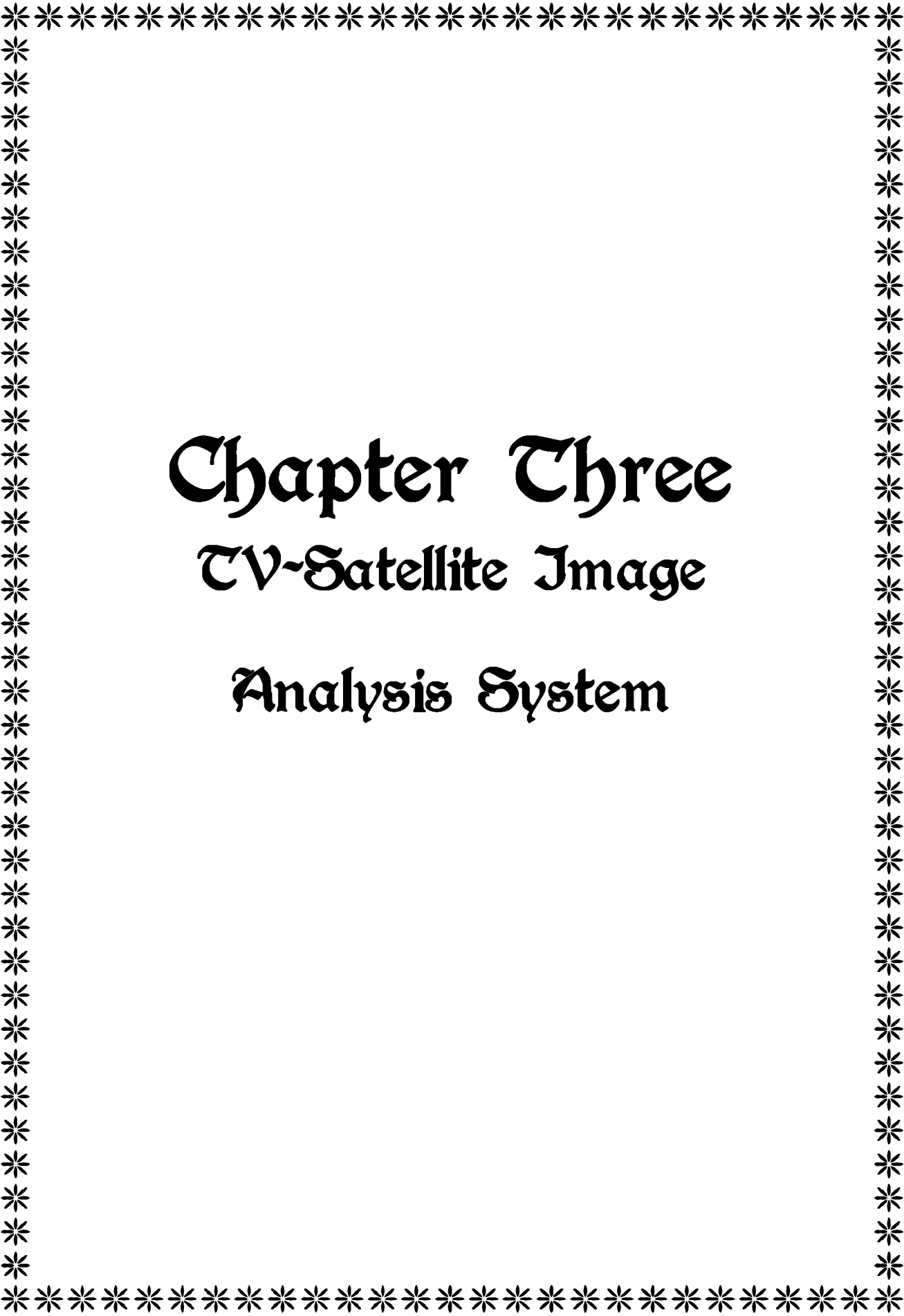
The principle use of correlation is for matching. In matching, $I_1(i,j)$ is an image containing object or region. If we want to determine whether I_1 contains a particular object or region in which we are interested, we let $I_2(i,j)$ be that object or region (we normally call this image a template). Then if there is a match, the correlation of the two functions will be maximum at the location where I_2 finds a correspondence in I_1 [Gon02].

In the special case when the image function I_1 and I_2 are the same, the correlation operation is called autocorrelation. This is used to combine all parts of the image to find repetitive structures. By sliding the top image laterally in any direction, the degree of match with the underlying original is measured by the autocorrelation function. Where features still reside on themselves, the match is high. Likewise, when a large shift brings a feature onto another similar one, the match is again high [Rus07].

Cross correlation is an algorithm for the location of corresponding image patches based on the similarity of gray levels. A reference point is given in the reference image, and its coordinates are searched for in the

search image. That is why, the reference image is moved in the search image, and the position of maximum similarity of gray levels is searched for. For that purpose, at each position of the reference image in the search image, a similarity value [Kro01].

Finally, we point out that the term cross correlation often is used in place of the term correlation to clarify that the images being correlated are different. This is as opposed to autocorrelation, in which both images are identical [Gon02].

Chapter Three
TV-Satellite Image
Analysis System

Chapter Three
TV-Satellite Image Analysis System

3.1 Introduction

The fundamental idea of this study is to analyze the TV-Satellite images using different image quality measures. In this chapter we will explain the system of how to analyze these TV-Satellite images and illustrate the quality measures. A number of different techniques have been proposed including statistical measures, new contrast of edges measures and local similarity measures as methods to determine the quality of TV-Satellite images.

3.2 TV-Satellite Video Capture Processing

This study has used a number of TV-Satellite images which have been captured using TV-Satellite system; this system consists of:

- Satellite dish of Type (G-Gard).
- LNB attached to the Dish of type StarSat, which is shown in figure (3.1a) with its properties in figure (3.1b).
- Satellite home receiver of type (Strong SRT 4620).
- TV Tuner card of type (easy capture TV) shown in figure (3.2), which is attached to the computer. Later will be used after installing it to the computer by its software program (Inter-Video Win DVR) that comes with the product.

After completing the installation process of the TV Tuner card different video clips have been captured from a channel broadcasted

over different satellites (Arabsat, Hotbird, Nilesat). The considered satellite channel in this study is an Arab channel called (Abu Dhabi). The recorded video clips will be cut into frames (about 30 frames in a second) by using a software program called (Ulead Video Studio 0.9), according to SECAM TV standard, and then save these frames as BMP images.

| (a) | (b) |

Figure (3.1): (a) The type of used LNB, (b) The properties of the LNB

Figure (3.2): The TV Tuner Card

3.3 TV-Satellite Image Analysis System

An overview of the developed system architecture in this study is presented in figure (3.3). The steps of the involved processes are discussed in the following sections. A number of TV-Satellite images

were saved first as bitmap images from the captured video clip of the considered channel over three satellites (Arabsat, Hotbird, and Nilesat). These images will be processed according to different methods. Differernt contrast of edges methods and correlation methods have been introduced as main steps in the whole system.

Several contrast of image edges measures were suggested in this stage including maximum and minimum contrast of edges, maximum and minimum mean of contrast edges, horizontal and vertical contrast of edges, and finally main and second diagonal contrast of edges. Also there are different measures applied after the edge extraction process, these are, amount of edges and SNR of edges methods. All of these methods will be discussed later in this chapter with their corresponding equations and algorithms.

Correlation method is applied on the selected homogenous regions of the image; the selection process is made according to two different ways, the manual and the automatic selection process. The manual selection homogenous regions will be selected from the single image and also from the scene (consists of six consequence images). The correlation of the automatic selection is based on searching for the regions that have minimum standard deviation values of the image. The maximum and minimum correlation of the image will be computed as a different correlation method. The correlation will be discussed later in this chapter with its implementation algorithms.

Input Digital TV-Satellite Images

The Correlation of the Manual Selected regions of the Image

The Correlation of the Manual Selected regions of the Scene

The Correlation of the Automatic Selected regions of the Image

The Maximum and Minimum Correlation

Correlation Methods

Edge Detection

Calculate Amount of Edges

Calculate SNR of Edges

Contrast of Edges

Maximum Contrast

Minimum Contrast

Max Mean Contrast

Min Mean Contrast

Horizontal Contrast

Vertical Contrast

Main Diagonal Contrast

Second Diagonal Contrast

The Contrast of Statistical Image Measures
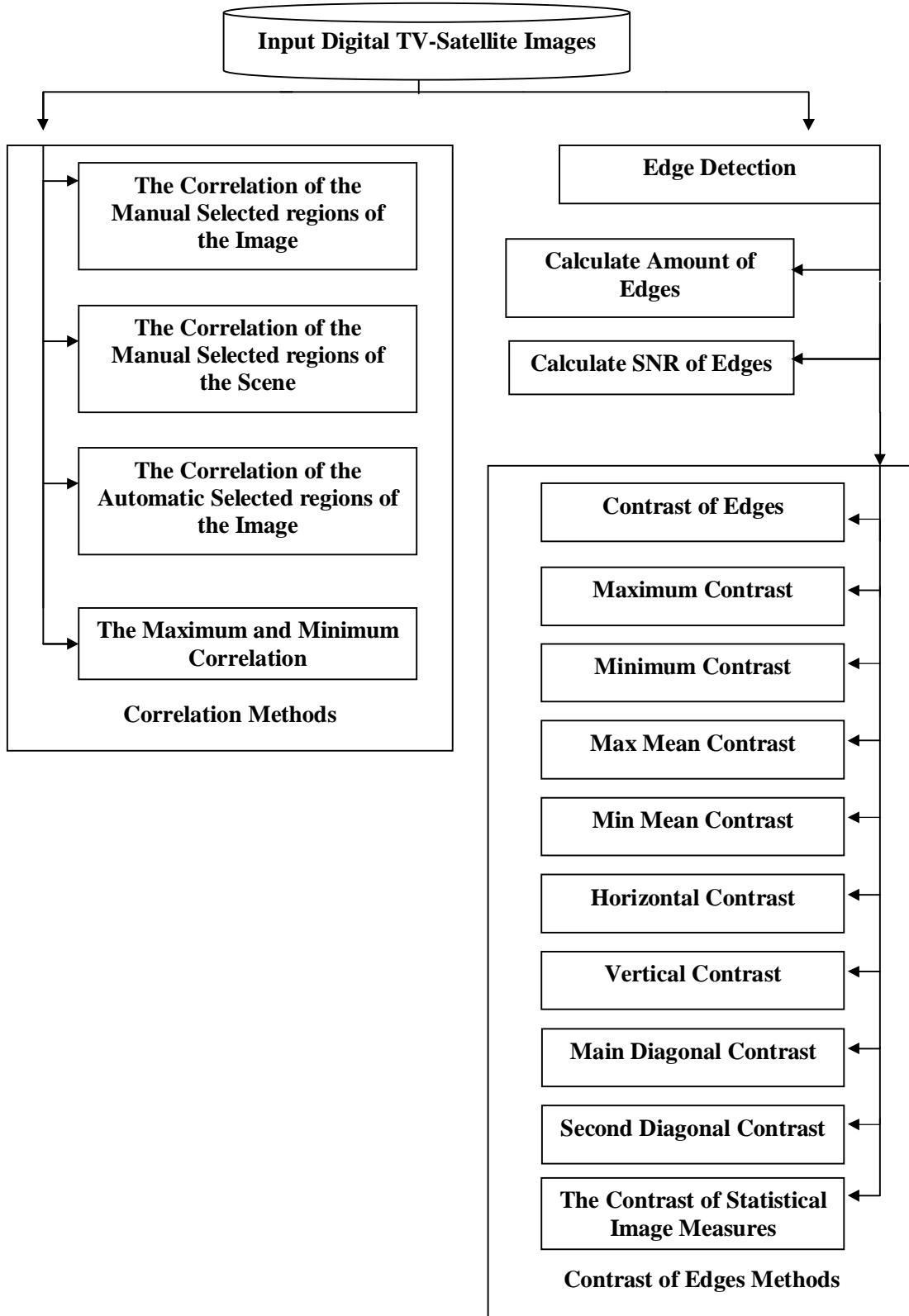
Contrast of Edges Methods

Figure (3.3): TV-Satellite Image Analysis System

3.4 Edge Extraction Using Sobel Filter

The process of edge extraction is the conversion of the colored image to the edged image, which the edged image consists of the three primary (RGB bands) and L component that represent the colored edges. Each color components is represented by one byte. The luminance (L) value is obtained from the equation (2.1). This equation has applied on all image pixels in order to obtain the L value.

Edge detection is used to find the edges of the TV-Satellilte images. In this study, sobel filter, shown in the figure (3.4) have been used to obtain the edges from the image.

-1	-2	-1
0	0	0
1	2	1

-1	0	1
-2	0	2
-1	0	1

      Row Mask   Column Mask

Figure (3.4): The sobel edge detector's two masks

Sobel filter is passed over all pixels in the colored image, the filter output is determined according to the following equations:

$g_x = |\,(img(i+1,j-1)+2*img(i+1,j)+img(i+1,j+1)) -$

$\qquad (img(i-1,j-1)+2*img(i,j-1)+img(i-1,j+1))\,| \qquad \qquad \dots (3.1)$

$g_y = |\,(img(i-1,j+1)+2*img(i,j+1)+img(i+1,j+1)) -$

$\qquad (img(i-1,j-1)+2*img(i,j-1)+img(i+1,j-1))\,| \qquad \qquad \dots (3.2)$

A threshold value should be defined in the edge extraction for comparison process; the colored image is converted to edged image by testing g_x or g_y values; if either of them is greater than the threshold value then the pixel is set to (255) for all RGB-L component otherwise, it is converted to black (0).

The pseudo code (3.1) illustrates the implementation steps to perform the sobel filter. The input is the colored TV-Satellite image, which read from a Bmp file as an RGBL array of records. Each record consists of RGB-L component and the threshold value, the output is the image of edges, which is represented as a two dimensional array contains the edge values of the image.

Pseudo code list (3.1) Sobel edge detection routine

<u>**Input**</u>

Th: Threshold value for edge detection.

imag: Image array in RGB-L data of known Ih and Iw.

{Where Ih and Iw is the image height and width}

<u>**Output**</u>

Edge: Image array of edges only.

<u>**Variables**</u>

gx, gy: Sobel orientation variables.

Max1: Maximum value for comparison.

<u>**Procedure**</u>

For i   {where i=2..ih-1}

   i1=i-1, i2=i+1

  For j {where j=2..iw-1}

     j1=j-1, j2=j+1

     {*Calculate gx, gy for each RGB-L valuess*}

     gx ⟵   Abs([img(i2,j1)+2*img(i2,j)+img(i2,j2)]–[img(i1,j1)+2*img(i,j)+img(i1,j2)])

     gy ⟵   Abs([img(i1,j2)+2*img(i,j2)+img(i2,j2)]–[img(i1,j1)+2*img(i,j1)+img(i2,j1)])

     max1 ⟵ 0

     if gx > Th or gy > Th then   max1=255

     Edge (i,j) ⟵ max1

   End For i, j

<u>**End Procedure**</u>

3.5 Determining the Amount of Edges

The image edges which has been produced by applying sobel edge detector on the colored image, need to be used to determine the rate of edges. In this study, the amount of edges has been considered as one of image quality measures, whereas the amount of edges increases, the image quality increases. The amount of edges method process is implemented according to the following steps:

Step 1: Check each point of the image edges if it is an edge or not.

$$If \quad edge(i, j) = 255 \quad \{ \text{ an edge for all RGB and L } \}$$

$$\{ \text{ where } i=2 .. ih, j=2 .. iw \}$$

$$Rate = Rate + 1 \quad \{ \text{ for all RGB and L } \}$$

Step 2: After tracing the edge pixels over the image edges, the total number of edges (Rate) will be divided by the total number of pixels in the original image (N).

$$Rate = Rate / N \quad \{ \text{ for all RGB and L, Where N is the total}$$

$$\text{number of Pixels in the image } ih*iw \}$$

The following pseudo code (3.2) will illustrate this method briefly.

Pseudo code list (3.2) Amount of Edges routine

Input

      Th: Threshold value for edge detection.

      img: Image array in RGB-L data of known Ih and Iw.

    {Where Ih and Iw is the image height and width}

      Edge: Image array of edges of RGB-L.

Output

      Rate: Amount of edges of RGB-L.

Variables

      i, j: Image array indices.

      N: Total number of pixels of the image.

Continued

Procedure

     N ⟵ ih * iw

     Rate ⟵ 0

    For i   {where i=2..ih-1}

     For j {where j=2..iw-1}

         {*Calculate number of edges for each RGB-L valuess*}

         If edge(i,j) = 255 then

              Rate ⟵ Rate + 1

     End For

    End For

    Rate ⟵ Rate / N

End Procedure

3.6 Calculating the SNR of Edges

The highly SNR values indicate that the image has a good quality. After determining the image edges for RGB-L components, the SNR has been computed. The implanted method is illustrated in the following steps:

Step 1: Check each pixel of the image of edges whether is an edge or not. If it is an edge (if edge(i,j) = 255) then calculate the standard deviation (σ_E) of the edge pixel by taking the pixel real value not the (255) but the value from the colored image before the conversion process by sobel filter. Otherwise if the pixel is not an edge then move to the next pixel and so on. Repeat this step until the last pixel of the image of edges.

    If edge = 255 then

        Calculate σ_E from the colored image.

   Else Go to the next edge.

Step 2: Divide the colored image (the image before the extraction process) into blocks of size (16×16), calculate the (σ) for each block

for each RGB-L components and find the minimum standard deviation (Min$_{\sigma I}$).

Step 3: After determining (σ_E) and (Min$_{\sigma I}$), Calculate the SNR for each RGB-L components according to the following equation:

$$SNR = 10 \times \log \left(\frac{\sigma_E}{Min_{\sigma I}} \right) \qquad \ldots (3.3)$$

The following pseudo code list (3.3) will illustrate the SNR method:

Pseudo code list (3.3) SNR of Edges routine

Input

      img: Image array in RGB-L data of known Ih and Iw.

      {Where Ih and Iw is the image height and width}

      Edge: Image array of edges of RGB-L.

Output

      SNR: Signal to Noise Ratio.

Variables

      m,m1: mean variables.

      STD1,minSTD: Standard derivation and minimum Standard derivation.

Procedure

    n1 ⟵ 0 :   m ⟵ 0:   sm ⟵ 0

   For i   {where i=2..ih-1}

       For j {where j=2..iw-1}

     {*Calculate the mean and the variance of the edges* for each RGB-L}

          If edge(i,j) = 255 then

             m ⟵ m + img(i,j)

             sm ⟵ sm+img(i,j)^2

             n1 ⟵ n1+1

         End if

        End For j

      End For i

    m ⟵ m / n1

    STD1 ⟵ $\sqrt{\left(\frac{sm}{n1} \right) - m\char`\^2}$

Continued

*{ Now searching for the minimum STD value after dividing the image into blocks of size (16*16) }*

MinSTD ⟵ 1000

n2 ⟵ 16*16

bsz ⟵ 16

bsz1 ⟵ bsz-1

m1 ⟵ 0:   sm1 ⟵ 0

For i Step bsz :   i1 ⟵ i+bsz1   *{ Where i=1..ih }*

 For j   Step bsz: j1 ⟵ j+bsz1   *{ Wher j=1..iw }*

  If   i1 > ih   then   i1 ⟵ ih

  If   j1 > iw   then j1 ⟵ iw

  For ii   *{ Where ii=i..i1 }*

   For jj   *{ Wher jj=j..j1 }*

{ Calculate the Mean, the Variance and the STD for each RGB and L }

         m1 ⟵ m1+img(ii,jj)

         sm1 ⟵ sm1+img(ii,jj)^2

      End For jj

     End For ii

     m1 ⟵ m1 / n2

     STD2 ⟵ $\sqrt{\dfrac{sm1}{n2} - m1\text{\textasciicircum}2}$

      If MinSTD > STD2   then   MinSTD ⟵ STD2

   End For j

 End For i

 SNR ⟵ $10 * \log\left(\dfrac{STD\_1}{MinSTD}\right)$

End Procedure

3.7 Contrast of Edges Methods

The contrast considered as one of the most important measures used to evaluate the amount of image information, and to estimate the quality of the image. In this study, the contrast has been calculated for

image edges. Most of the images details concentrate on edges. Also, contrast appears intensively in the edges (in the different image intensity values areas of the image). The contrast of edges calculated according to the Michelson formula in additional to the number of different suggested methods of contrast that based on modifying Michelson formula. These methods will be illustrated in the following sections.

3.7.1 Contrast of Edges

After applying sobel filter on the TV-satellite colored image and determining its edges, then the contrast has used on the obtained image edges. The contrast of image edges is computed according to Michelson contrast formula (2.14), the implementation steps of this method have been discussed below:

Step 1: Check each pixel of the image of edges whether it is an edge or not, if it is so (edge=255), then take a moved mask window of size (3×3) around the edge pixel.

Step 2: Searching for the maximum (I_{max}) and minimum (I_{min}) intensity for each RGB values and L-component of the mask window (where the values of the mask will take the values of the image before applying sobel filter on it). After find the maximum and minimum intensity values, replace them in the Michelson contrast formula (2.14).

Step 3: This step represent the computation of the histogram of the contrast values. Histogram of contrast of edges shows the distribution of contrast values for each edge pixel in the image within the range of the contrast values. If the minimum value of the contrast of edges is (0) and the maximum value of the contrast of edges is (1), then the

histogram of the contrast of edges shows the distribution of contrast of edges values ranging from (0) to (1).

Step 4: Calculate the mean and STD of probability of contrast according to the equation (2.2) and (2.5). This process performed four times for each RGBL values. These steps are illustrated in the pseudo code list (3.4).

Pseudo code list (3.4) Contrast of edges

Input

      img: Image array of RGB-L data of known ih and iw.

   {Where ih and iw are the height and the width of the image}

      Edge: Image array of edges of RGB-L data.

Output

      hist: Array of histogram of contrast of edges.

      m: Mean of probability of contrast of edges.

      std: STD of probability of contrast of edges.

Variables

      Imax, Imin: Highest and lowest pixel intensities of RGB-L data.

      Cont: Contrast of edges.   Sm: Variance.

Procedure

      n←0

      For i,j   *{Where i=2..ih-1, j=2..iw-1}*

      {Check whether the pixel is an edge or not}

        If Edge(i,j)=255 then

            n←n+1

          i1←i-1, i2←i+1

          j1←j-1, j2←j+1

          a1←img(i,j)

          imax←a1,   imin←a1

        For ii, jj   *{Where ii=i1..i2, jj=j1..j2}*

          a2←cimg(ii,jj)

           if a2>imax then

Continued

imax←a2

if a2<imin then   imin←a2

End For

If (imax=0 and imin=0) then

Cont←0

Else   *{Calculate the stretched contrast of edges and the histogram}*

$$\text{Cont} \leftarrow \text{Round\_integer}(255 * (\frac{I_{Max} - I_{Min}}{I_{Max} + I_{Min}}))$$

hist(cont) ←hist(cont)+1

End if

End For

{Calculation of Mean and STD of contrast of edges}

m←0, sm←0

For k   {Where k=0 .. 255}

hist (k) ←hist(k)/n

gl← k / 255

m←m+gl*hist(k)

sm←sm+ gl^2 * hist(k)

End For   *{This loop will apply for all RGB-L components}*

std← $\sqrt{sm - m^2}$

End Procedure

3.7.2 Maximum and Minimum Contrast of Edges

Using Michelson contrast formula and modifying it into different equations to determine two new methods of computing contrast. These two methods are maximum and minimum contrast of edges. The two methods are applied on the image of edges, these edges extracted by using sobel filter. This method is illustrated in the following steps:
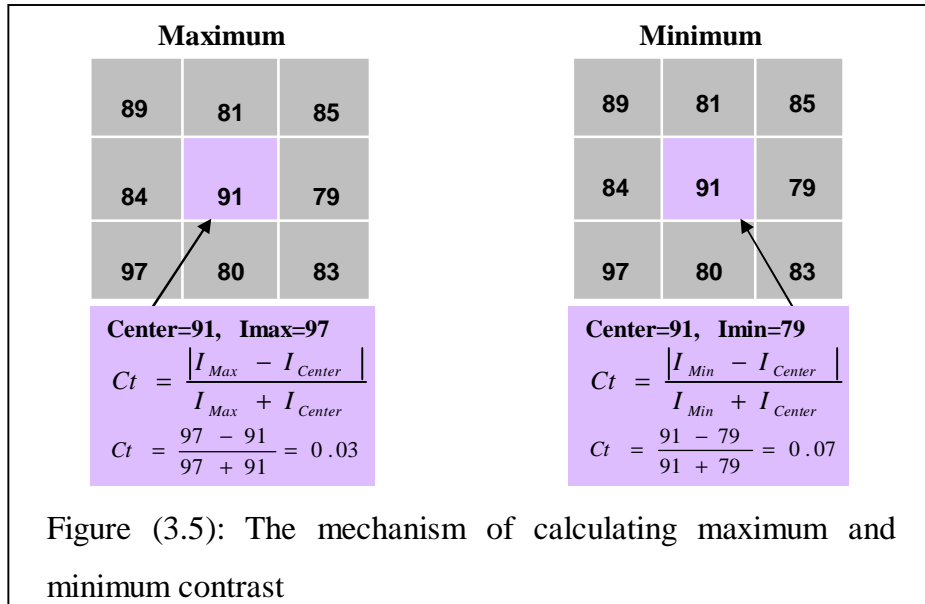
Step 1: Check the pixel of the image whether it is an edge or not, if it is so then go to the step 2, if it is not check the next pixel and so on.

Step 2: Take a moved window of size (3×3) around each edge pixel and get the values of this mask from the colored image (the image before the extraction process).

Step 3: Search for the maximum value among the edged pixel of the original image then replace it by the value of I_{Max} from the Michelson formula while I_{Min} will take the center value of the matrix($I_{Min} = I_{Center}$), which is illustrated in the following equation:

$$Ct = \frac{\left| I_{Max} - I_{Center} \right|}{I_{Max} + I_{Center}} \qquad \qquad ...(3.4)$$

Where I_{Max} is the maximum intensity of the center surroundings of the moved (3×3) matrix of the original image, while I_{Center} is the intensity of the center pixel from the original image. Figure (3.5) illustrates the maximum and minimum contrast of edges examples.

Maximum				Minimum		
89	81	85		89	81	85
84	91	79		84	91	79
97	80	83		97	80	83

Center=91, Imax=97

$$Ct = \frac{\left| I_{Max} - I_{Center} \right|}{I_{Max} + I_{Center}}$$

$$Ct = \frac{97 - 91}{97 + 91} = 0.03$$

Center=91, Imin=79

$$Ct = \frac{\left| I_{Min} - I_{Center} \right|}{I_{Min} + I_{Center}}$$

$$Ct = \frac{91 - 79}{91 + 79} = 0.07$$

Figure (3.5): The mechanism of calculating maximum and minimum contrast

Minimum contrast has the same mechanism of maximum contrast except this method is searching for the minimum intensity

pixel around the center as shown in figure (3.5) and then calculates the minimum contrast according to equation (3.5).

$$Ct = \frac{\left| I_{Min} - I_{Center} \right|}{I_{Min} + I_{Center}} \qquad ...(3.5)$$

Step 4: After computing the contrast of the two methods and obtained their values, the two histograms of them are calculated to represent the distribution of these contrast methods. The mean of probability of them will be determined as well for all RGB-L component.

Pseudo code list (3.5) illustrates the maximum contrast of edges method.

Pseudo code list (3.5) Maximum contrast of edges

Input

img: Image array of RGB-L data of known ih and iw.

{Where ih and iw are the height and the width of the image}

Edge: Image array of edges of RGB-L data.

Output

hist: Array of histogram of contrast of edges.

m: Mean of probability of contrast of edges.

Variables

Imax, ICenter: Highest and center of mask intensities of RGB-L data.

Cont: Contrast of edges.

Center: Center of the moved matrix.

Procedure

n ← 0

For i,j   *{Where i=2..ih-1, j=2..iw-1}*

{Check whether the pixel is an edge or not}

If edge(i,j)=255 then

n ← n+1

i1 ← i-1, i2 ← i+1

j1 ← j-1, j2 ← j+1

a1 ← img(i,j)

I_{max} ← img(i1,j1)

Continued

$I_{Center} \longleftarrow a1$

For ii, jj do   *{Where ii=i1..i2,   jj=j1..j2}*

$a2 \longleftarrow img(ii,jj)$

if $a2 > I_{max}$ then

$I_{max} \longleftarrow a2$

End For

If $I_{max} <= I_{Center}$ then

$Cont \longleftarrow 0$

Else   *{Calculate the stretched contrast of edges and the histogram}*

$$Cont \longleftarrow Round\_Integer(255*(\frac{I_{Max} - I_{Center}}{I_{Max} + I_{Center}}))$$

$hist(cont) \longleftarrow hist(cont)+1$

End if   End if

End For *{This loop will apply for all RGB-L components}*

{Calculation of Mean of contrast of edges}

$m \longleftarrow 0$

For k   {Where k=0..255}

$hist(k) \longleftarrow hist(k) / n$

$gl \longleftarrow k / 255$

$m \longleftarrow m+gl*hist(k)$

End For   *{This loop will apply for all RGB-L components}*

End Procedure

3.7.3 Maximum and Minimum Mean Contrast of Edges

This is another suggested method of computing the contrast of edges. Also the equation (2.14) has been modified into two different equations to produce these two methods. These two methods are applied on the image of edges. The implementation process of these methods is illustrated in the following steps:

Step 1: Take 3×3 moved window around the pixel from the original image after checking if the pixel is an edge (255), else if it is (0) then move to the next pixel to check and so on.

Step 2: Calculate the mean of the pixels surrounding the edge pixel (center of the moved mask).

Step 3: Check whether the computed mean is greater than the center, if it is so then consider the following equation to estimate the contrast, else go to the next (3x3) block.

$$Ct = \frac{\left| I_{mean} - I_{center} \right|}{I_{mean} + I_{center}} \qquad ...(\,3.6\,)$$

Where I_{mean} is the mean of the pixels around the edge pixel, while I_{Center} is the intensity of the edge pixel (center of the moved window). Figure (3.6) illustrates two examples of the maximum and minimum mean contrast of edges.

The main difference between minimum mean contrast of edges and the maximum mean is that, in minimum mean method we checked if I_{mean} is smaller than I_{center} , if it is so then apply equation (3.6).

Step 4: After computing the contrast of the two methods and obtained their values, the two histograms of them are calculated to represent the distribution of these contrast methods. The mean of probability of them will be determined as well for all RGB-L component.

The following pseudo code list (3.6) presents the method of maximum mean contrast of edges.

Pseudo code list (3.6) Maximum mean contrast of edges

<u>Input</u>

        img: Image array of RGB-L data.

{Where ih and iw are the height and the width of the image}

        Edge: Image array of edges of RGB-L data.

<u>Output</u>

        hist: Array of histogram of contrast of edges.

        m: Mean of probability of contrast of edges.

<u>Variables</u>

        Imean: mean of pixels around the center of RGB-L data.

        Cont: Contrast of edges.   ICenter: Center of the moved matrix.

<u>Procedure</u>

       $n \leftarrow 0$

       For i,j   *{Where i=2..ih-1, j=2..iw-1}*

       {Check whether the pixel is an edge or not}

        If Edge (i,j)=255 then

            $n \leftarrow n+1$

            $i1 \leftarrow i-1,\ \ i2 \leftarrow i+1$

            $j1 \leftarrow j-1,\ \ j2 \leftarrow j+1$

            $I_{mean} \leftarrow 0$

            $I_{Center} \leftarrow imge(i,j)$

            For ii, jj   *{Where ii=i1..i2, jj=j1..j2}*

                $I_{mean} \leftarrow I_{mean}+img(ii,jj)$

           End For

           $I_{mean} \leftarrow Round(Imean\ /\ 9)$

       {Calculate the stretched contrast of edges and the histogram}

           $cont \leftarrow Round\_integer(255 * (\frac{|I_{mean} - I_{Center}|}{I_{mean} + I_{Center}}))$

           $hist(cont) \leftarrow hist(cont)+1$

        End if

       EndFor *{This loop will apply for all RGB-L components (i.e. computed 4-times for each RGBL-values}*

Continued

{Calculate Mean of contrast of image edges}
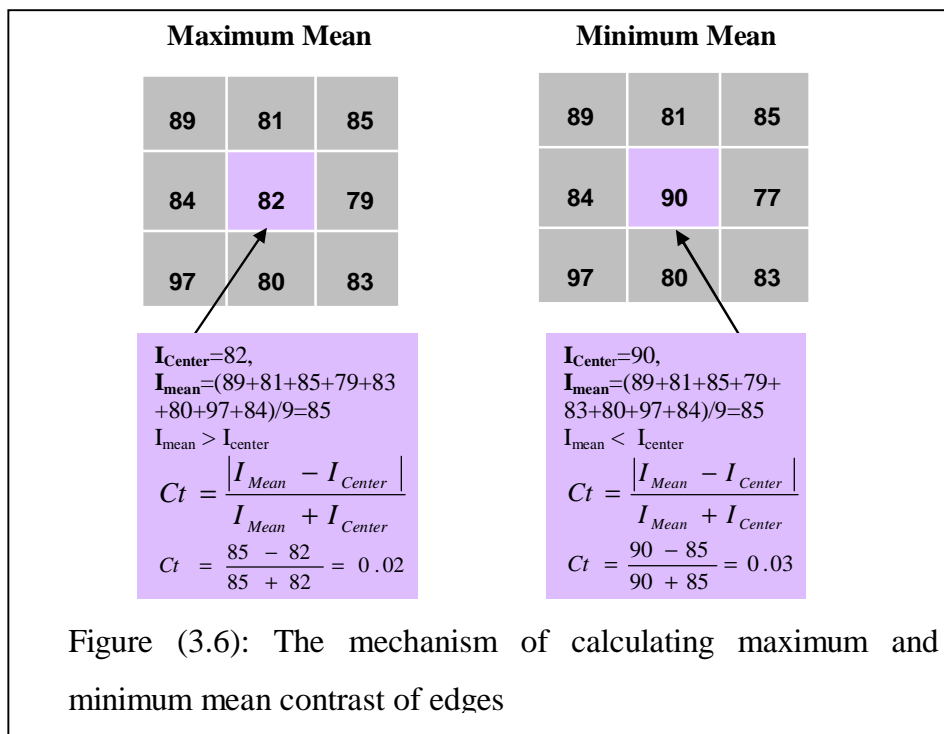
m←0

For k   {Where k=0..255}

　　　hist(k) ← hist(k) / n

　　　gl← k / 255

　　　m←m+gl*hist(k)

End For   *{This loop will apply for all RGB-L components}*

End Procedure

Figure (3.6) will show maximum mean contrast of edges and minimum mean contrast of edges with examples.

Maximum Mean　　　　**Minimum Mean**

89	81	85
84	82	79
97	80	83

89	81	85
84	90	77
97	80	83

I_{Center}=82,
I_{mean}=(89+81+85+79+83+80+97+84)/9=85
$I_{mean} > I_{center}$

$$Ct = \frac{\left| I_{Mean} - I_{Center} \right|}{I_{Mean} + I_{Center}}$$

$$Ct = \frac{85 - 82}{85 + 82} = 0.02$$

I_{Center}=90,
I_{mean}=(89+81+85+79+83+80+97+84)/9=85
$I_{mean} < I_{center}$

$$Ct = \frac{\left| I_{Mean} - I_{Center} \right|}{I_{Mean} + I_{Center}}$$

$$Ct = \frac{90 - 85}{90 + 85} = 0.03$$

Figure (3.6): The mechanism of calculating maximum and minimum mean contrast of edges

3.7.4 Horizontal and Vertical Contrast of Edges

This method is calculated according to the number of steps discussed in the following section. First, read the TV image then

apply Sobel filter to extract the edges. The following steps and pseudo code list (3.5) will illustrate the horizontal contrast of edges.

Step 1: Take 3×3 moved window around the pixel from the original image after checking if the pixel is an edge (255), else if it is (0) then move to the next pixel to check and so on.
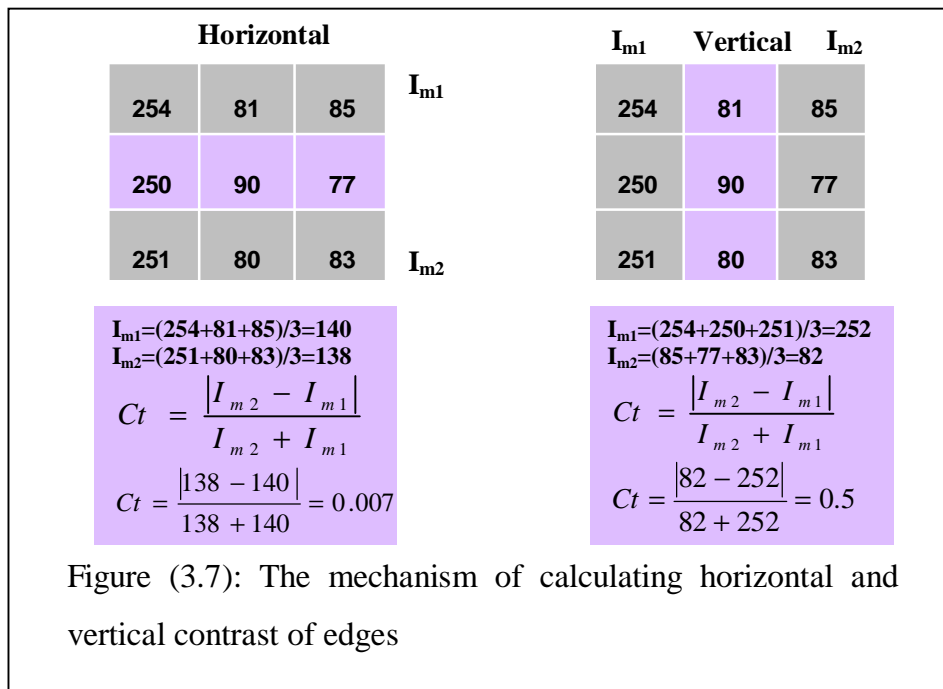
Step 2: Calculate the mean of each horizontal lines of the mask except the line that contains the center pixel, which the two mean lines will take respectively the variables name I_{m1}, and I_{m2}.

Step 3: Compute the contrast using the following equation:

$$Ct = \frac{|I_{m2} - I_{m1}|}{I_{m2} + I_{m1}} \qquad ...(3.8)$$

, and then calculate the histogram of the horizontal contrast of edges and the mean of the probability for all RGB-L component.

The determination of vertical contrast of edges has same steps mentioned in previous method except taking the mean of the vertical two lines of the mask window. Figure (3.7) illustrates the two methods with examples.

Horizontal			I_{m1} Vertical I_{m2}		
254	81	85	254	81	85
250	90	77	250	90	77
251	80	83	251	80	83

I_{m1}=(254+81+85)/3=140
I_{m2}=(251+80+83)/3=138

$$Ct = \frac{|I_{m2} - I_{m1}|}{I_{m2} + I_{m1}}$$

$$Ct = \frac{|138 - 140|}{138 + 140} = 0.007$$

I_{m1}=(254+250+251)/3=252
I_{m2}=(85+77+83)/3=82

$$Ct = \frac{|I_{m2} - I_{m1}|}{I_{m2} + I_{m1}}$$

$$Ct = \frac{|82 - 252|}{82 + 252} = 0.5$$

Figure (3.7): The mechanism of calculating horizontal and vertical contrast of edges

The following pseudo code list (3.7) shows the horizontal contrast of edges method.

Pseudo code list (3.7) Horizontal contrast of edges

Input

      img: Image array of RGB-L data.

{Where ih and iw are the height and the width of the image}

      Edge: Image array of edges of RGB-L data.

Output

      hist: Array of histogram of contrast of edges.

      m: Mean of probability of contrast of edges.

Variables

      I_{m1}, I_{m2}: mean of the two lines of the matrix.   cont: Contrast of edges.

Procedure

      n←0

      For i   *{Where i=2..ih-1}*

      i1←i-1, i2←i+1

        For j *{Where j=2..iw-1}*

        j1←j-1, j2←j+1

        If Edge(i,j)=255 then *{Check whether the pixel is an edge or not}*

    {Calculate the stretched contrast for RGBL values}

            I_{m1}←(img(i1,j1)+img(i1,j)+img(i1,j2))/3

            I_{m2}←(img(i2,j1)+img(i2,j)+img(i2,j2))/3

           $Cont = Round\_integer(255 * \frac{\mid I_{m2} - I_{m1} \mid}{I_{m2} + I_{m1}}))$

            hist(cont)=hist(cont)+1,   n←n+1

        End if

      End For j   End For i

   m←0

    For k   *{where k=0..255}*

      hist(k)←hist(k)/n

      gl←k/255

      m←m+gl*hist(k)

    End For   *{This method will apply for all RGB-L components}*

End Procedure

3.7.5 Main and Second Diagonal Contrast of Edges

This is the last suggested contrast method which also considered one of the main methods used in this study. Here is the explanation of the diagonal contrast of edges. Loading the image and determining the edges from it has done first. The following steps will illustrate the implementation process of the main diagonal of contrast of edges:

Step 1: Take 3×3 moved window around the pixel from the original image after checking if the pixel is an edge (255), else if it is (0) then move to the next pixel to check and so on.

Step 2: Calculate the mean of the pixel values over and under the diagonal of the mask and give those variables name I_{m1} and I_{m2} respectively.

Step 3: Calculate the contrast of edges according to equation (3.8) mentioned in the previous section, and then calculate the histogram of the main diagonal contrast of edges and the mean of the probability for all RGB-L component. Pseudo code list (3.8) illustrates the diagonal contrast of edges.

Pseudo code list (3.8) The Main Diagonal contrast of edges

Input

      img: Image array of RGB-L data.

{Where ih and iw are the height and the width of the image}

      Edge: Image array of edges of RGB-L data.

Output

      hist: Array of histogram of contrast of edges.

      m: Mean of probability of contrast of edges.

Variables

      I_{m1}, I_{m2}: mean of the two lines of the matrix.

      cont: Contrast of edges.

Continued

Procedure

    n ← 0

    For i   *{Where i=2..ih-1}*

    i1 ← i-1, i2 ← i+1

      For j   *{Where j=2..iw-1}*

      j1 ← j-1, j2 ← j+1

  {Check whether the pixel is an edge or not}

     If Edge (i,j)=255 then

        n ← n+1

        I_{m1} ← (img(i1,j)+img(i1,j2)+img(i,j2))/3

        I_{m2} ← (img(i,j1)+img(i2,j1)+img(i2,j))/3

    {Calculate the stretched contrast and the probability of contrast}

$$\text{Cont=Round\_integer}(255 * \frac{\left| I_{m2} - I_{m1} \right|}{I_{m2} + I_{m1}}))$$

        hist(cont)=hist(cont)+1

    End For

   End For

   m ← 0

   For k   *{where k=0..255}*

     hist(k) ← hist(k) / n

     gl ← k / 255

     m ← m+gl*hist(k)

  End For   *{This method will apply for all RGB-L components}*

End Procedure

The method of second diagonal contrast of edges implies some calculation steps as the main diagonal contrast of edges. This method is based on calculating the mean of the values over and under the second diagonal of the moved mask. Figure (3.8) illustrates the two methods with two examples one for each.

Main Diagonal   **Second diagonal**

89	81	85	I_{m1}
254	82	79	
250	253	83	

I_{m2}

I_{m1}	89	81	85
	254	90	79
	250	253	83

I_{m2}

$I_{m1}=(81+85+79)/3=82$
$I_{m2}=(254+250+253)/3=252$

$$Ct = \frac{|I_{m2} - I_{m1}|}{I_{m2} + I_{m1}}$$

$$Ct = \frac{|252 - 82|}{252 + 82} = 0.5$$

$I_{m1}=(81+89+254)/3 =141$
$I_{m2}=(79+83+253)/3 =138$

$$Ct = \frac{|I_{m2} - I_{m1}|}{I_{m2} + I_{m1}}$$

$$Ct = \frac{|138 - 141|}{138 + 141} = 0.01$$

Figure (3.8): The mechanism of calculating the main the second diagonal contrast of edges
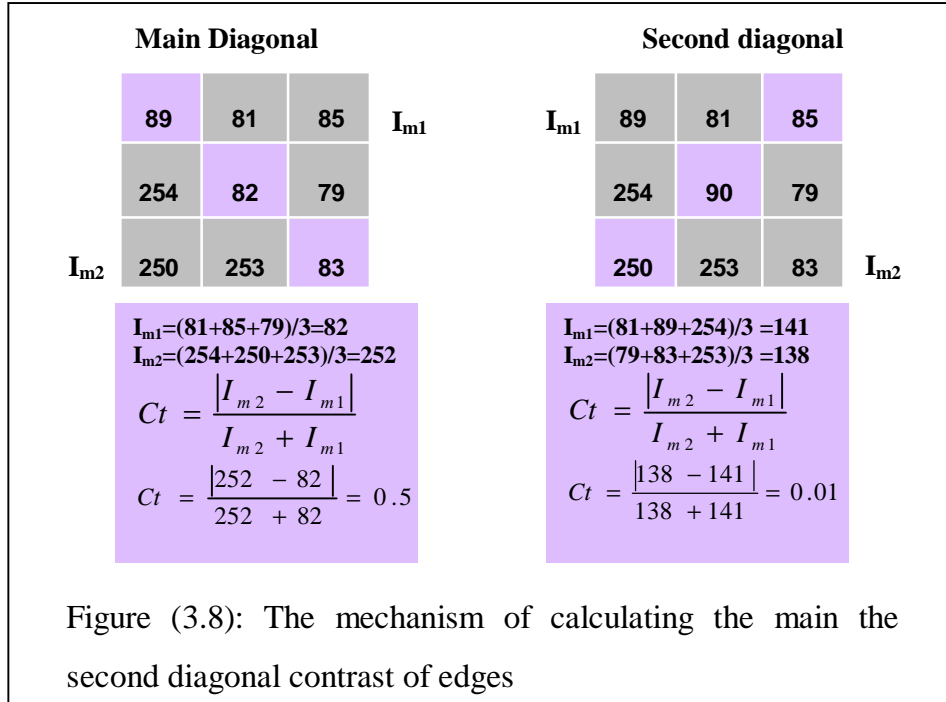
3.7.6 Contrast Assessment Using Statistical Image Measures

In this method the statistical measures of the image edges have been used to determine the contrast. The mean (μ) and the standard deviation (σ) of the image edges were calculated to evaluate the contrast. In the previous techniques of the contrast, it has been determined the contrast by using only two pixels of the image edge mask window which are I_{min} and I_{max}. In this method all the edge pixels of the image will be taken in the consideration of contrast evaluation. Equation (2.14) is applied after computing both I_{min} and I_{max} according to the following equations to produce equation (3.11):

$$I_{max} = \mu + \sigma \qquad\qquad\qquad\qquad\qquad \dots (3.9)$$

$$I_{min} = \mu - \sigma \qquad\qquad\qquad\qquad\qquad \dots (3.10)$$

This method is applied after extracting the edges of the image by using sobel filter. This method is illustrated in the following steps:

Step 1: After determining the edges of the image using sobel filter, then calculate the (μ) and the (σ) of the image.

Step 2: Open two loops to trace all the points of the image of the edges.

Step 3: Check if the pixel of the image edges whether is an edge (255) or not (0). If it is an edge then go to step 4, otherwise go to step 3 to shift to the next pixel.

Step 4: Calculate the (μ) and the (σ) for the edges pixels by taking their values from the image before the edge extraction process applied on it.

Step 5: After the end of the two loops that used to trace the image edges, calculate the contrast according to the equation bellow:

$$Ct_{\frac{\sigma}{\mu}} = \frac{\sigma}{\mu} \qquad\qquad \dots (3.11)$$

This method was applied on all RGB-L components of the image. Pseudo code (3.9) illustrates the implementation steps to perform this method. The input is the colored TV-Satellite image, which read from a Bmp file as an RGBL array of records. Each record consists of RGB-L component, the output is the value of the computed contrast for all RGB-L component.

Pseudo code list (3.9) The Contrast Using Statistical Measures

Input

      img: Image array of RGB-L data.

{Where ih and iw are the height and the width of the image}

      Edge: Image array of edges of RGB-L data.

Output

      Cont: Contrast of Image Edges.

Variables

      m: Mean of Image Edges.

      s: Standard deviation of the image edges.

      ne: Number of edges in the image.

Continued

Procedure

m←0,   s←0, ne←0

For i   *{Where i=2..ih-1}*

  For j *{Where j=2..iw-1}*

  If Edge (i,j)=255 then   *{Check whether the pixel is an edge or not}*

  {Calculate the Mean and the Standard deviation of the image edges}

        m←m + img (i,j)

        s←s + img (i,j) ^ 2

        ne←ne + 1

     end if

  end for i   end for j

  m←m / ne

  s← $\sqrt{\dfrac{s}{ne} - m^2}$

  cont = s / m

End Procedure   *{This method will apply for all RGB-L components}*

3.8 Similarity Measures

Similarity measures methods is used in simple or complicated different fields of digital image, starting from a simple comparison between two pixels to the most complicated ones that are used to determine how two events are similar or correlated. There are different methods to measure the similarity; one of them is used in this study, which is the correlation among the pixels of the selected homogenous region of TV-Satellite images.

The correlation method in this research based on using equation (2.15), which is, applied on regions of the TV images. These regions are homogenous regions selected from the image (automatically or manually). The mechanism of this method is to find how much the

selected block and the next adjacent block by one pixel is correlated. In the next sections, the methods of the correlation that used to determine the quality of the image will be explained.

3.8.1 The Correlation of the Manual Selected Regions

The correlation method was applied on the selected homogeneous regions of the image. The selection was made manually. The correlation method has been calculated using a single image and a single video clip which are the same image and same clip on three satellites. The figure (3.9) illustrates the correlation method after selecting (manually) homogenous regions from the image. The figure shows determining the correlation between the selected block (B1) and the block next to it (B2) shifted to the right direction by only one pixel (t=1).

Figure (3.9): The correlation method of the selected region
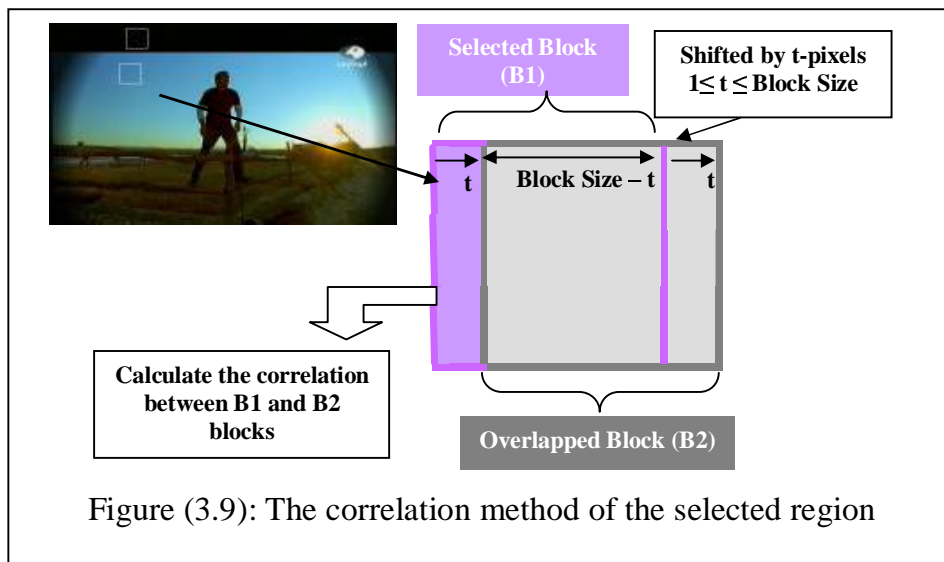
a) Single Image Correlation

After loading the image the following steps will applied on it to determine the correlation for each RGBL values:

Step 1: Select a homogenous region of size 40×40.

Step 2: Calculate the mean for RGBL components of the selected block (B1) and the overlapped block (B2) which shifted by one (t=1) pixel, where (B1) and (B2) have the same size.

Step 3: Calculate the correlation for each RGB and L between the two blocks according to the equation (2.15). Pseudo code list (3.9) will shows the method of correlation.

Pseudo code list (3.9) Image Correlation

Input

  img: Image array of RGB-L data.

{Where Ih and Iw are the height and the width of the image}

  Sblock: Selected block size.

  Nblock: Number of selected blocks.

  x1,y1: Block starting points.

Output

  cor: Correlation between the Two Blocks.

Variables

  m_1,m_2: mean of the two blocks.

  std, sm: the variance and the standard derivation of the selected block.

  cor_1,cor_2,cor_3,cor: Correlation variables.

Procedure

  $x_2 \leftarrow x_1+(\text{Sblock}-1)$

  $y_2 \leftarrow y_1+(\text{Sblock}-1)$

  $m_1 \leftarrow 0$, $m_2 \leftarrow 0$, $n \leftarrow (\text{Sblock}*\text{Sblock})$

  For i, j   *{where i=(y1+1)..y2, j=(x1+1)..x2}*

 {Calculate the Mean and STD for all RGB bands and L component}

    $m_1 \leftarrow m_1+\text{img}(i,j)$

    $m_2 \leftarrow m_2+\text{img}(i,j+1)$

    $sm \leftarrow sm+(\text{img}(i,j))$ ^ 2

   End For j, i

   $m_1 \leftarrow m_1/n$

   $m_2 \leftarrow m_2/n$

   $std \leftarrow ((sm/n)-(m_1)^2)$ ^ 0.5

Continued

$cor_1 \leftarrow 0$, $cor_2 \leftarrow 0$, $cor_3 \leftarrow 0$

For i,j   *{where i=(y1+1)..y2,   j=(x1+1)..x2}*

{Calculate the correlation for each RGB bands and L component}

    If   std>=0 and std<=h then   cor $\leftarrow$ 1

   Else

    $cor_1 \leftarrow cor_1 + (img(i,j)-m1)*(img(i,j+1)-m2)$

    $cor_2 \leftarrow cor_2 + (img(i,j)-m1)\wedge 2$

    $cor_3 \leftarrow cor_3 + (img(i,j+1)-m2)\wedge 2$

   End if

  End For

  If cor=1 then Print cor

   Else If cor_1=0 and cor_2=0 and cor_3=0 then   cor $\leftarrow$ 1

    Else if cor_2=0 or cor_3=0 then   cor $\leftarrow$ 0

    Else   cor $\leftarrow$ Abs$\left(\dfrac{cor_1}{\sqrt{(cor_2 * cor_3)}}\right)$

   End If

End Procedure

---

b) Scene Correlation

Instead of applying the correlation method mentioned in the previous section on a single image, this method is applied on a scene (same scene) extracted from three satellites videos. This scene consists of six frames. From each frame more than one homogenous region will be selected manually. The selected regions should be of the same location in all the frames of the video, in order to find how much the frames of the video is correlated over the time.

3.8.2 The Correlation of the Automatic Selected Regions

Selecting the region automatically based on searching for the region that has minimum standard deviation (σ_{Min}), because the region

with less σ value considered to be homogenous and has no edges. This process is applied only on the L component, and it is accomplished in five steps.

Step 1: Input the size of the sliding window, the proposed size in this method is 30×30 from the loaded image.

Step 2: Calculate the σ of the sliding window.

Step 3: Check if the σ has the minimum value, if it is so save the values of the σ and the starting points of the blocks in the parameters and go to the next block, which is away from the previous block about four pixels, else take the next block to calculate the σ, and so on until we find the last minimum value of σ for L component.

Step 4: After finding σ_{Min} of L of the block, as mentioned in the previous step the σ_{Min} value and the starting points of the block (x,y) have saved, that can be later used to calculate the correlation, and that illustrated in pseudo code list (3.10).

Step 5: Calculate the correlation of the found block according to the pseudo code list (3.9) illustrated previously for all RGBL components.

Pseudo code list (3.10) describes the method of searching for the block σ_{Min}, where step 5 is illustrated in pseudo code list (3.9).

Pseudo code list (3.10) Image Correlation of automatic selection

Input

   img: Image array of RGB-L data.

{Where Ih and Iw are the height and the width of the image}

   Sblock: Selected block size.

Output

   Cor: Correlation between the two blocks.

Variables

   Ss, std1: Standard derivation.

   m1: mean of the moved window.

Procedure

   Std1 ←— 10000   *{Initial value for comparison}*

Continued

Bsz1 ← bsz-1,   n ← (bsz*bsz)

For i   Step 4   *{Where i=1..ih}*

        i1 ← i+bsz1

For j   Step4   *{Where j=1..iw}*

        j1 ← j+bsz1

        m1 ← 0,   Sm1 ← 0

        if i1 > ih then exit for

        if j1 > iw then exit for

    For ii, jj   *{Where ii=i..i1,   jj=j..j1}*

          m1 ← m1+img(ii, jj)

          sm1 ← sm1+(img(ii, jj)^2)

    end for jj, ii

        m1 ← m1/n

        ss1 ← $\sqrt{\left(\dfrac{sm_1}{n}\right) - m_1{}^2}$

        If ss1 <= std1 then

          Std1 ← ss1,   x ← ii – bsz,   y ← jj – bsz

        end if

   end for j, i {*After finding the minimum (std) block then apply pseudo code list (3.9) to determine the correlation for the block and the block next to it}*

End Procedure

3.8.3 Maximum and Minimum Correlation

The block proposed in this method is (40×40) elements in size; the way of selecting the block is quite different in comparison with the other methods. The method performed to find the blocks that have the maximum (or the minimum) correlation of L component in the image. The steps of calculating this correlation are listed below in pseudo code list (3.11) and they are:

Step 1: Take a moved mask of size (40×40) sliding over the image plane.

Step 2: Calculate the correlation of the sliding block.

Step 3: Check each block of the image to find the maximum correlation value of the L component.

Step 4: After finding the block that has the maximum correlation value, the starting point of the block will be saved to be used later in step 5.

Step 5: Calculate the correlation of the found block that has the maximum correlation of L for all RGB bands and L component.

Pseudo code list (3.11) Maximum Image Correlation

Input

  img: Image array of RGB-L data.

{Where Ih and Iw are the height and the width of the image}

  Sblock: Selected block size.

Output

  Cor: Correlation between the two blocks.

Variables

  m_1, m_2: mean of the two blocks.

  Cor_1, Cor_2, Cor_3, Cor: Correlation variables.

Procedure

  Max1 ⟵ 0, Bsz1⟵bsz-1, n⟵(bsz*bsz)

  For i step bsz *{where i=1..ih-1}*

  i1⟵i+bsz1

  For j step bsz *{where j=1..iw-1}*

   j1⟵j+bsz1

   m_1⟵0, m_2⟵0, sm1⟵0

   For ii, jj *{where ii=i..i1, jj=j..j1}*

    m_1⟵m_1+img(i,j)

    m_2⟵m_2+img(i,j+1)

    sm_1⟵sm_1+img(i,j) ^ 2

   End For ii, jj

  m1⟵m1/n

  m2⟵m2/n

68

Continued

std $\leftarrow$ ($(sm_1/n) - (m_1$ ^ 2)) ^ 0.5

$cor_1 \leftarrow$ 0, $cor_2 \leftarrow$ 0, $cor_3 \leftarrow$ 0

For i,j

{Calculate the correlation for all RGBL values}

If std>=0 and std <=h then cor $\leftarrow$ 1

Else

$cor_1 \leftarrow cor_1 + (img(i,j)-m_1)*(img(i,j+1)-m_2)$

$cor_2 \leftarrow cor_2 + (img(i,j)-m_1)$^2

$cor_3 \leftarrow cor_3 + (img(i,j+1)-m_2)$^2

End if

End For j, i

If cor=1 then goto *the step of determining the max. correlation*

ElseIf cor1=0 and cor_2=0 and cor_3=0 then cor $\leftarrow$ 1

Else if cor_2=0 or cor_3=0 then cor $\leftarrow$ 1

Else   cor $\leftarrow$ Abs($\dfrac{cor_1}{\sqrt{cor_2 * cor_3}}$)

End If

If cor >= max_1 then

$max_1 \leftarrow$ cor

x $\leftarrow$ ii $-$ bsz *{saving the starting top left point of the found block}*

y $\leftarrow$ jj $-$ bsz

End if

End For j, i   *{Then calculate the correlation for all RGB-L as mentioned in pseudo code list (3.9)}*

End Procedure

The minimum correlation works the same as the maximum correlation, but instead of searching for the block that has maximum correlation, the search will be base on searching block that has the minimum correlation of L of the image. After finding the minimum correlation block, the correlation method for all RGBL components will be calculated.

Chapter Four
Results and Discussions

Chapter Four
Results and Discussions

4.1 Introduction

In this study determining the quality of the image depends on measuring the contrast of image edges and the correlation of the homogeneous regions. The highly contrast of image edges and the highly correlated homogeneous regions give an image with a good quality. This chapter shows and discusses the results of the acquired TV satellite images. These results performed for various techniques included the statistical image analysis, the contrast based on edges, and the correlation of homogeneous regions. The TV-Satellite images are acquired from the (Abu Dhabi) channel broadcasted on three satellites (Arabsat, Hotbird, and Nilesat).

The image edges have been determined using Sobel edge detector for RGBL components of different threshold values (30, 50 and 70). Different contrast approaches applied on the image edges for RGBL components depending on using a Michelson contrast equation, these contrast methods are illustrated as follows:

- Maximum Contrast of Edges (Ct_{Max}).

- Minimum Contrast of Edges (Ct_{Min}).

- Maximum Mean Contrast of Edges ($Ct_{MaxMean}$).

- Minimum Mean Contrast of Edges ($Ct_{MinMean}$).

- Horizontal Contrast of Edges (Ct_H)

- Vertical Contrast of Edges (Ct_V).

- Main Diagonal Contrast of Edges (Ct_{D1}).

- Second Diagonal Contrast of Edges (Ct_{D2}).

The second image quality measure used in this study is the correlation method, this method is calculated for the homogeneous regions of the image of RGBL component, and this evaluation is performed as follows:

- Calculate the correlation for different homogeneous regions selected (manually and automatically) for the same image on three satellites and make a comparison among them to evaluate the results.

- Calculate the maximum and the minimum correlation for different homogeneous regions selected (automatically) of the same image on three satellites and make a comparison among them to evaluate the results.

- Calculate the correlation for different homogeneous regions selected (manually) of the same scene which consists of six images on three satellites and make a comparison among them to evaluate the results.

4.2 The Considered Images Used in This Study

This study has considered different TV satellite images of Abu Dhabi-channel that broadcasted through three commercial satellites (Arabsat, Hotbird, and Nilesat). Table (4.1) lists the characteristics of Abu Dhabi channel on the three mentioned satellites, and table (4.2) lists the properties for each of these images after saving them as a Bmp type.

Table (4.1): The characteristics of the (Abu Dhabi) channel			
Satellite	**Arabsat**	**Hotbird**	**Nilesat**
Frequency	11804 GHz	12380 GHz	11747 GHz
Symbol Rate	27500	27500	27500
Polarization	Horizontal	Vertical	Vertical

Table (4.2): The captured image properties	
Type of the Image	**Bmp Image**
Image Size	**740 kB**
Image Width	**640 Pixels**
Image Height	**395 Pixels**
Horizontal Resolution	**96 dpi**
Vertical Resolution	**96 dpi**
Bit depth	**24**

These images are divided into groups, these groups are:

1. People image, which illustrated in figure (4.1). Where this image has been taken after the moment of the changing the scene and starting another scene on the same video clip of each satellite. So the number of the images is(3 images); one for each satellite.

2. Twilight images, which shown in figure (4.2), where this image has been taken after the moment of the changing the scene and starting another scene on the same video of each satellite. And the number of the images is (3 images); one for each satellite.

3. The scene of the man standing next to the white horse, shown in figure (4.3), this scene has been taken after the moment of the changing scene. This scene consists of (6 images) for each satellite. So, there will be (18 images); one for each satellites.

The total number of the considered images in this study is about (24 images).

Arabsat   Hotbird

Nilesat

Figure (4.1): The images on the three satellites used in edge detection

Arabsat   Hotbird

Nilesat

Figure (4.2): The images from the three satellites broadcasts used in image correlation

Arabsat

Hotbird

Nilesat

Figure (4.3): The first and last frames from the three scenes extracted from the three satellites broadcast

4.3 Image Contrast Results

Sobel edge detector has been used first to extract the TV-satellite image edges, then different suggested contrast approaches have been applied on the images edges to estimate their quality. The results of these methods will be evaluated in this section.

Figure (4.1) shows the considered TV-Satellite images that have been taken from Abu Dhabi channel on three satellites (Arabsat, Hotbird, and Nilesat). To be certain that the tested images are the same images on

three satellites belong to same channel, is the first image at the moment of transition from scene to another; that means the moment of ending scene and staring the next scene of the video clip. As had mentioned earlier Sobel filter applied on the image by different threshold values. Figures [from (4.4) to (4.33)] show the histograms of computed contrast for different Sobel edge detector threshold values (30, 50 and 70).

Threshold value 30 has considered to be the best value to determine the edges from the image, because as the threshold value increases, the image edges decreases. The histograms [from(4.4) to (4.33)] will be illustrated as follows:

4.3.1 Histograms of Edges

Figure (4.4) presents the histogram of image edges for three RGB-L component respectively for three satellites (Arabsat, Hotbird, and Nilesat). The x-axis presents the RGB-L component which scaled (from 0 to 255). The y-axis presents the histogram of image edge points. This method is illustrated in section (3.4) in both pseudo code lists (3.1) and (3.2) of chapter three. The corresponding figure illustrates the histograms of image edges for all RGB-L components that show the distribution of the edge points of the image from the low intensity areas (0) to the high intensity ones (255). The histograms consist of different intensity areas and that obvious for all RGB-L components, and seemed approximately similar for all images on Arabsat, Hotird and Nilesat. It has been found that as the threshold value increases, the differentiation of the histograms peaks decreases. The shape of them became more flatted and had less clear peaks, and extended from the dark areas (less intensity) to the bright ones (high intensity) especially in the high threshold values. The mean of image edges illustrated on the figures (4.4), (4.14) and (4.24) increased as the threshold increased, where most weak edges of the image are in the

bright areas (high intensity) which are omitted during the increment of the threshold values. Due to the increment of the threshold values the number of image edges will decrease cause mean of image edges to increase. The indicated histograms show that the image on the Nilesat has the highest amount of edges, then Arabsat comes second and Hotbird comes last.

4.3.2 Image Contrast Based on Edges

Figure (4.5) presents the histograms of contrast of image edges for RGB-L component for the satellites (Arabsat, Hotbird, and Nilesat). The x-axis shows the contrast values that scaled (from 0 (low contrast value) to 1 (high contrast value)). The y-axis shows the probability of contrast of image edges. The contrast is calculated according to the Michelson equation (3.1) discussed in section (3.5.1) in pseudo code (3.3). The contrast is calculated for the image edges, whereas the edges is considered one of the most important features of the image because it contains high details that isolate the object from the background in the image. However, as the edges have high contrast, the image has a good quality. The histograms in figure (4.5) illustrate the distribution of the contrast of image edges values for all RGB-L component. It had been found that the indicated histograms contained low probability of contrast values in the low contrast area (where Ct=0..0.2) and high probability of contrast values in the high contrast areas (where Ct=1) which take vertical line shape. The middle areas of the histograms were flatted with small peaks which indicated for different edge values in the image. As the threshold value increases, the shape of the histograms curves start to expand to the high values of the contrast and the peaks start to get smaller in the low contrast area of the histograms. In the middle areas of the histograms the curves got extended, with obvious increment of

probability of contrast of edges at Ct=1 taking vertical line shape. The mean of contrast of edges increases as the threshold value decreases. This method indicated that the Nilesat has the best contrast of image edges; Arabsat comes in the second place while Hotbird comes last.

4.3.3 Maximum and Minimum Contrast of Edges (Ct_{Max}, Ct_{Min})

Figure (4.6) and (4.7) present the Ct_{Max} and Ct_{Min} of edges for the RGB-bands and L component of the satellites (Arabsat, Hotbird, and Nilesat). Ct_{Max} and Ct_{Min} are illustrated in section (3.5.2) in the pseudo code list (3.4). The figure (4.6) illustrates the distribution of Ct_{Max} values for the RGB-L components, the histograms in this figure contain high probability of contrast values in the low contrast areas and medium probability of contrast values in the high contrast area when Ct=1 for RGB bands only, while the histograms of L contain low probability of contrast value when Ct=1. The histograms become more flatted with low peaks for all RGB-L components when the threshold value increases.

In figure (4.7) the histograms indicate that the Ct_{Min} method gave contrast results higher than the results in the previous method for all RGB-L components, because the contrast value in the low intensity values of the image more than the intensity values in the high intensity ones. The shapes of the histograms of the Ct_{Min} are similar to the previous method except they have higher contrast of image edges values. The histograms show high probability of contrast values in the low contrast area and high probability of contrast values when Ct=1 which presented as a vertical line shape. For both methods, as the threshold value increases the histograms become more flatted and extended from the low to the high contrast areas. The mean of contrast of edges for the two methods will increase when the threshold value increases because of the

increment of number of image edges. According to the mean of contrast of edges for the both methods, it has been found that the contrast of edges for the images on the Nilesat is better than Arabsat and Hotbrid.

4.3.4 Maximum and Minimum Mean Contrast of Edges ($Ct_{MaxMean}$, $Ct_{MinMean}$)

The histograms presented in figures (4.8) and (4.9) belong to the $Ct_{MaxMean}$ and $Ct_{MinMean}$ methods, where mentioned in section (3.5.3). The histograms for both methods show high probability of contrast values in the low contrast area while the middle area of the histograms extended and flatted with low probability of contrast values that reach to zero in some places. The probability of contrast values start to increase for RGB bands as shown in figure (4.8), taking the vertical line shape in the high contrast area (Ct=1). The mean of contrast of edges for the both methods indicates that the image on the Nilesat has the best contrast values, Arabsat has the second place, while Hotbird comes last.

4.3.5 Horizontal and Vertical Contrast of Edges (Ct_H, Ct_V)

According to the obtained results shown in the figures (4.10) and (4.11), it has been found that Ct_V method gave higher contrast of edges values than Ct_H method, that because the vertical edges of the image have high contrast than the horizontal edges for all RGB-L components for Arabsat, Hotbird and Nilesat. Ct_H histograms in figure (4.11) have high probability of contrast values in low contrast area with low increment of probability of contrast value when Ct=1, while Ct_V histograms show higher increment in probability of contrast values when Ct=1 more than Ct_H histograms, which taking the vertical line shape. The mean of

contrast of edges for the both methods indicates that the image on the Nilesat has the best contrast values, Arabsat has the second place, while Hotbird comes last.

4.3.6 Main and Second Diagonal of Edges (Ct_{D1}, Ct_{D2})

Figures (4.12) and (4.13) present the histograms Ct_{D1} and Ct_{D2} of the image edges for the RGBL components of the satellites (Arabsat, Hotbird, and Nilesat); they discussed in section (3.5.5). The shapes of the histograms of the two figures are almost same and the mean of contrast almost equal. The histograms indicated that the Nilesat also has the best contrast than Arabsat and Hotbird.

4.3.7 The Contrast Using Statistical Image Measures

After the implementation of this method, it has been found that the contrast of image edges values decreases when the threshold value increases and that illustrated in the tables (4.3), (4.4), (4.5). The threshold value (30) showed the best contrast of edges values in all three satellites and for all RGB-L component. As illustrated in the three mentioned tables, the results of this method especially threshold (30) indicated that the image on Nilesat gave high contrast of edges values more than those on Arabsat and Hotbird for all RGB-L component.

From the above discussions we can conclude that the Nilesat has the best contrast value by using different approaches to determine the contrast, then Arabsat comes on the second place and Hotbird comes last.

Threshold=30

Arabsat
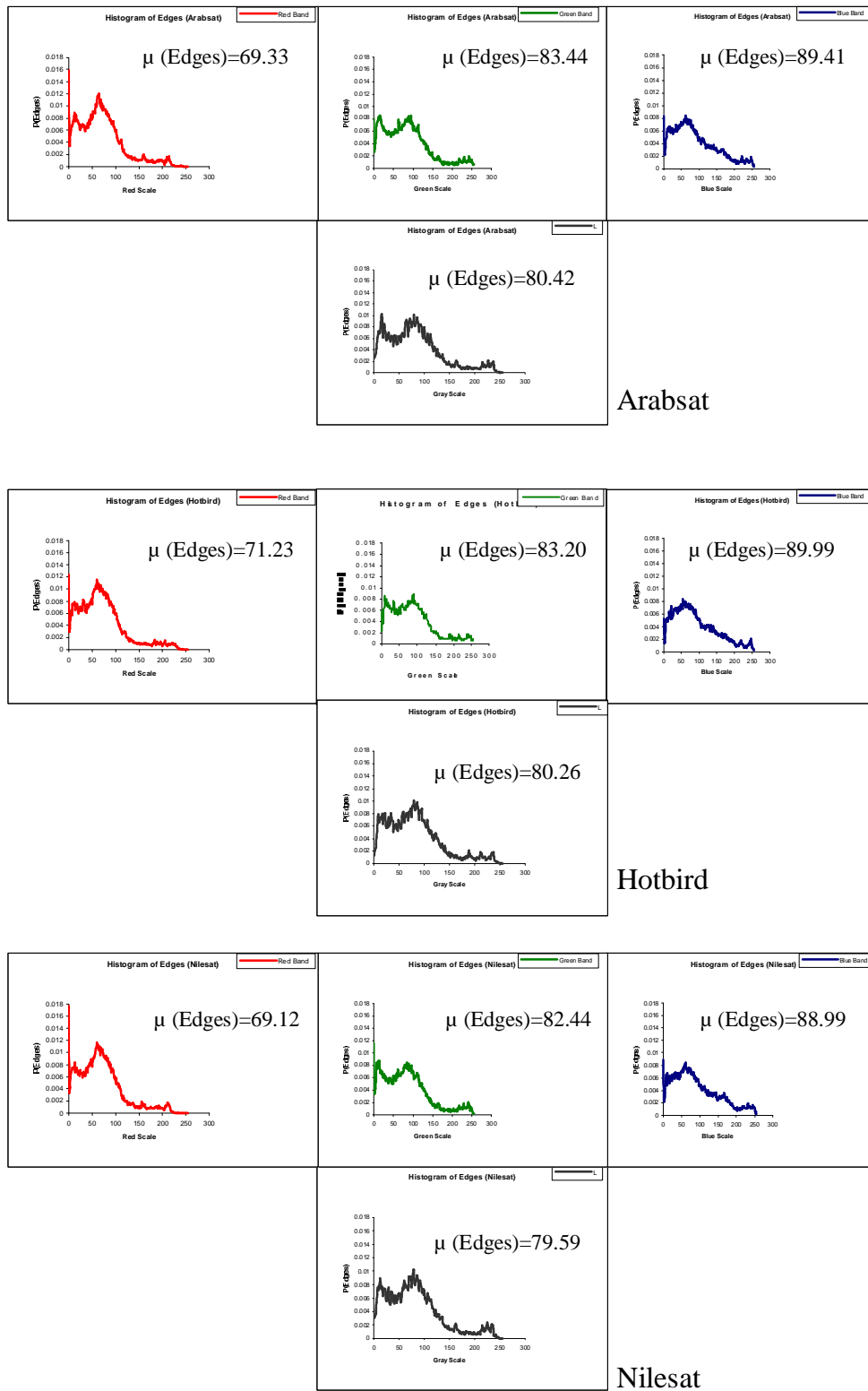
Hotbird

Nilesat

Figure (4.4): The histogram of image edges for RGBL components using threshold=30 for (Arabsat, Hotbird and Nilesat)

Arabsat
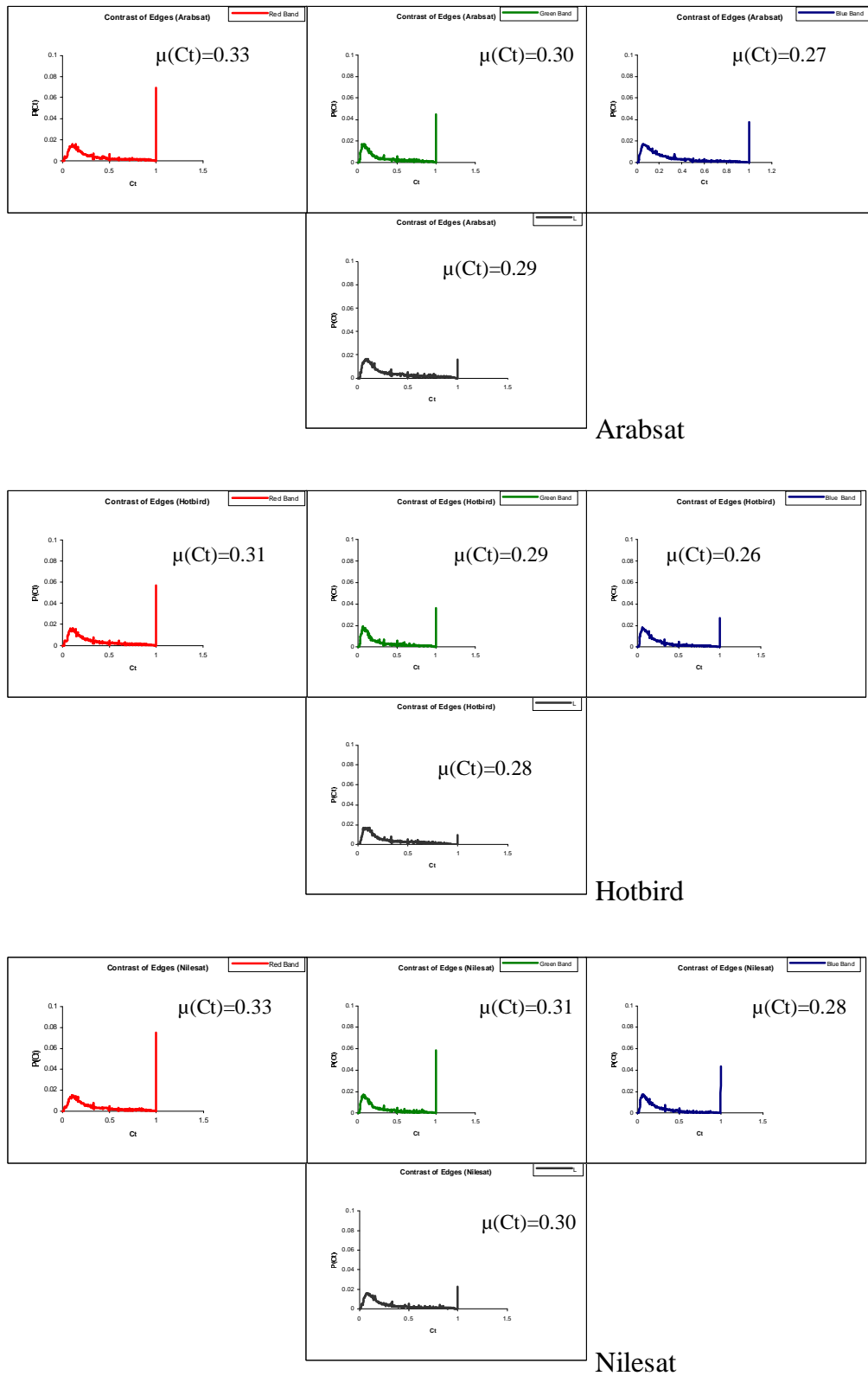
Hotbird

Nilesat

Figure (4.5): Contrast of image edges for RGBL components by using threshold=30 for (Arabsat, Hotbird and Nilesat)

Arabsat
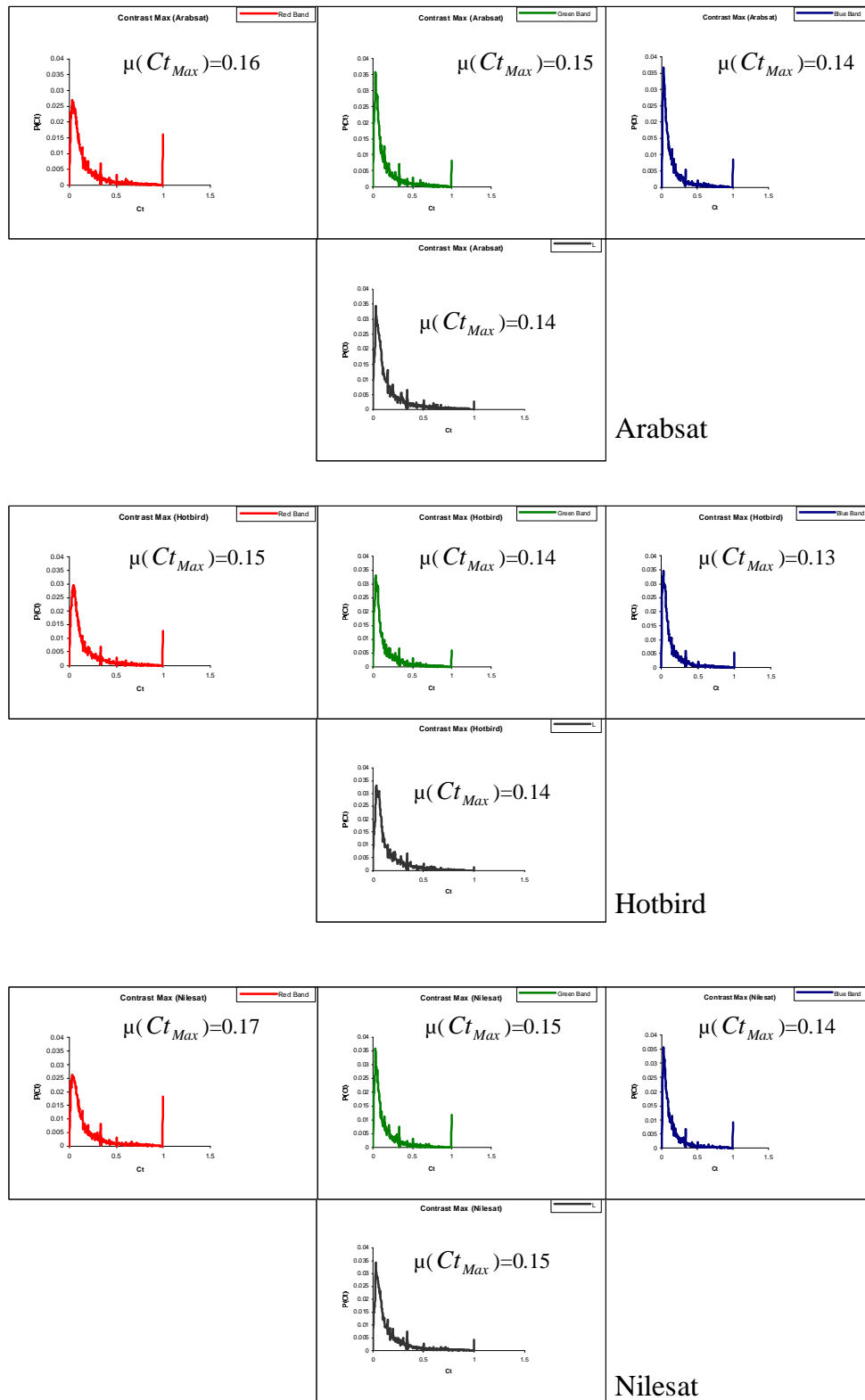
Hotbird

Nilesat

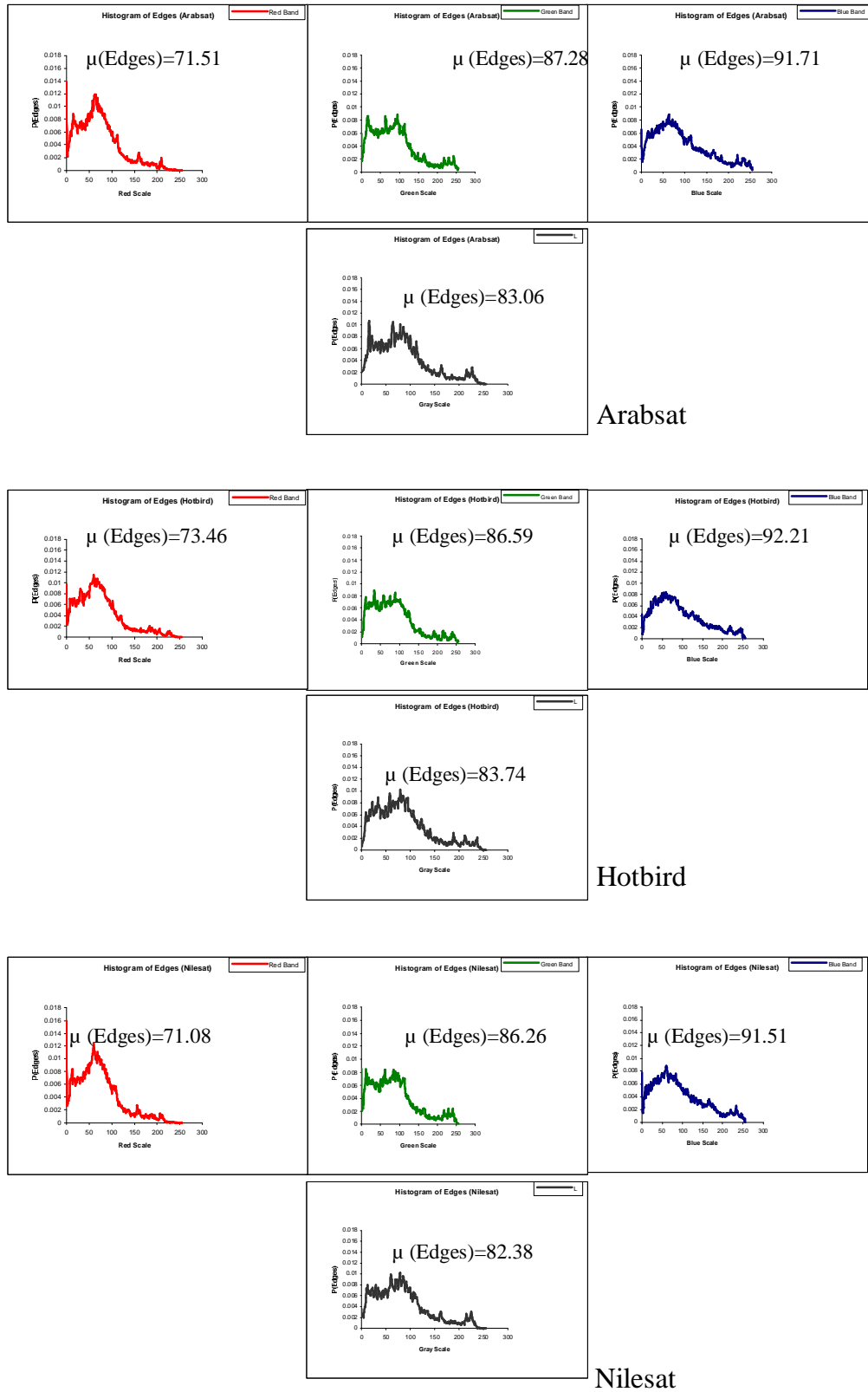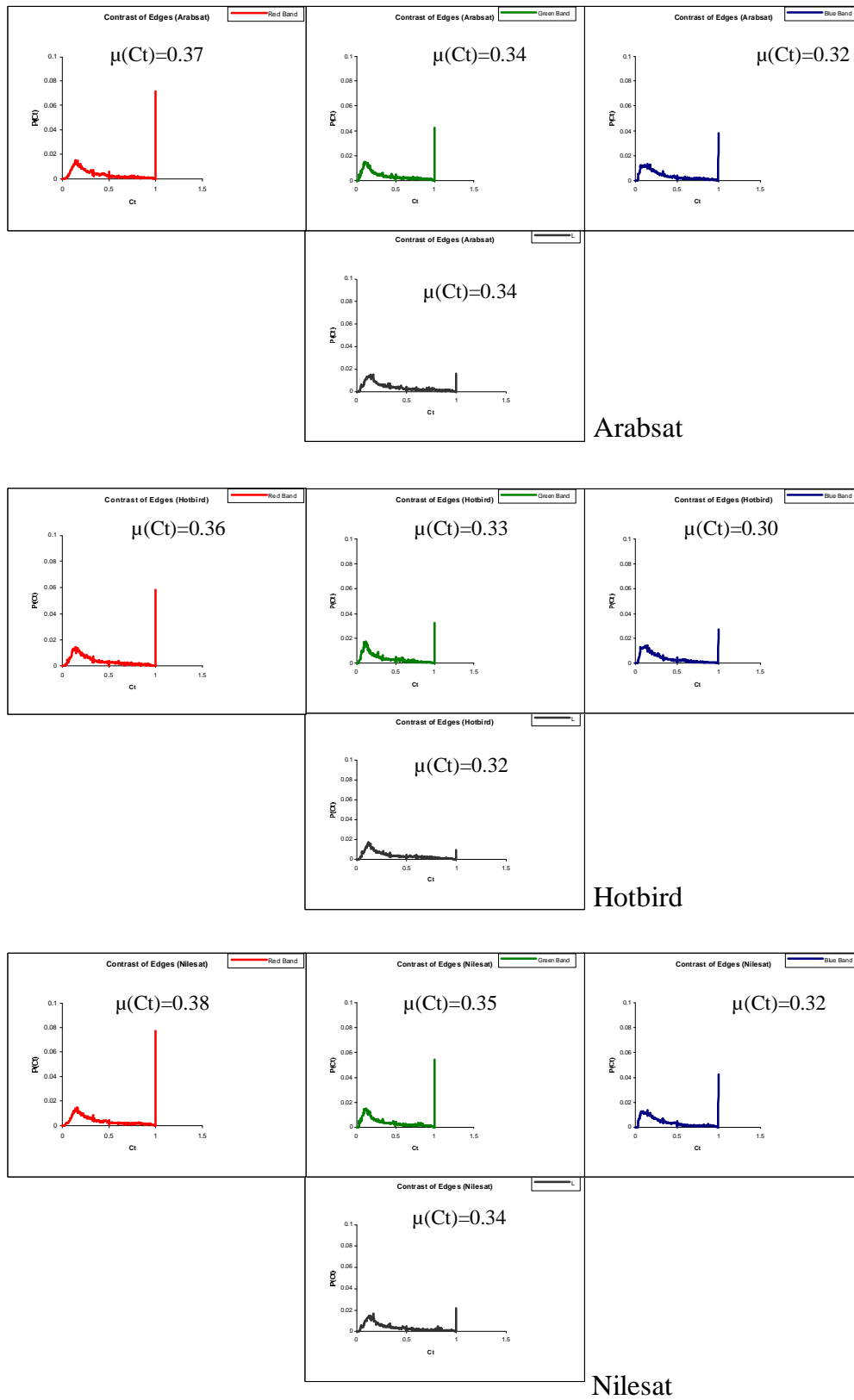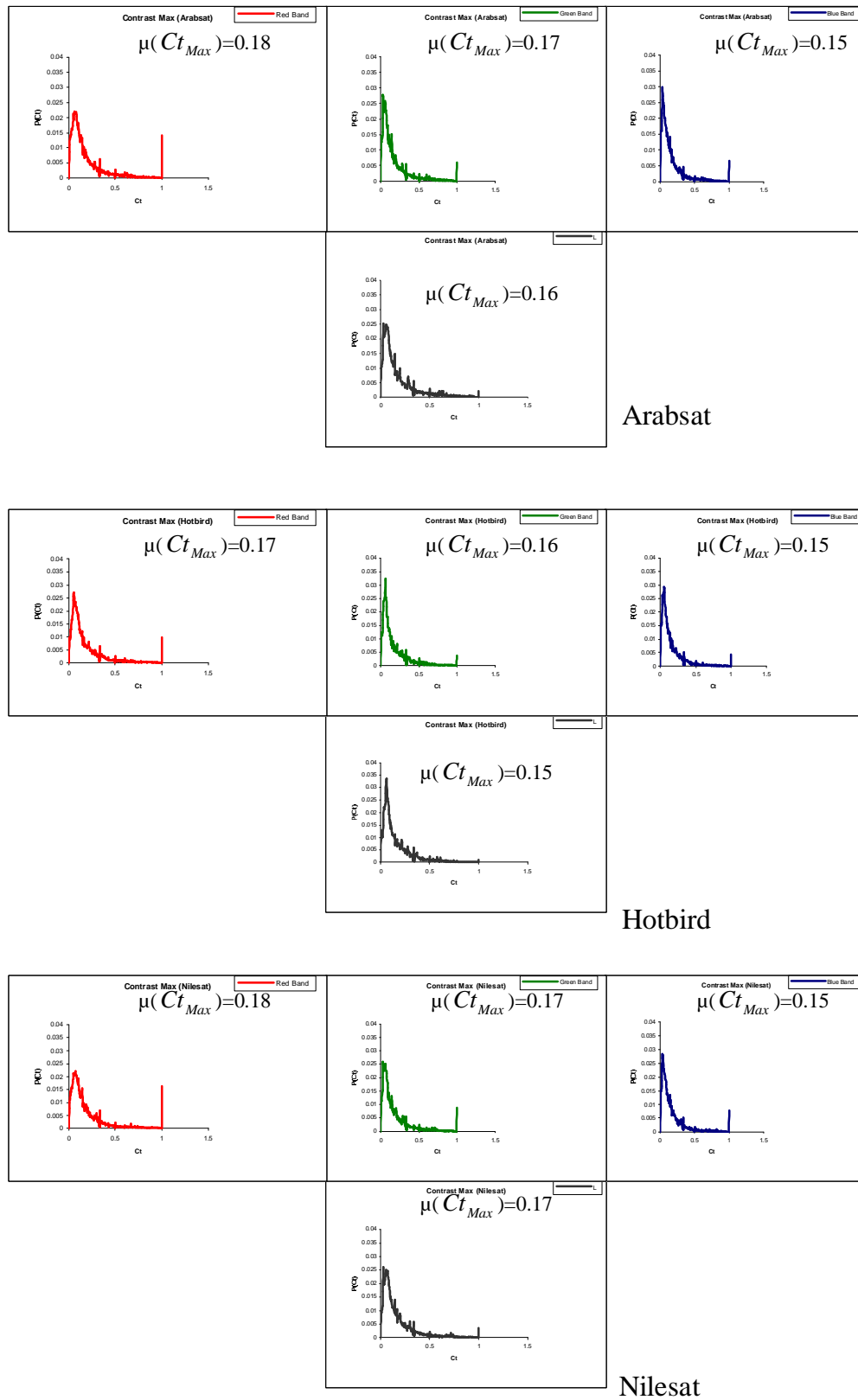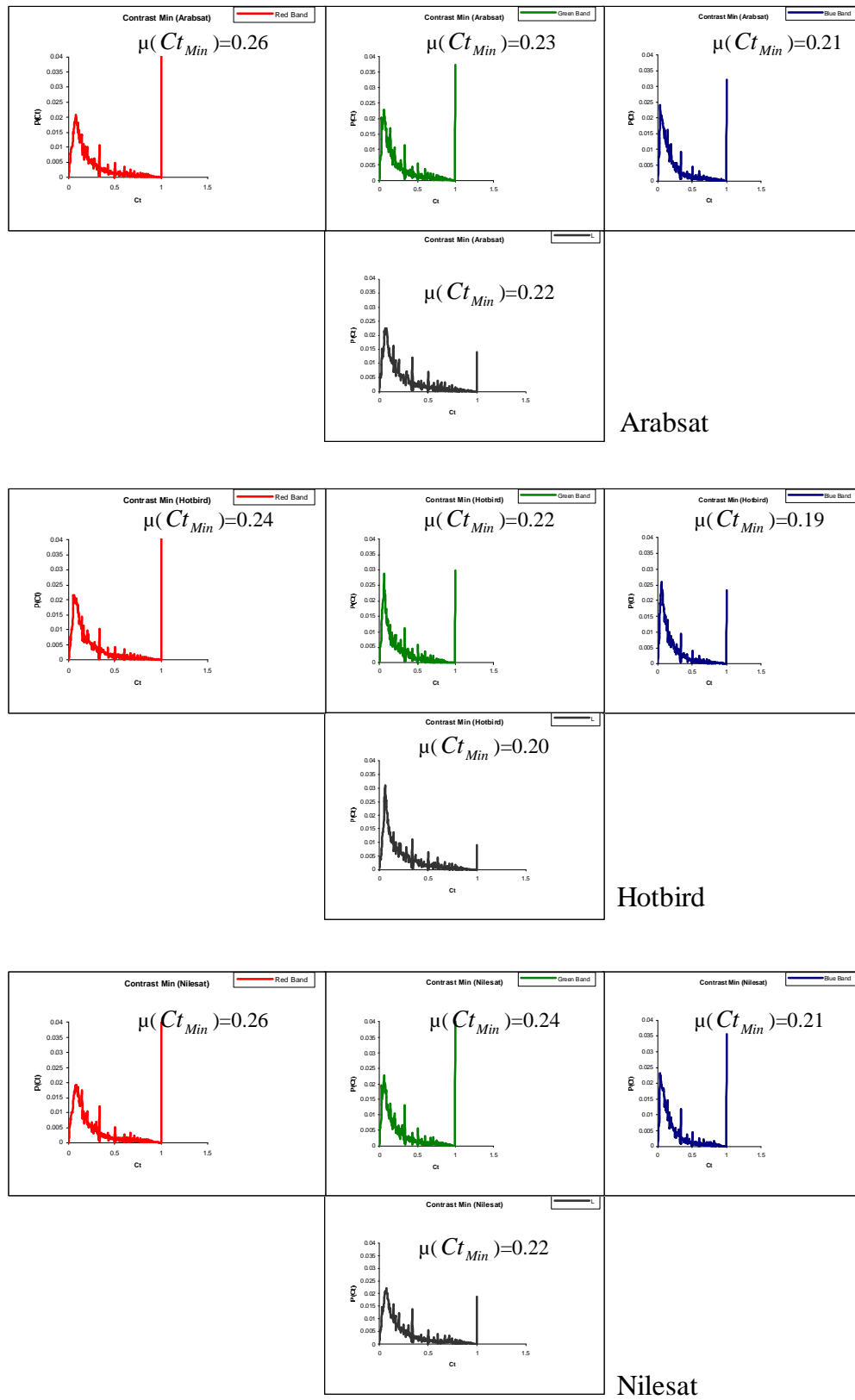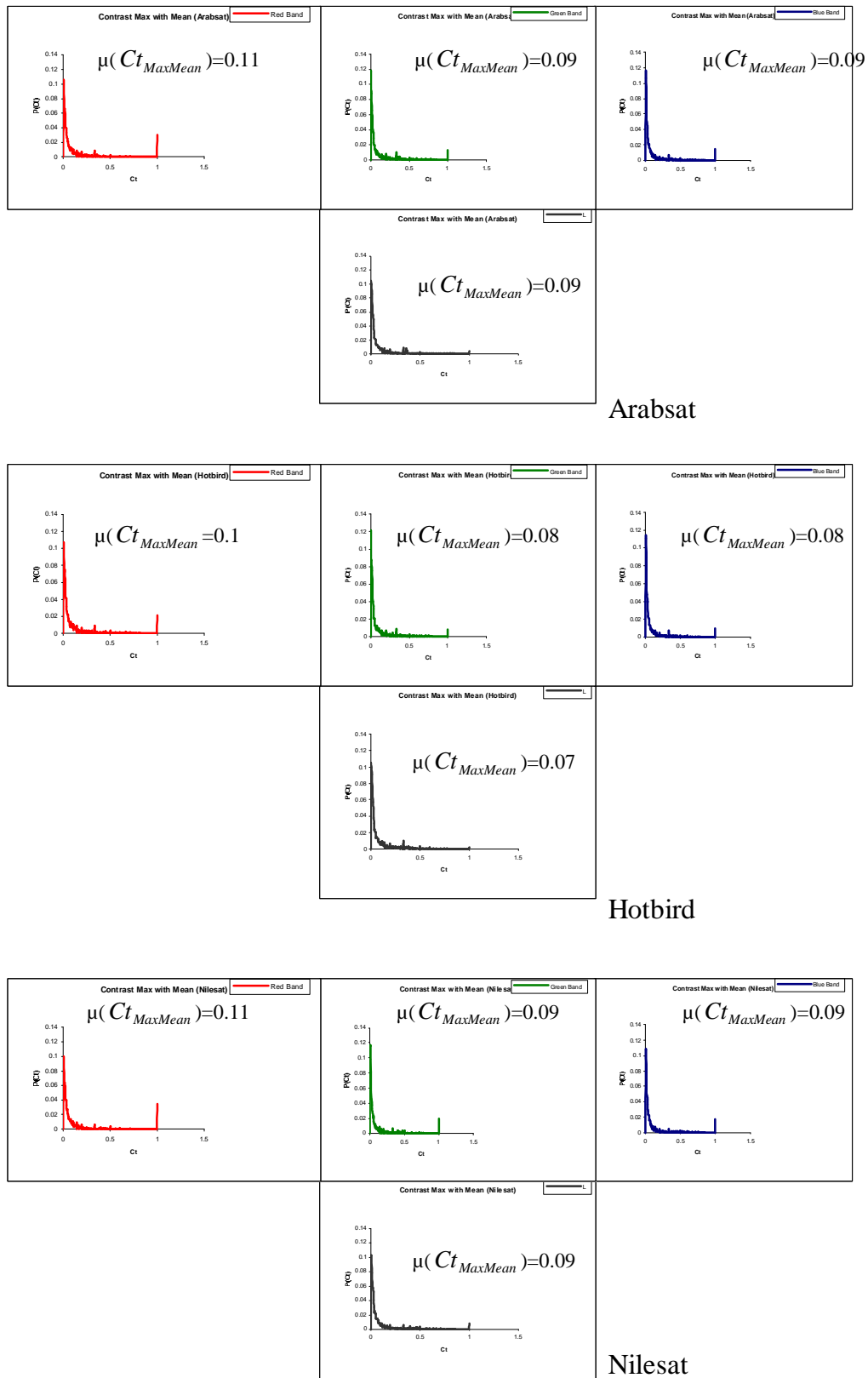Figure (4.6): Ct_{Max} for RGBL components using threshold=30 for (Arabsat, Hotbird and Nilesat)

Arabsat
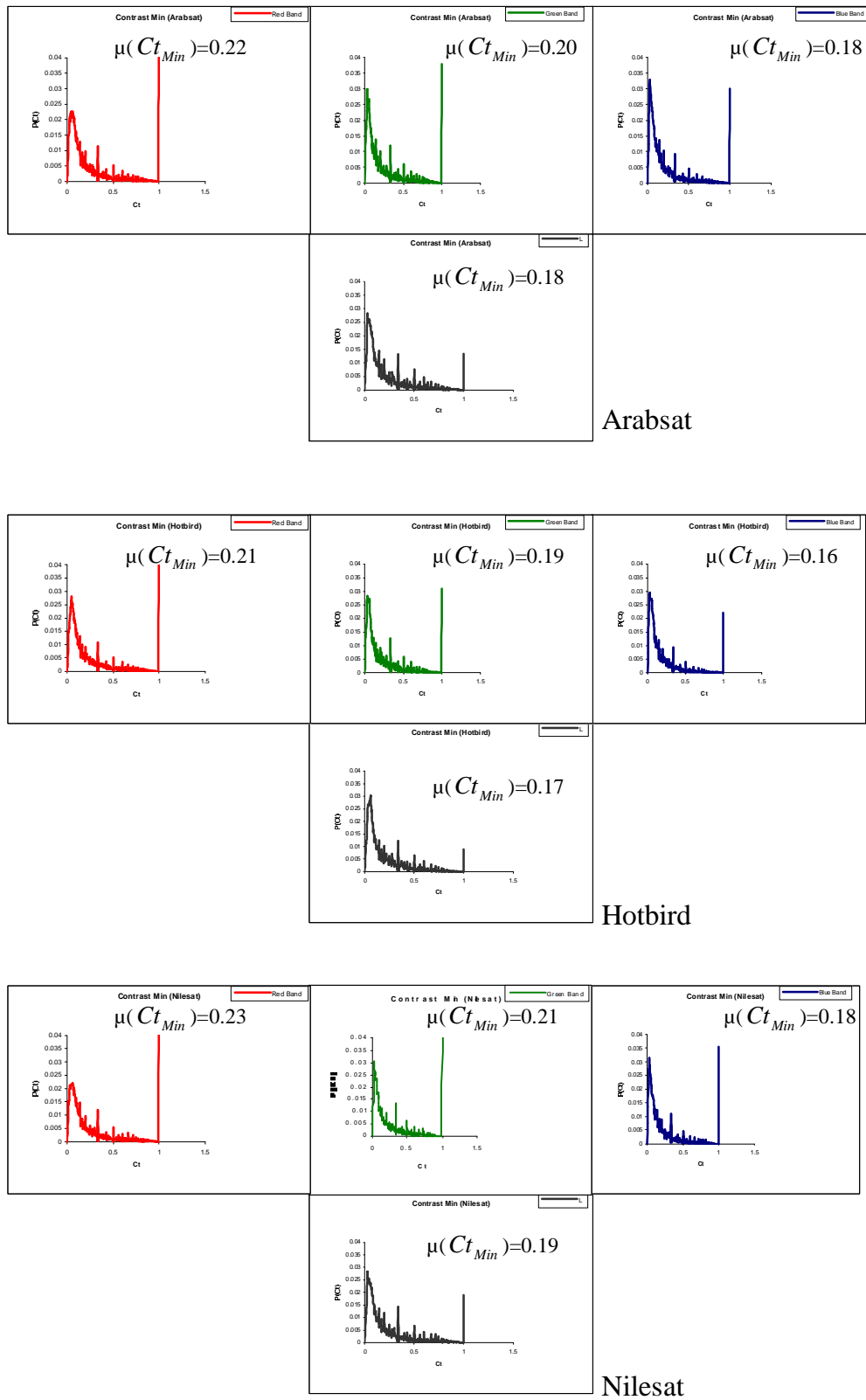
Hotbird

Nilesat

Figure (4.7): Ct_{Min} RGBL components using threshold=30 for (Arabsat, Hotbird and Nilesat)

Arabsat
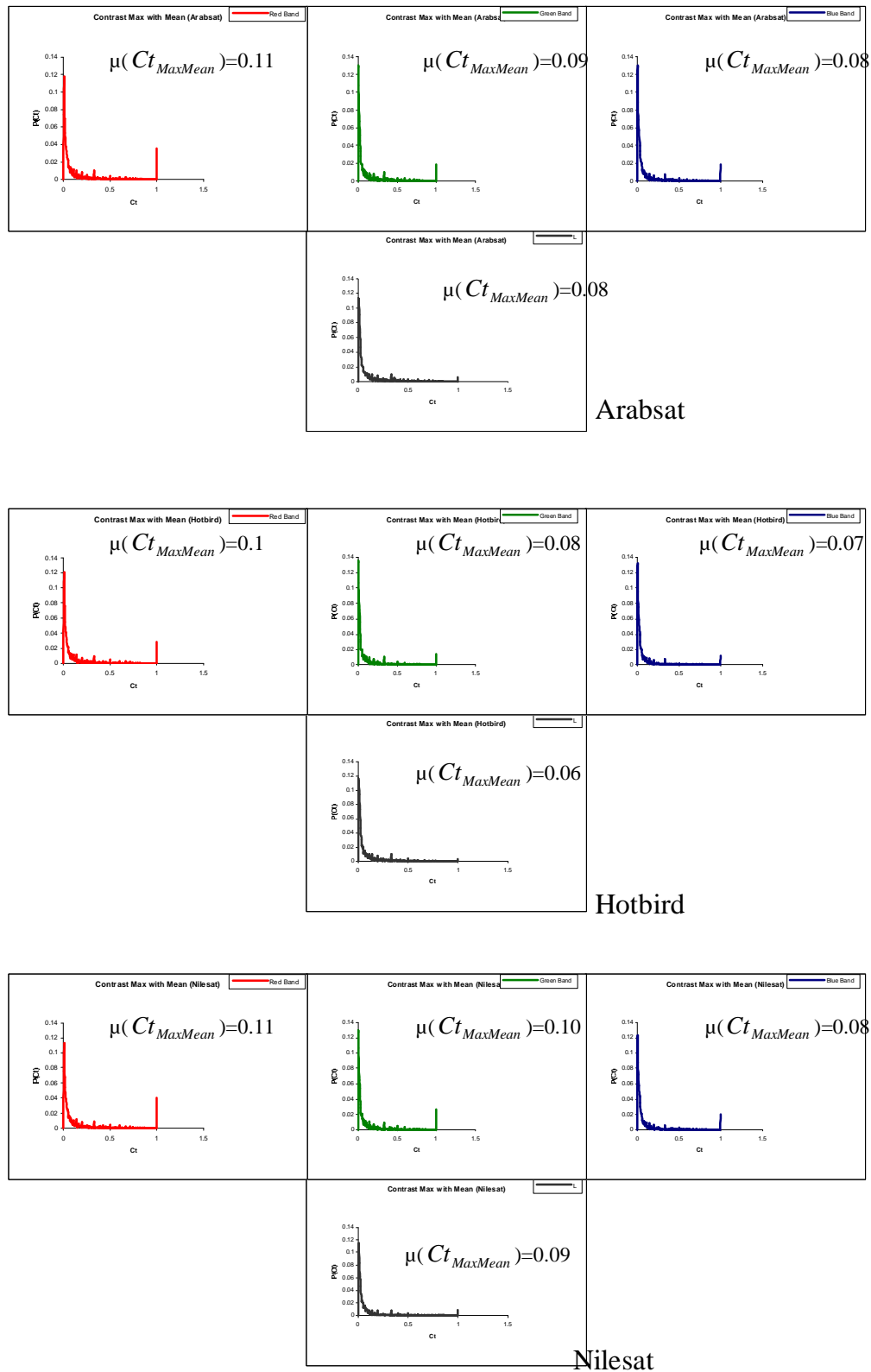
Hotbird

Nilesat

Figure (4.8): $Ct_{MaxMean}$ for RGBL components using threshold=30 for (Arabsat, Hotbird and Nilesat)
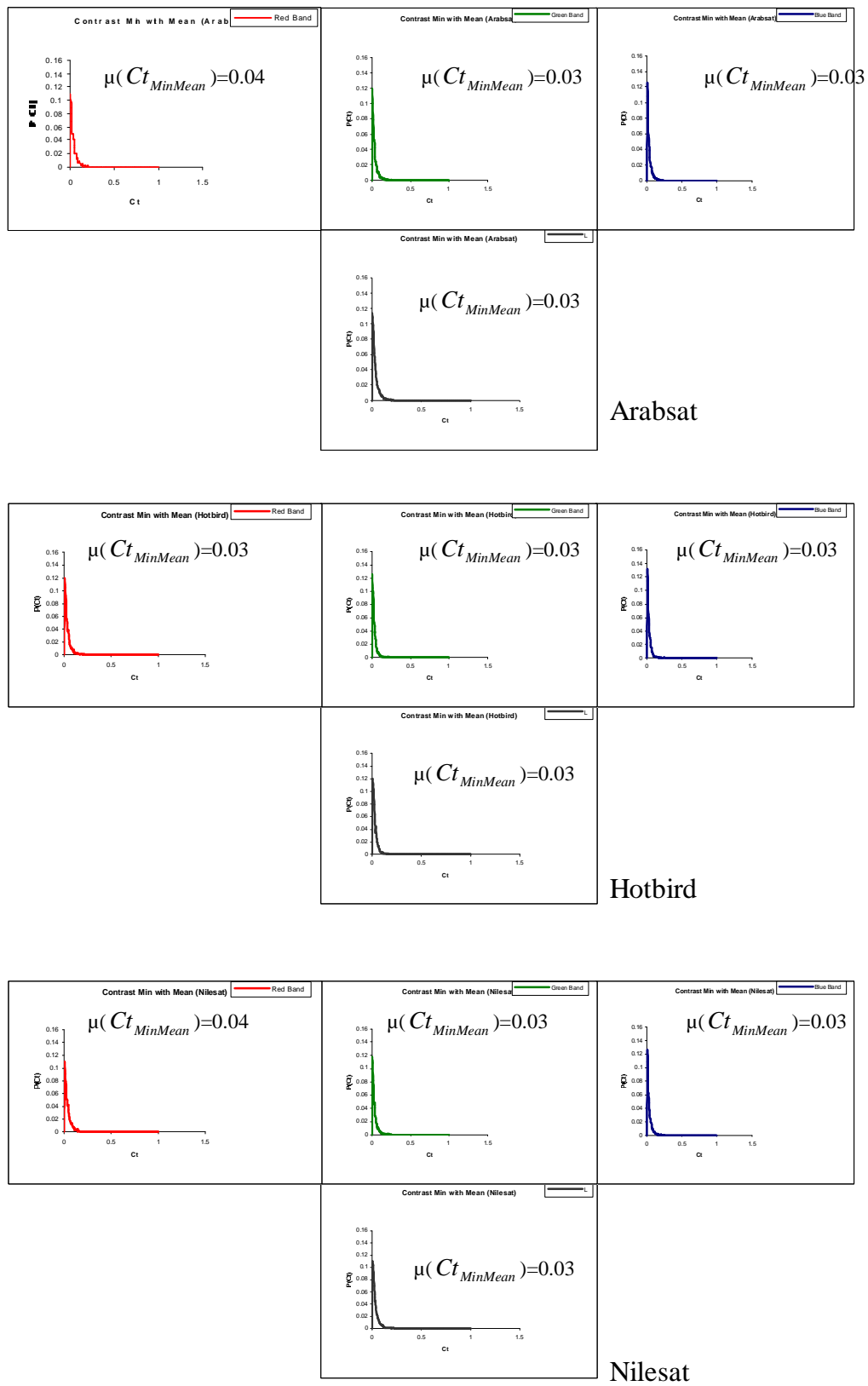
Arabsat
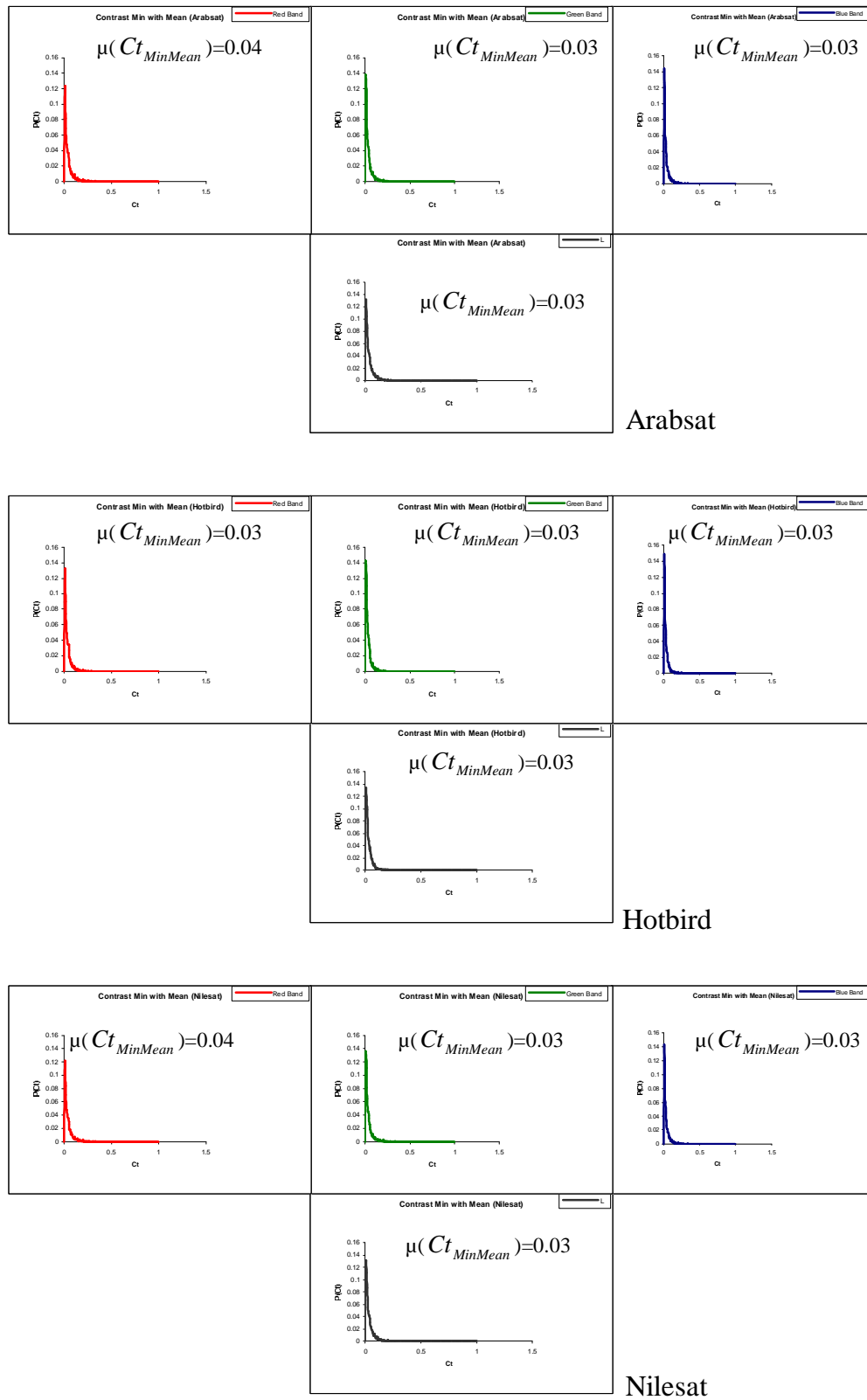
Hotbird

Nilesat

Figure (4.9): $Ct_{MinMean}$ for RGBL components using threshold=30 for (Arabsat, Hotbird and Nilesat)
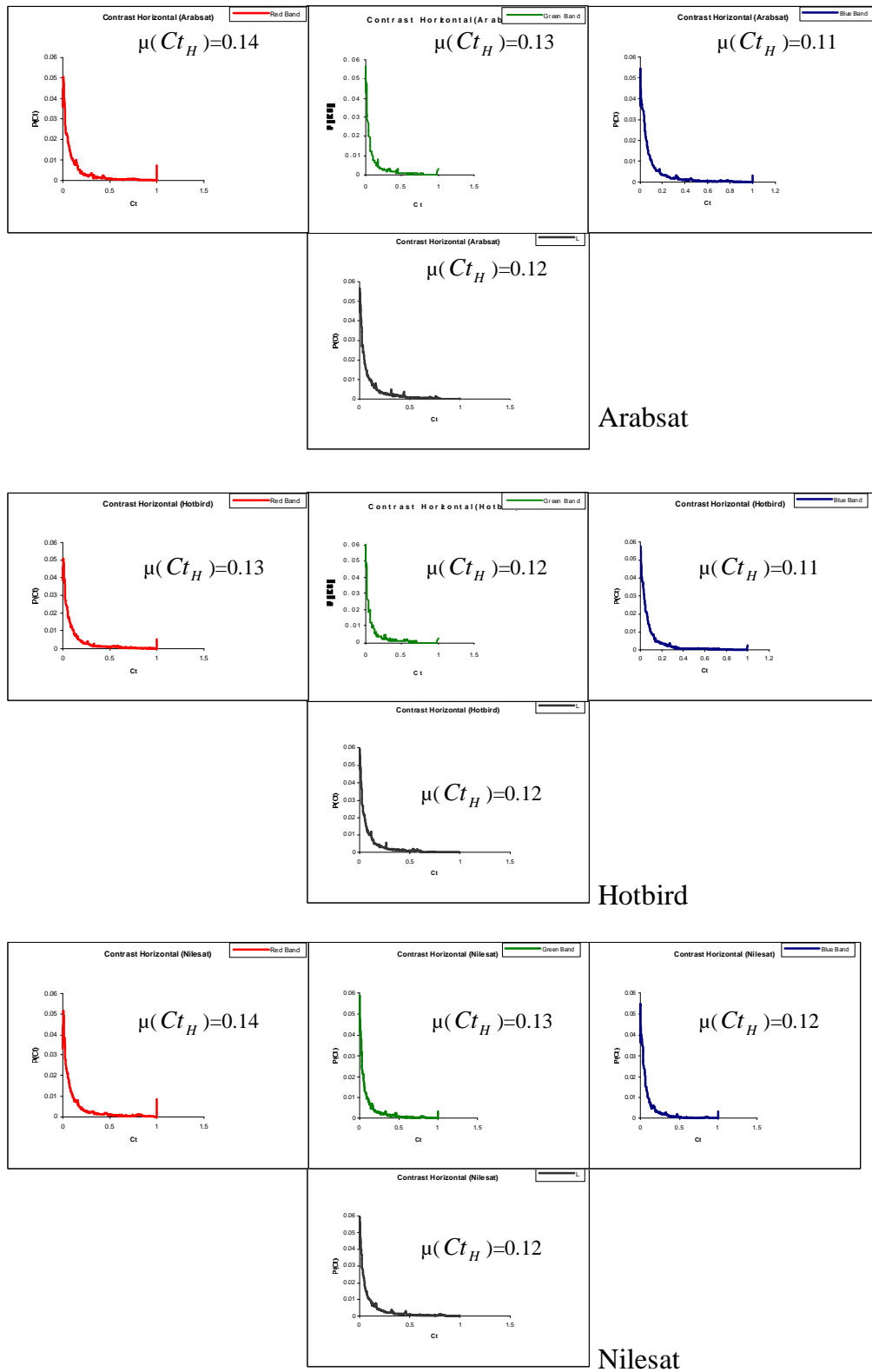
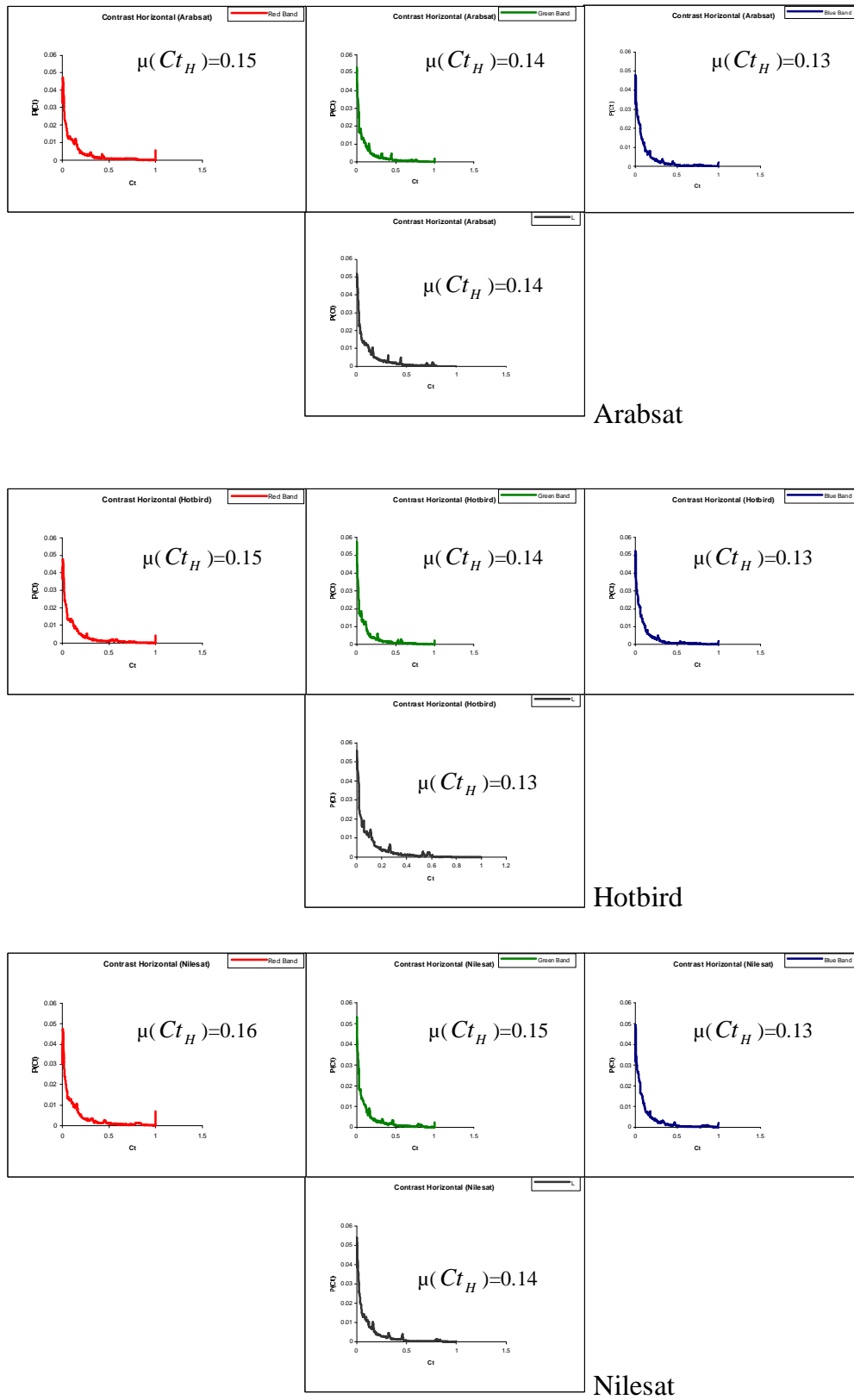Figure (4.10): Ct_H for RGBL components using threshold=30 for (Arabsat, Hotbird and Nilesat)
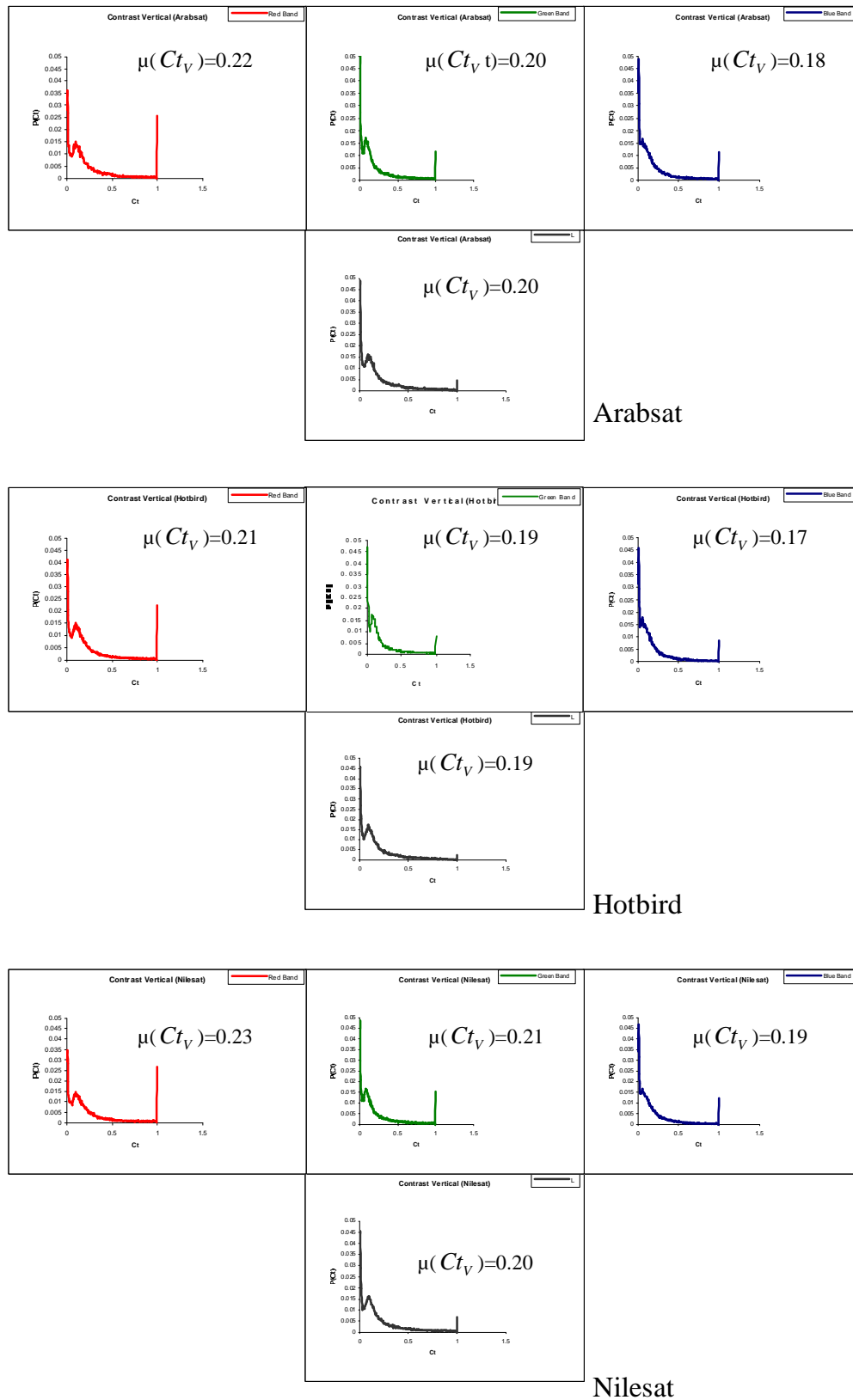
Arabsat
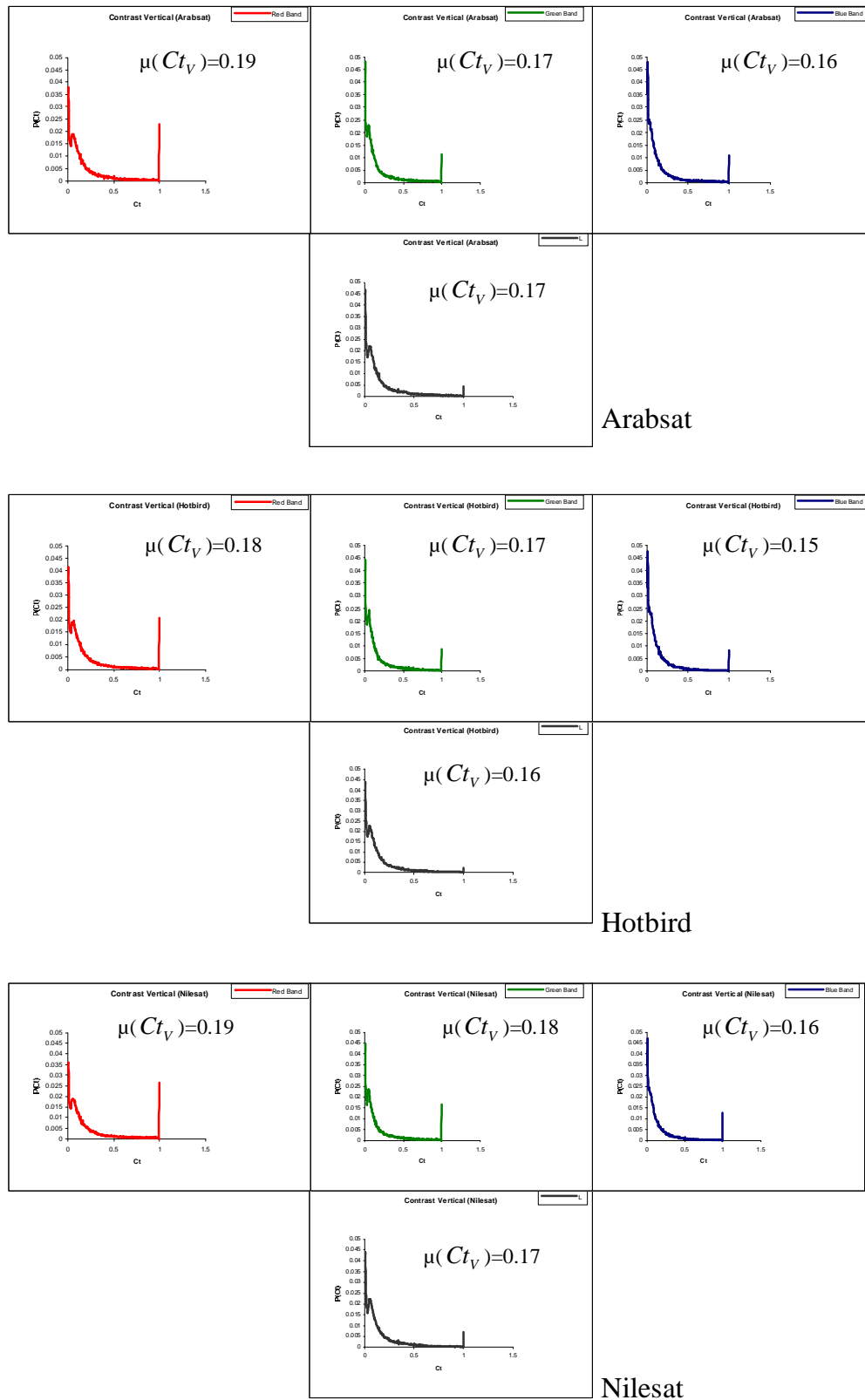
Hotbird

Nilesat

Figure (4.11): Ct_V for RGBL components using threshold=30 for (Arabsat, Hotbird and Nilesat)
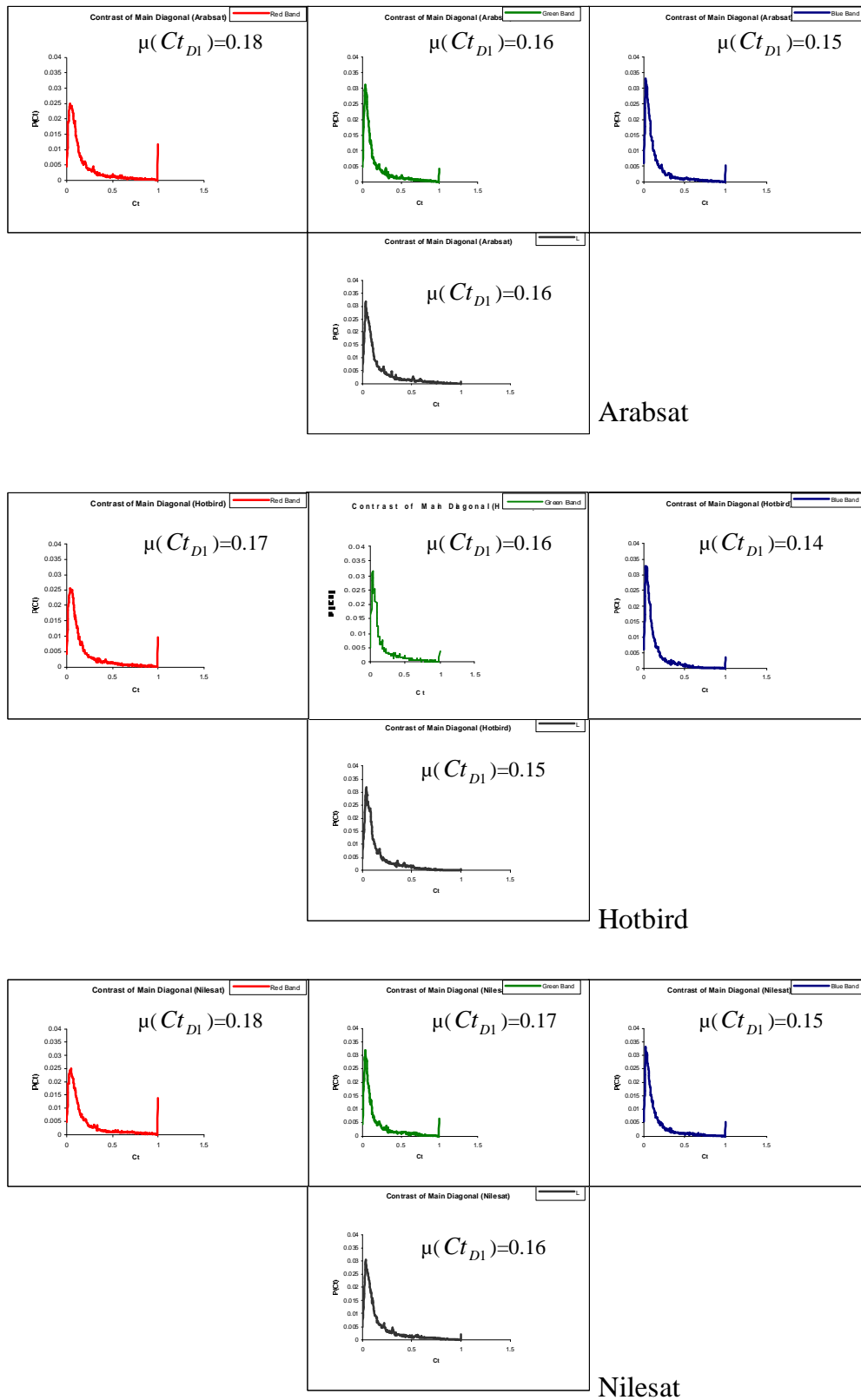
Figure (4.12): Ct_{D1} for RGBL components using threshold=30 for (Arabsat, Hotbird and Nilesat)
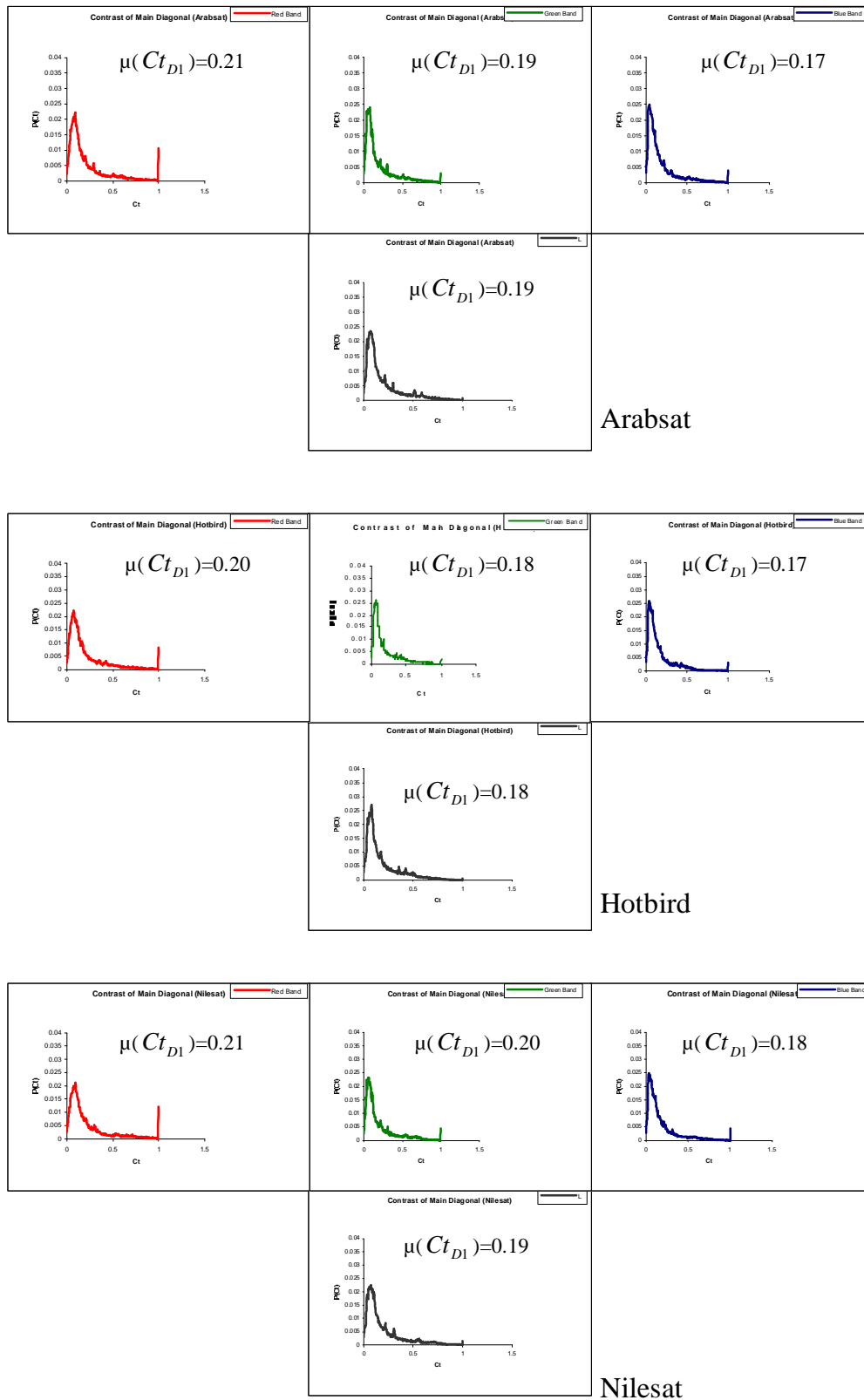
Arabsat
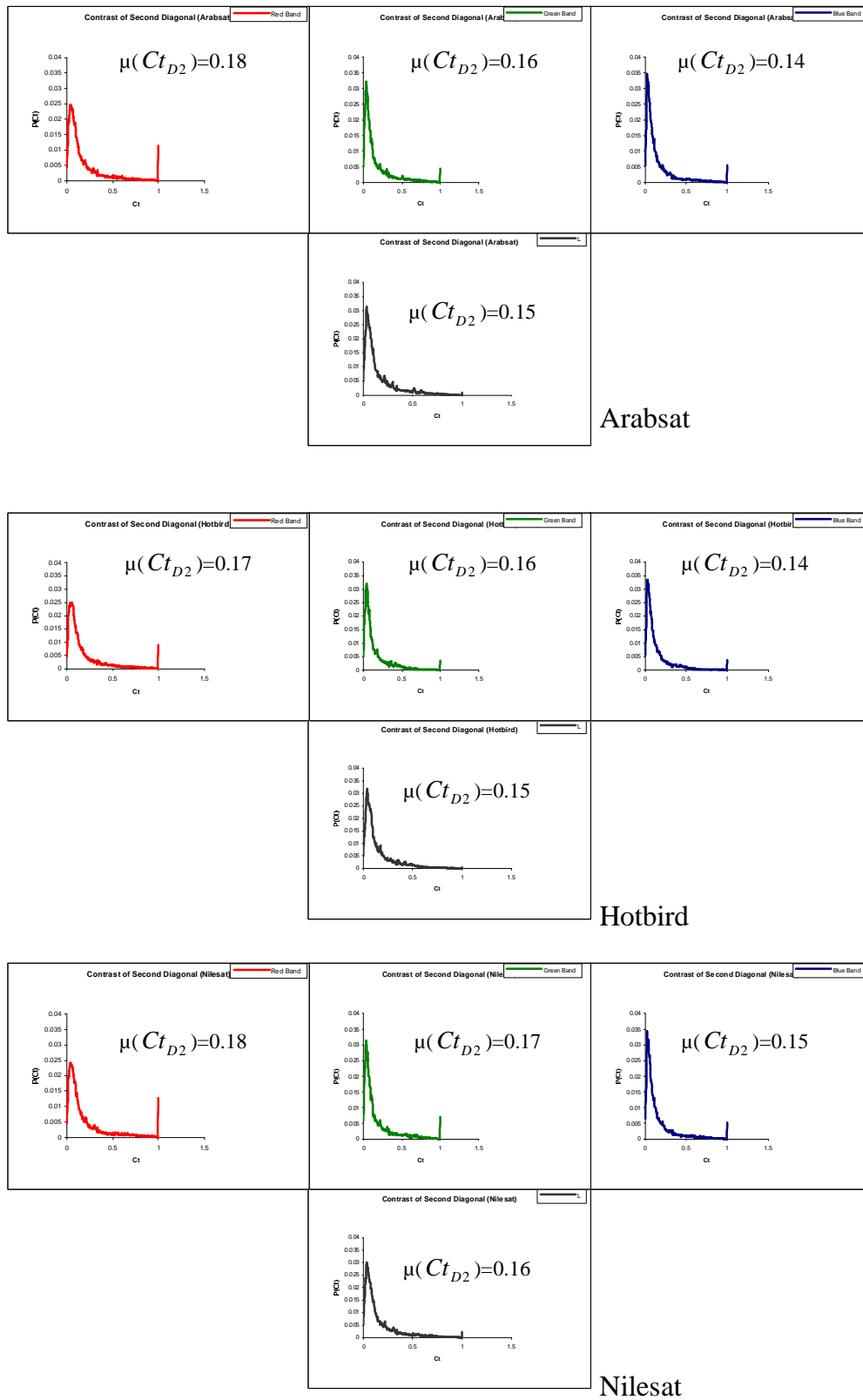
Hotbird

Nilesat

Figure (4.13): Ct_{D2} for RGBL components using threshold=30 for (Arabsat, Hotbird and Nilesat)

Threshold=50

Arabsat

Hotbird

Nilesat

Figure (4.14): Histogram of image edges for RGBL components using threshold=50 for (Arabsat, Hotbird and Nilesat)

Figure (4.15): Contrast of image edges for RGBL components
using threshold=50 for (Arabsat, Hotbird and Nilesat)

Arabsat

Hotbird

Nilesat

Figure (4.16): Ct_{Max} for RGBL components using threshold=50 for (Arabsat, Hotbird and Nilesat)

Arabsat

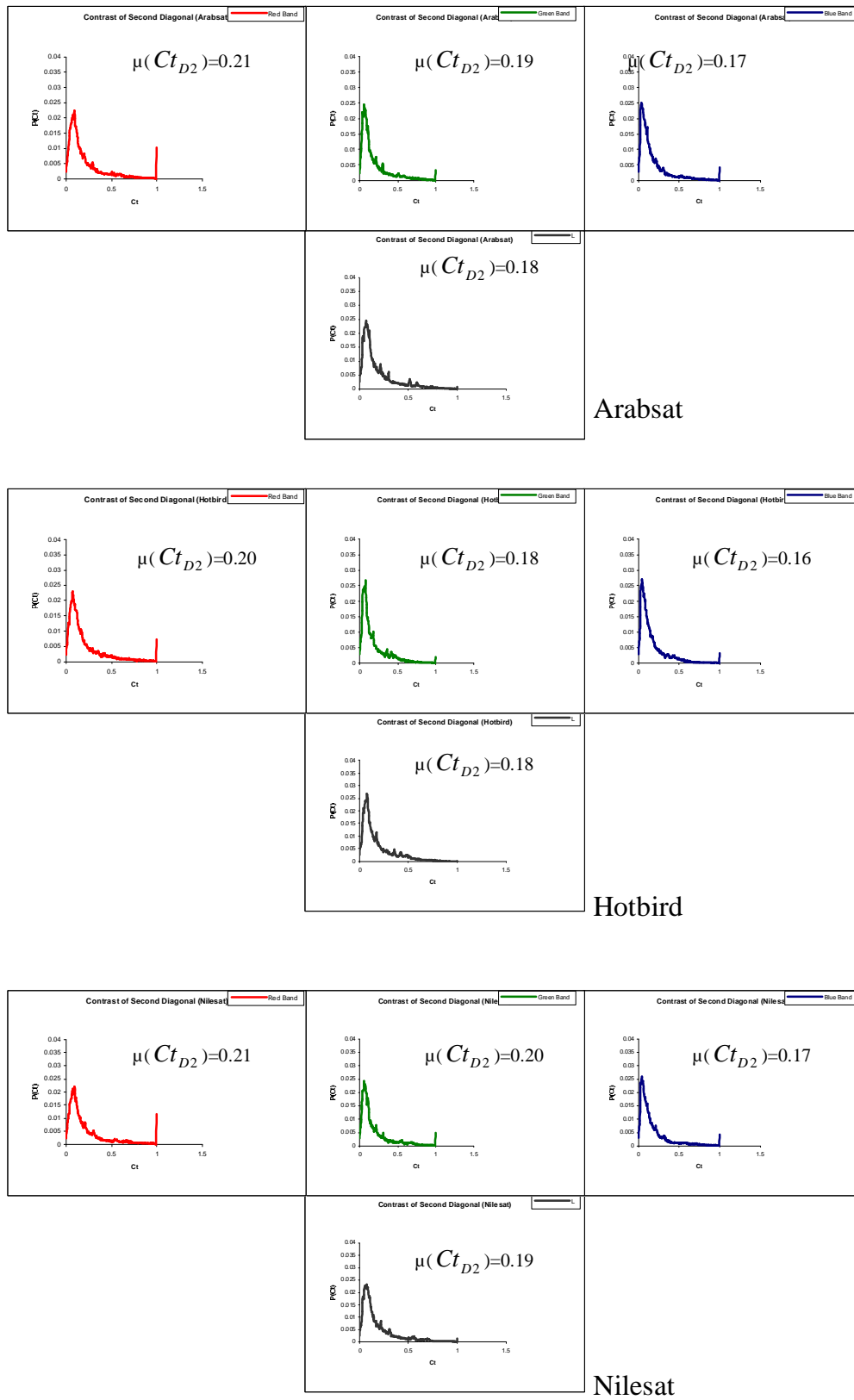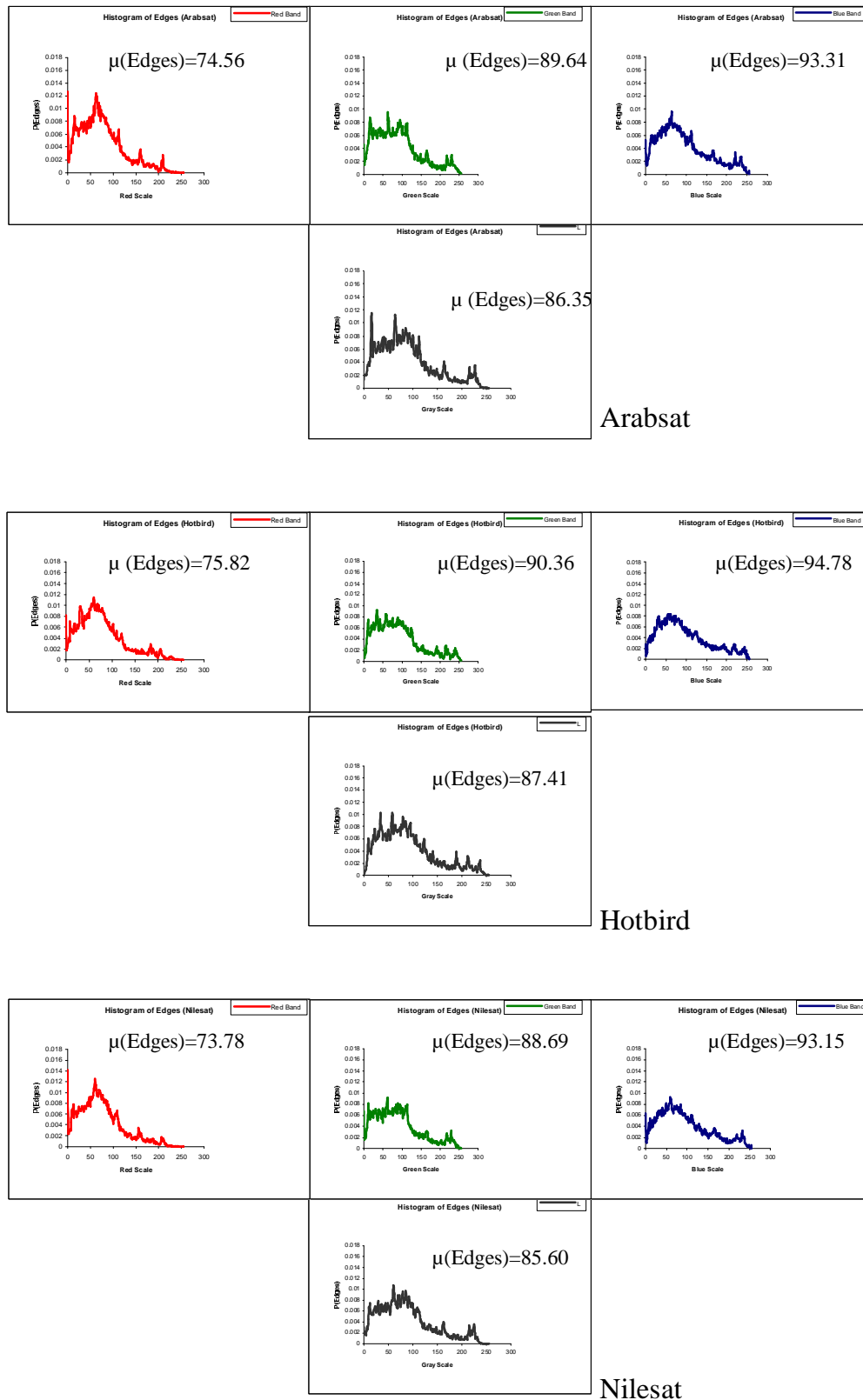Hotbird

Nilesat

Figure (4.17): Ct_{Min} for RGBL components using threshold=50 for (Arabsat, Hotbird and Nilesat)

Arabsat

Hotbird

Nilesat

Figure (4.18): $Ct_{MaxMean}$ for RGBL components using threshold=50 for (Arabsat, Hotbird and Nilesat)

94

Arabsat

Hotbird

Nilesat

Figure (4.19): $Ct_{MinMean}$ for RGBL components using threshold=50 for (Arabsat, Hotbird and Nilesat)

95

Arabsat

Hotbird

Nilesat

Figure (4.20): Ct_H for RGBL components using threshold=50 for (Arabsat, Hotbird and Nilesat)

Arabsat

Hotbird

Nilesat

Figure (4.21): Ct_V for RGBL components using threshold=50 for (Arabsat, Hotbird and Nilesat)
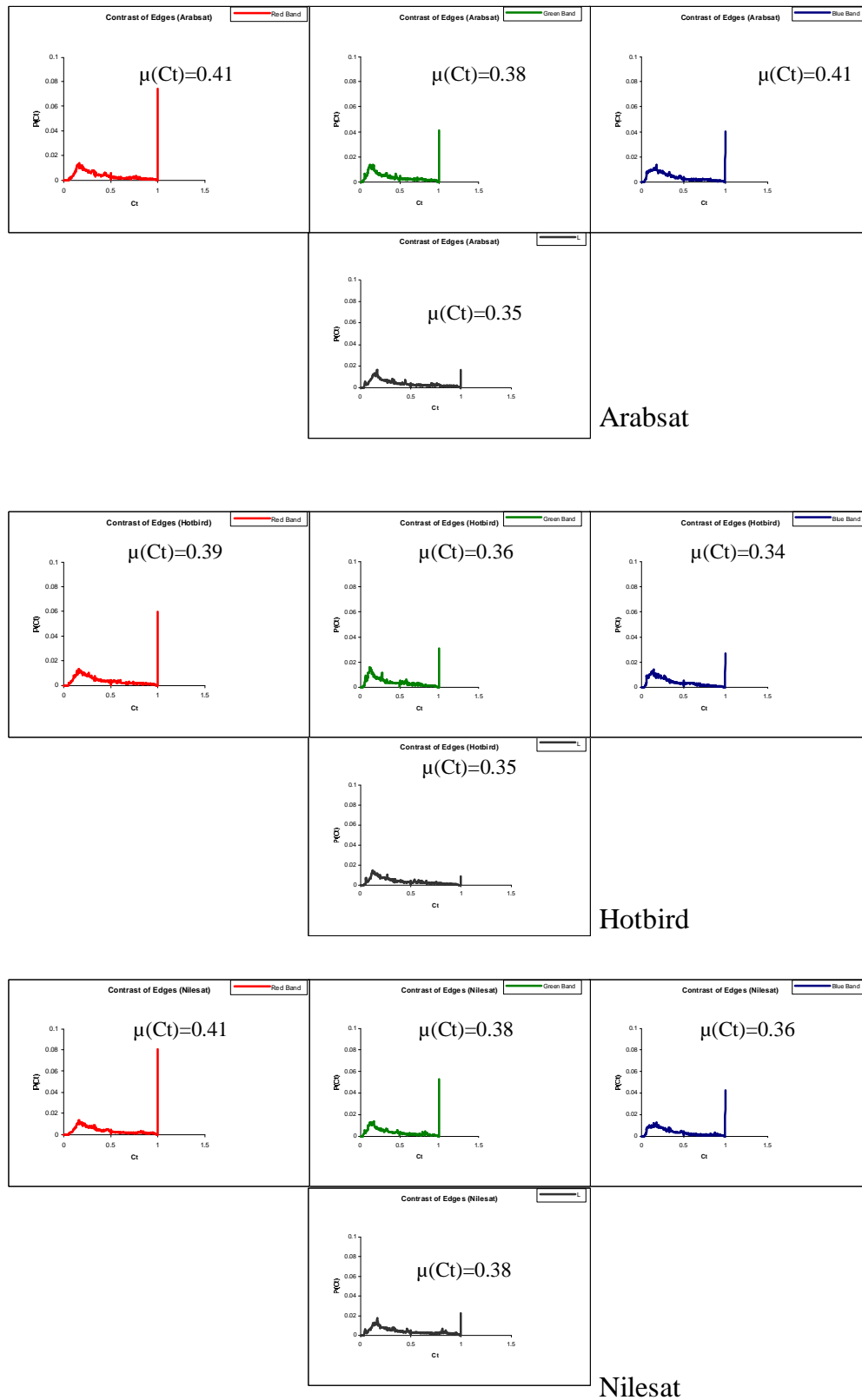
97

Arabsat

Hotbird

Nilesat

Figure (4.22): Ct_{D1} for RGBL components using threshold=50 for (Arabsat, Hotbird and Nilesat)

98

Figure (4.23): Ct_{D2} for RGBL components using threshold=50 for (Arabsat, Hotbird and Nilesat)

Threshold=70

Arabsat

Hotbird

Nilesat

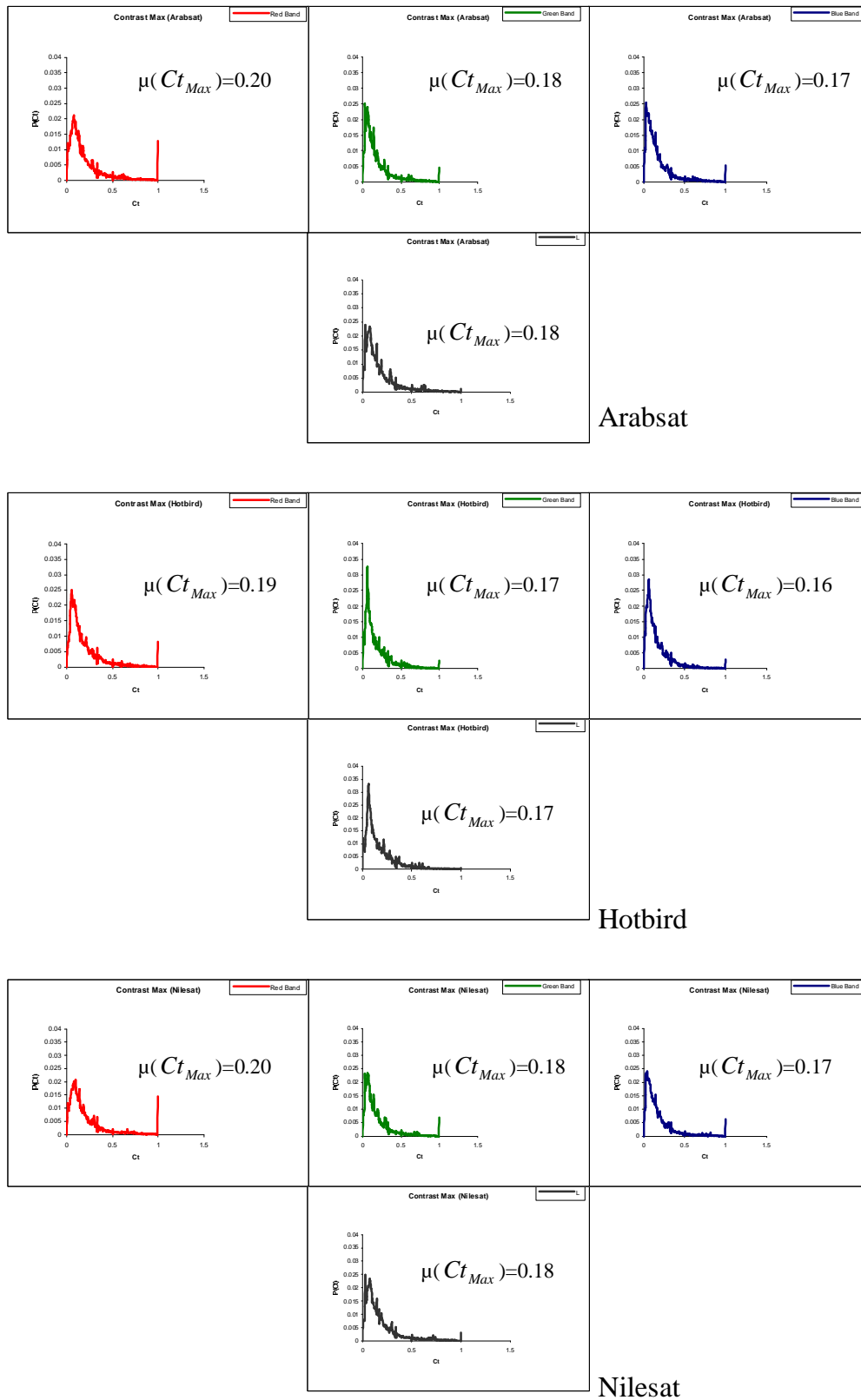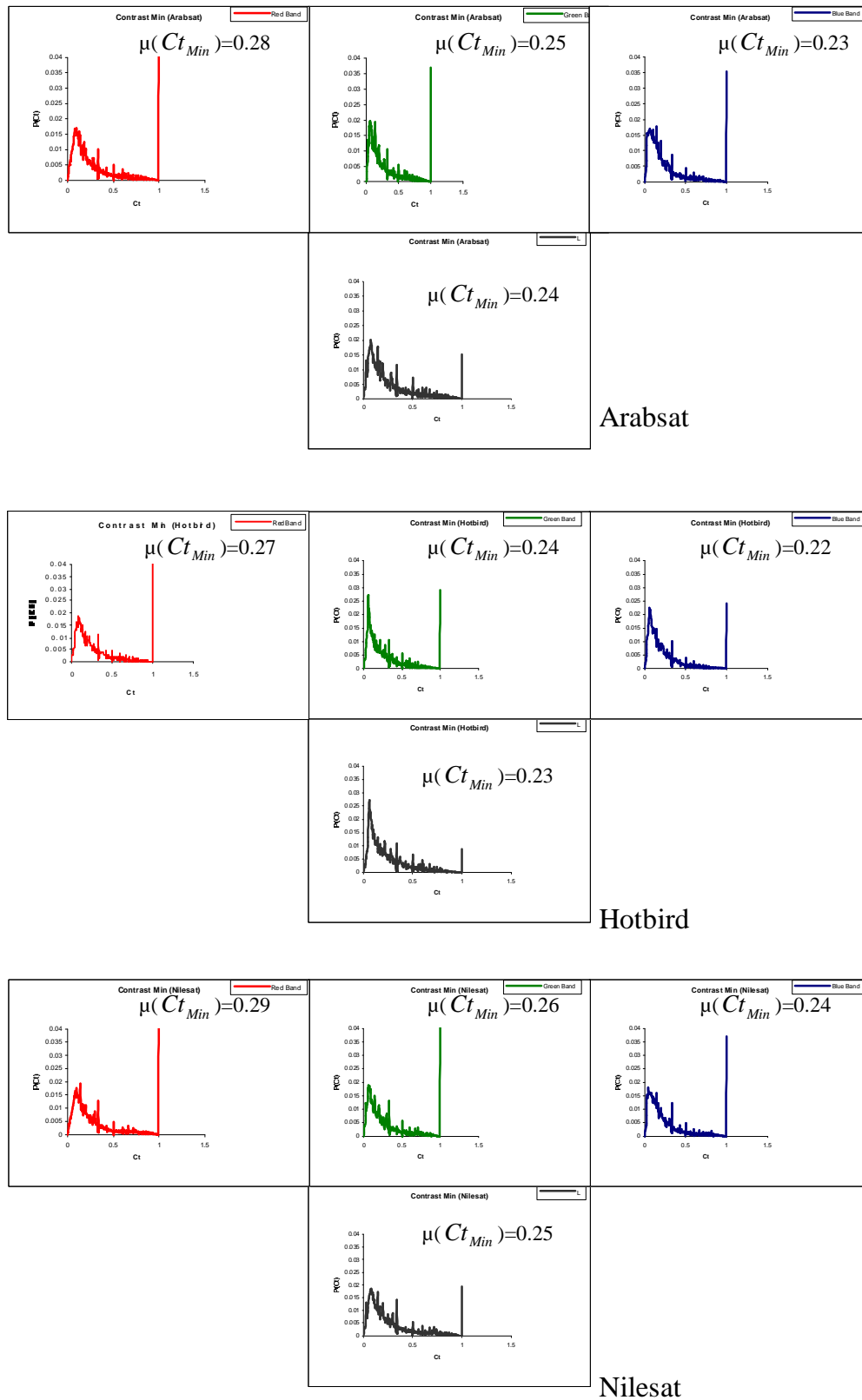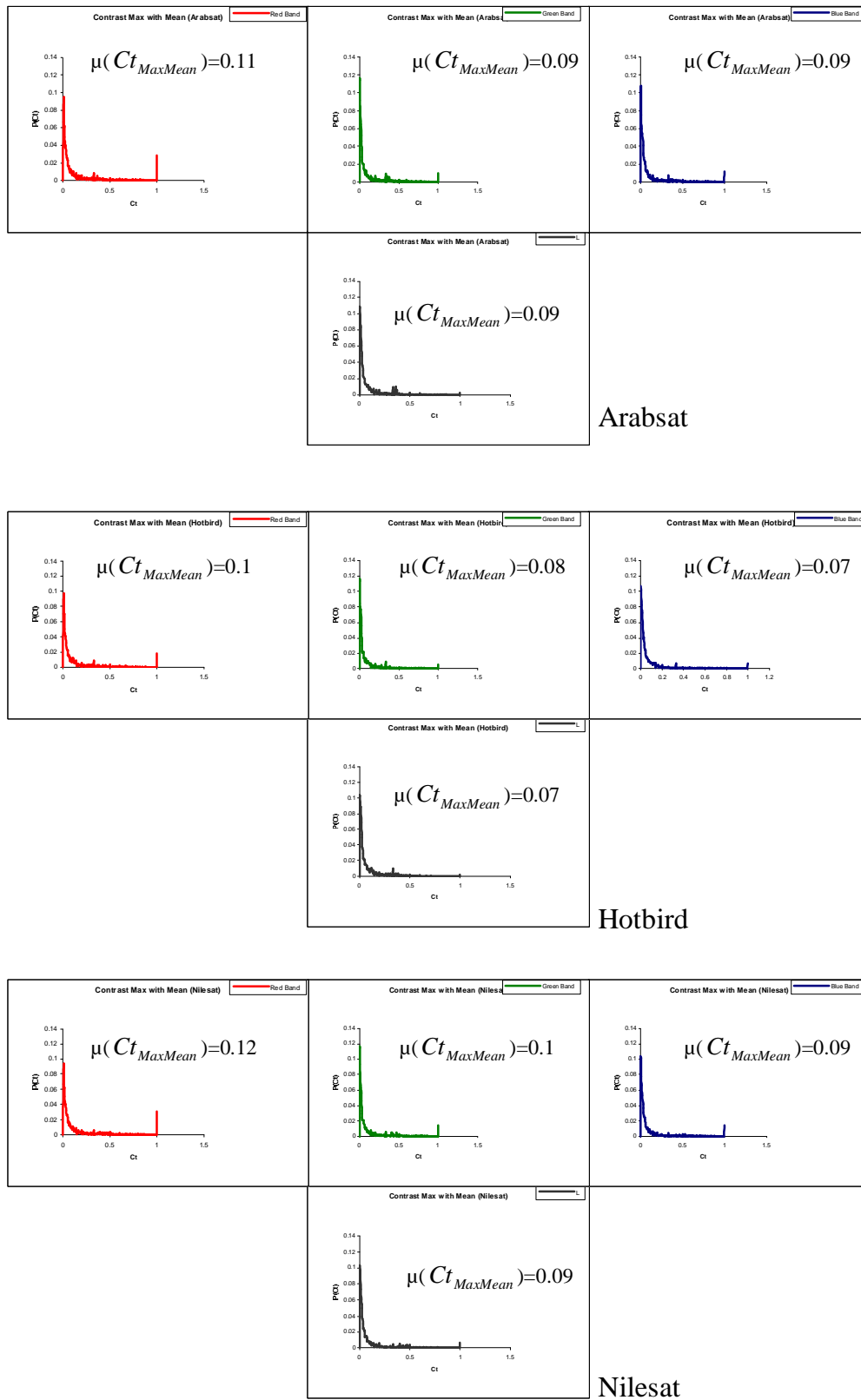Figure (4.24): Histogram of image edges for RGBL components using threshold=70 for (Arabsat, Hotbird and Nilesat)

Arabsat

Hotbird

Nilesat

Figure (4.25): Contrast of image edges for RGBL components using threshold=70 for (Arabsat, Hotbird and Nilesat)

Contrast Max (Arabsat) — Red Band

$\mu(Ct_{Max})=0.20$

Contrast Max (Arabsat) — Green Band

$\mu(Ct_{Max})=0.18$

Contrast Max (Arabsat) — Blue Band

$\mu(Ct_{Max})=0.17$

Contrast Max (Arabsat) — L

$\mu(Ct_{Max})=0.18$

Arabsat

Contrast Max (Hotbird) — Red Band

$\mu(Ct_{Max})=0.19$

Contrast Max (Hotbird) — Green Band

$\mu(Ct_{Max})=0.17$

Contrast Max (Hotbird) — Blue Band

$\mu(Ct_{Max})=0.16$

Contrast Max (Hotbird) — L

$\mu(Ct_{Max})=0.17$

Hotbird

Contrast Max (Nilesat) — Red Band

$\mu(Ct_{Max})=0.20$

Contrast Max (Nilesat) — Green Band

$\mu(Ct_{Max})=0.18$

Contrast Max (Nilesat) — Blue Band

$\mu(Ct_{Max})=0.17$

Contrast Max (Nilesat) — L

$\mu(Ct_{Max})=0.18$

Nilesat

Figure (4.26): Ct_{Max} for RGBL components using threshold=70 for (Arabsat, Hotbird and Nilesat)

Arabsat

Hotbird

Nilesat

Figure (4.27): Ct_{Min} for RGBL components using threshold=70 for (Arabsat, Hotbird and Nilesat)

Arabsat

Hotbird

Nilesat

Figure (4.28): $Ct_{MaxMean}$ for RGBL components using threshold=70 for (Arabsat, Hotbird and Nilesat)

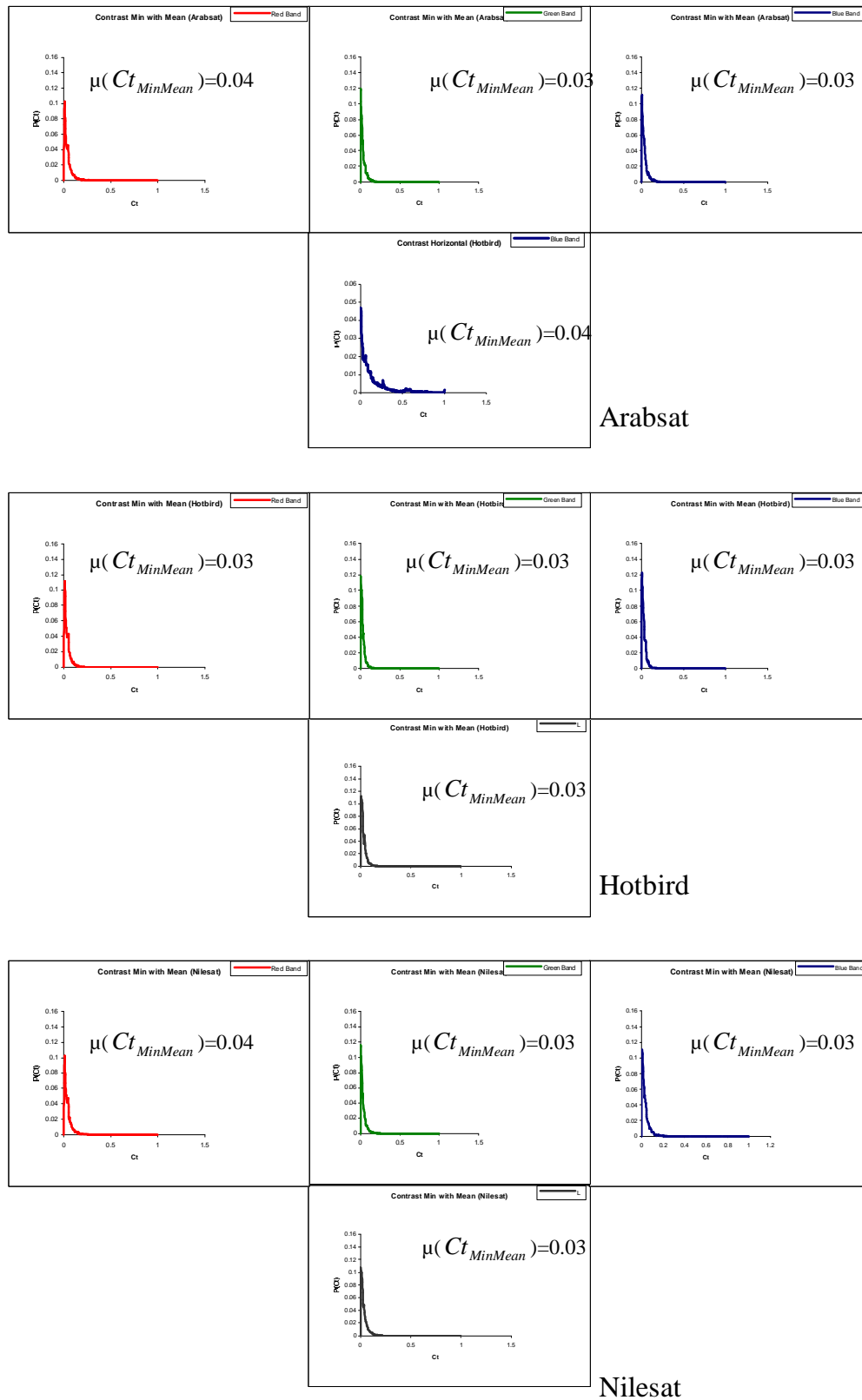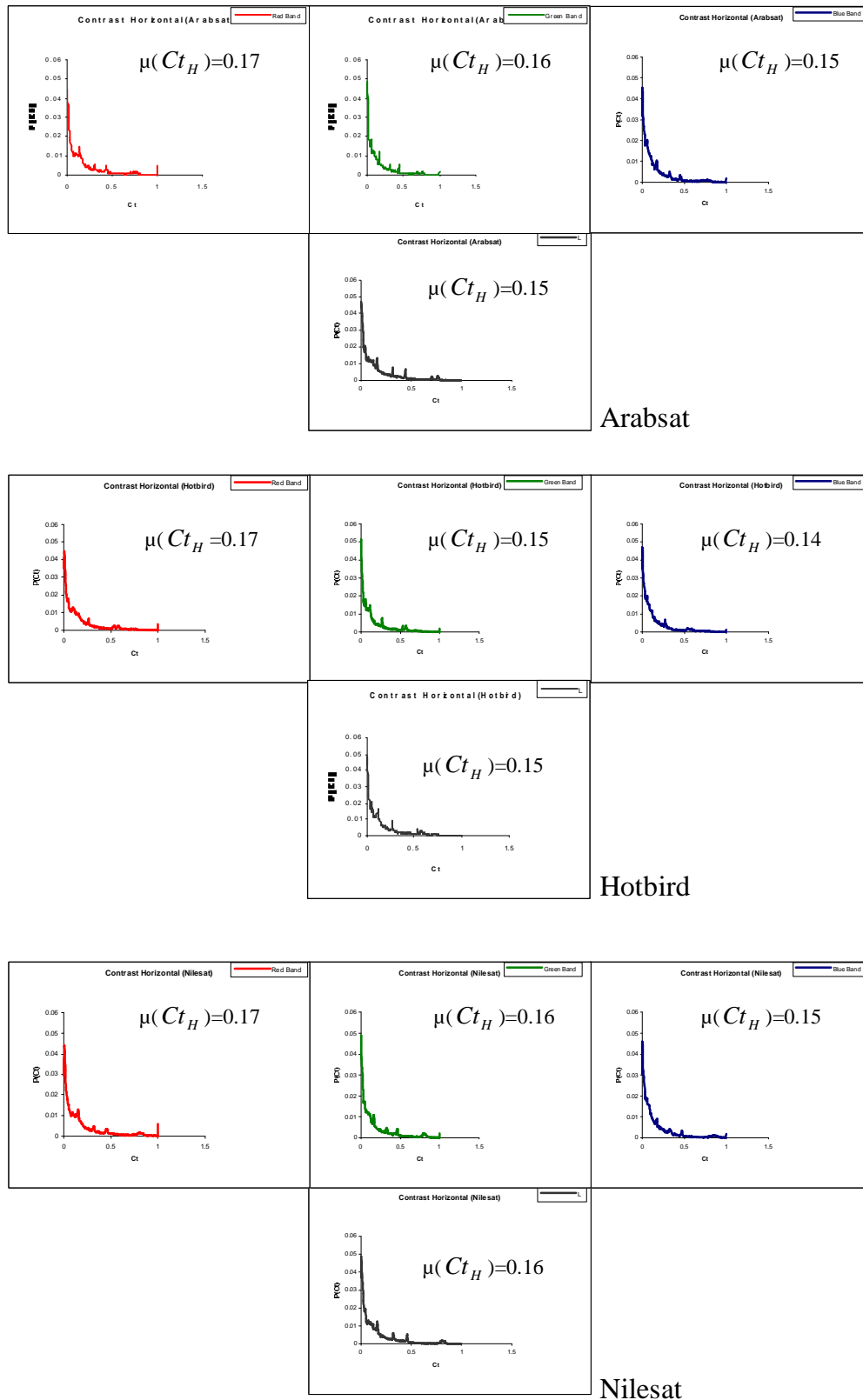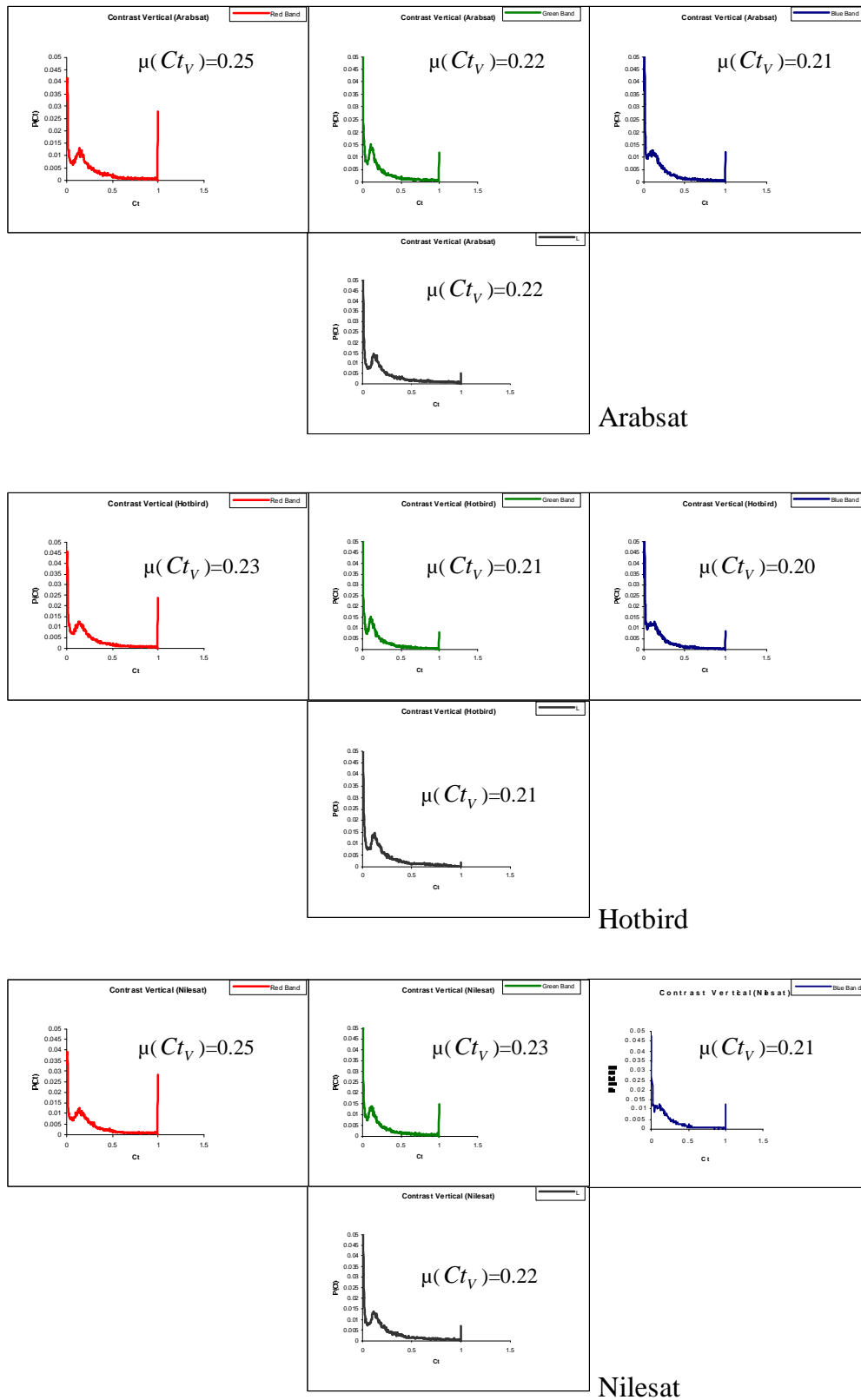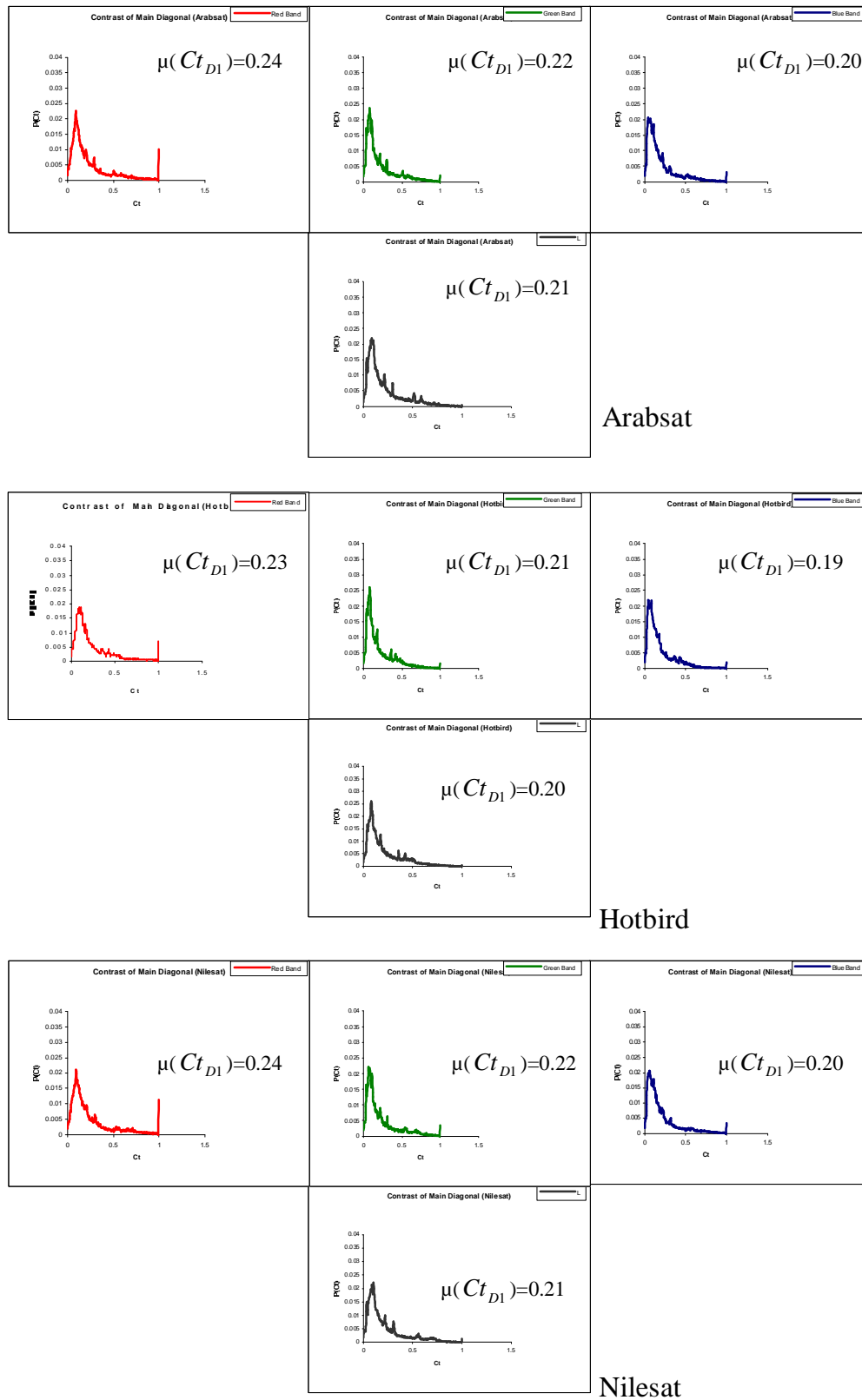Figure (4.29): $Ct_{MinMean}$ for RGBL components using threshold=70 for (Arabsat, Hotbird and Nilesat)

Arabsat

Hotbird

Nilesat

Figure (4.30): Ct_H for RGBL components using threshold=70 for (Arabsat, Hotbird and Nilesat)

Arabsat

Hotbird

Nilesat

Figure (4.31): Ct_V for RGBL components using threshold=70 for (Arabsat, Hotbird and Nilesat)

107

Arabsat

Hotbird

Nilesat

Figure (4.32): Ct_{D1} for RGBL components using threshold=70 for (Arabsat, Hotbird and Nilesat)
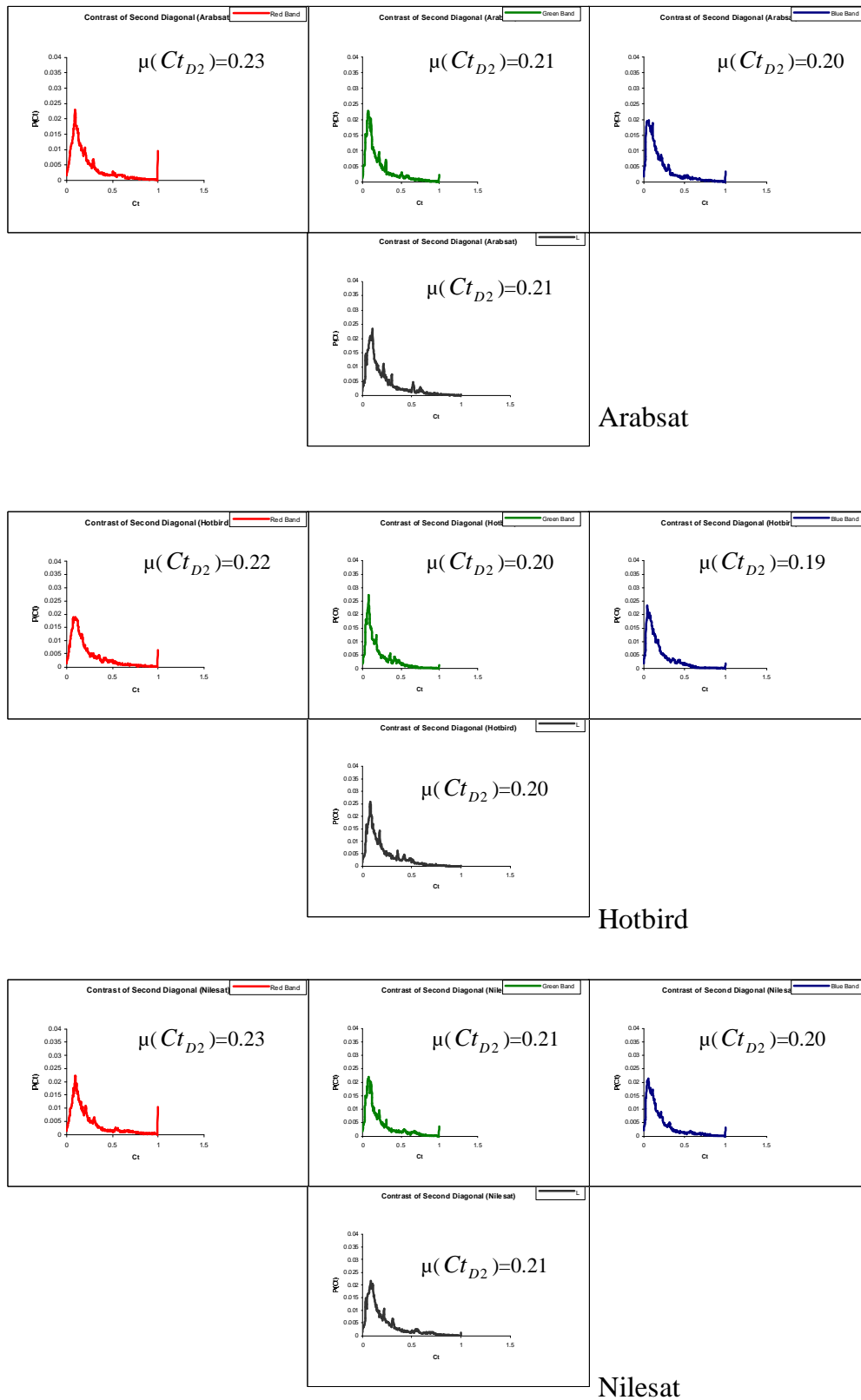
Arabsat

Hotbird

Nilesat

Figure (4.33): Ct_{D2} for RGBL components using threshold=70 for (Arabsat, Hotbird and Nilesat)

Table (4.3): Results of contrast of image edges for RGB-L components of Image on Arabsat.

Threshold value	Ct$_R$	Ct$_G$	Ct$_B$	Ct$_L$
30	0.67	0.69	0.68	0.67
40	0.65	0.68	0.67	0.66
50	0.64	0.67	0.66	0.65
60	0.63	0.66	0.65	0.64
70	0.63	0.65	0.64	0.63
80	0.62	0.64	0.63	0.63
90	0.62	0.64	0.63	0.62
100	0.61	0.63	0.62	0.61

Table (4.4): Results of contrast of image edges for RGB-L components of image on Hotbird

Threshold value	Ct$_R$	Ct$_G$	Ct$_B$	Ct$_L$
30	0.68	0.68	0.66	0.65
40	0.66	0.67	0.65	0.65
50	0.65	0.66	0.64	0.64
60	0.65	0.65	0.64	0.64
70	0.63	0.65	0.63	0.63
80	0.63	0.64	0.63	0.63
90	0.62	0.64	0.62	0.63
100	0.61	0.63	0.61	0.61

Table (4.5): Results of contrast of image edges for RGB-L components of image on Nilesat

Threshold value	Ct$_R$	Ct$_G$	Ct$_B$	Ct$_L$
30	0.68	0.69	0.68	0.67
40	0.66	0.68	0.66	0.66
50	0.64	0.67	0.66	0.65
60	0.63	0.66	0.65	0.64
70	0.63	0.65	0.64	0.63
80	0.63	0.65	0.63	0.63
90	0.62	0.64	0.63	0.62
100	0.62	0.63	0.62	0.61

4.4 Results of Image Edges Quality Measure

The images that are used in these methods are illustrated in figure (4.1). The curves [in figures (4.34) to (4.43)] present the relationship between (the rate of image edges, the SNR, and the mean of the different suggested contrast of edges that discussed earlier) and the Sobel edge

detector threshold (30, 40, 50, 60, 70, 80, 90 and 100). The discussion of the obtained results are illustrated below:

1. The relationship between the rate of image edges and the different threshold values for all RGB-L components of Arabsat, Hotbird and Nilesat were presented in the figure (4.34). According to the curves, it has been found that the threshold value (30) has the highest amount of image edges for RGB-L components among the rest threshold values. Also the curves show that as the threshold value increases the amount of edges decreases. Where most weak edges in the considered image were in the bright areas (Bright intensity), so when the threshold value increased, the number of image edges decreased so as the amount of image edges.
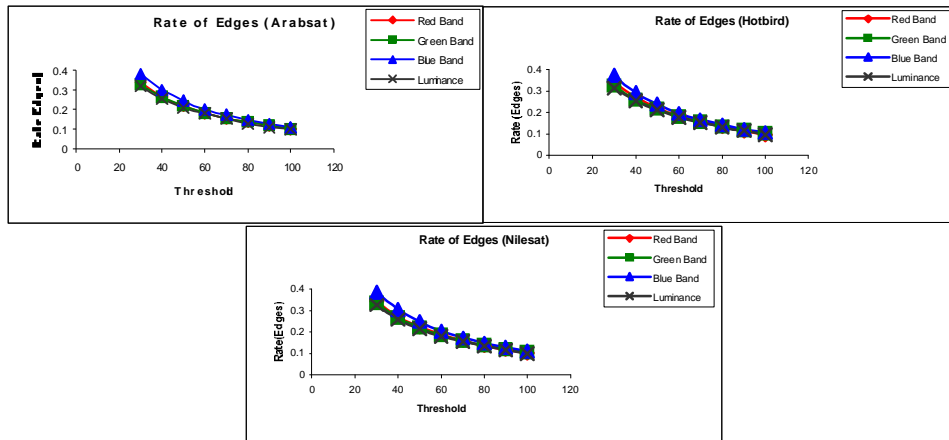

Figure (4.34): The relationship between rate of edges and the threshold values.

2. Figure (4.35) presents the curves of the SNR for all three bands RGB and L for three satellites. SNR method is illustrated in section (3.6) of chapter three. The curves indicate that all three satellites have high values of SNR which are more than (60 db) that led to discover that the noise is low of the images on the three satellites. The curves of Arabsat and Hotbird have almost the same shape of SNR which have

the same values for all threshold values. The curves of Nilesat show the highest SNR values for RGBL components among the considered satellites.
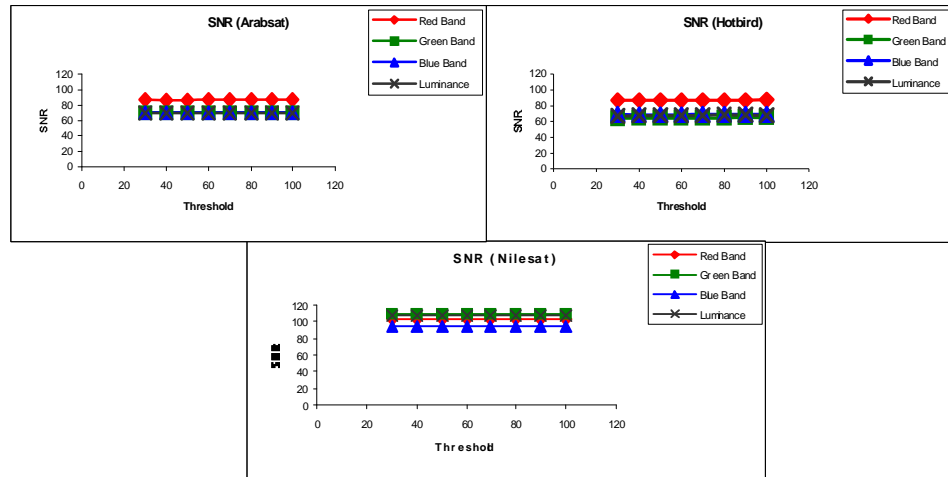

Figure (4.35): The relationship between the SNR of edges and the threshold values

3. The figures [from (4.36) to (4.44] illustrate the relationship between the mean of different suggested contrast of image edges measures and the threshold values. The indicated figures show obvious increment of the mean of contrast of image edges of the different methods as the threshold value increase. Where most of the weak image edges of the considered image are in the bright areas that have high intensity values, so as the threshold value increased the mean of contrast of image edges will increase. So in the high threshold values the only image edges remained are the strong image edges that have high contrast.
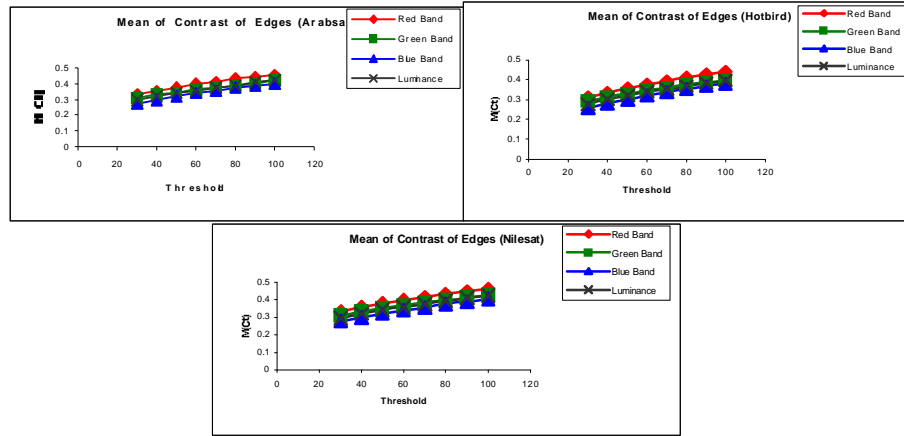
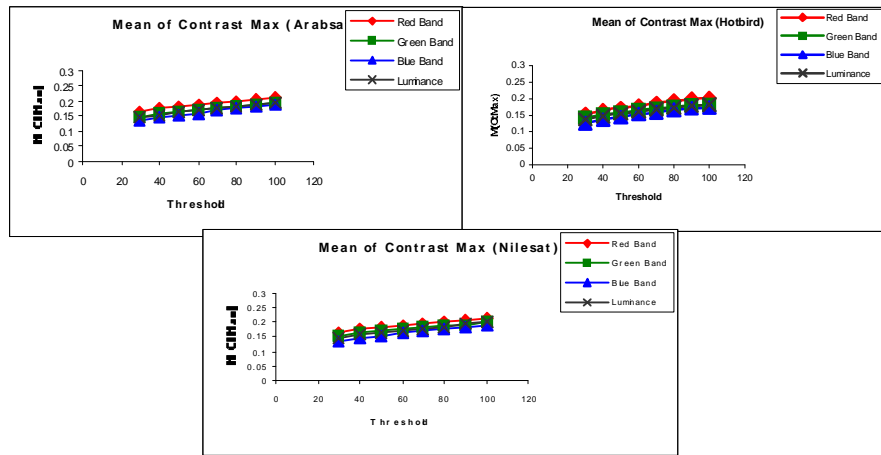Figure (4.36): The relationship between the mean of contrast of edges and the threshold values

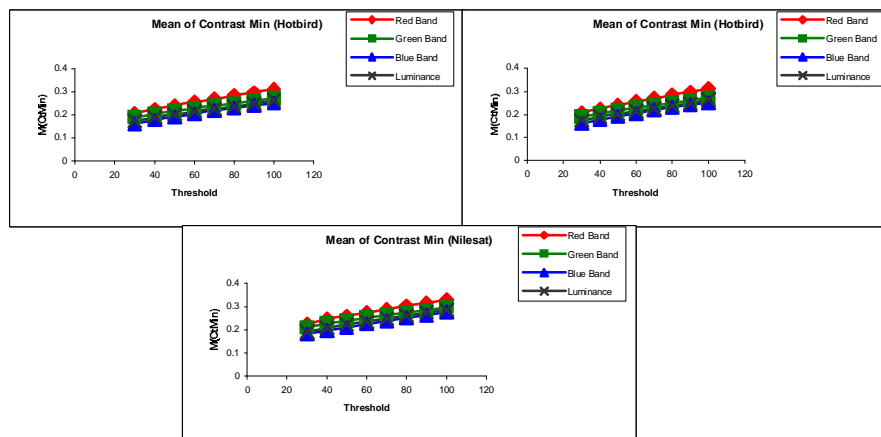Figure (4.37): The relationship between the Ct_{Max} of edges and the threshold values

Figure (4.38): The relationship between the Ct_{Min} of edges and the threshold values
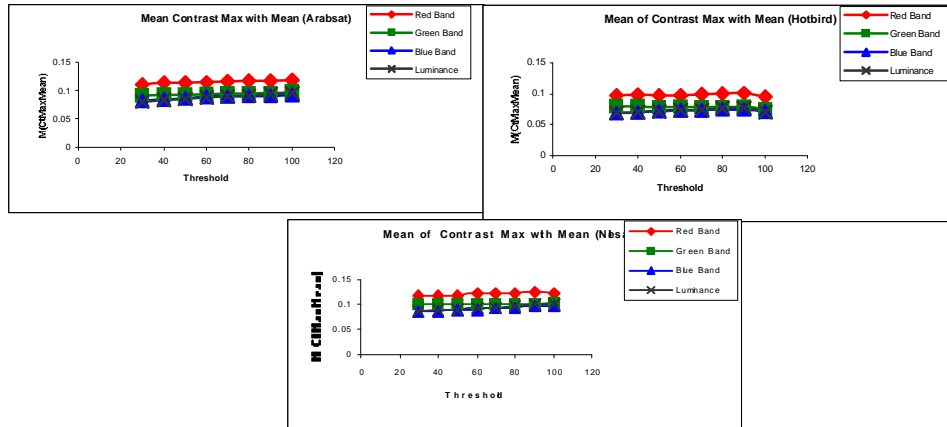
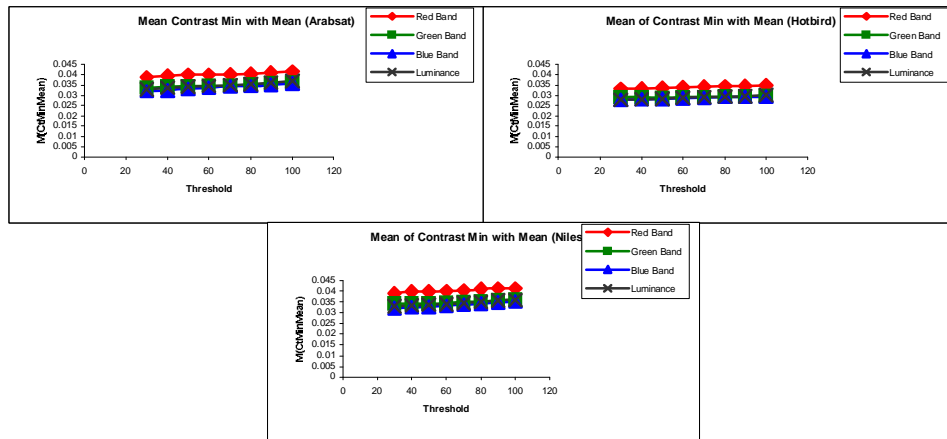Figure (4.39): The relationship between the $Ct_{MaxMean}$ of edges and the threshold values

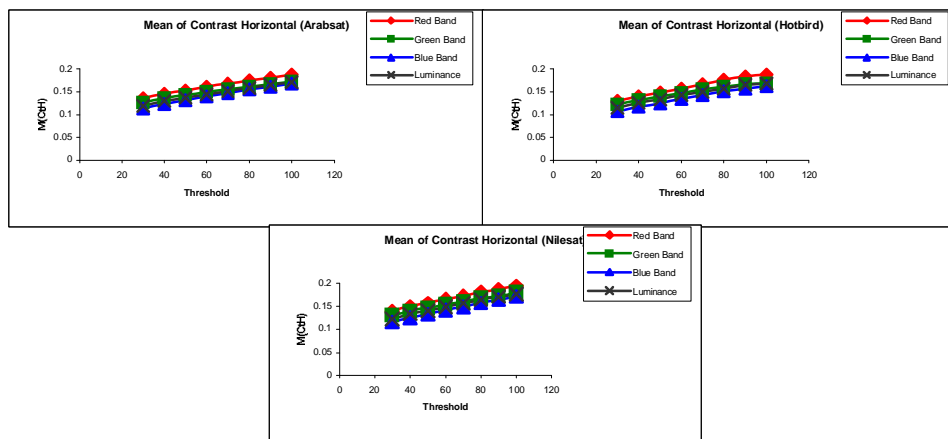Figure (4.40): The relationship between the $Ct_{MinMean}$ of edges and the threshold values

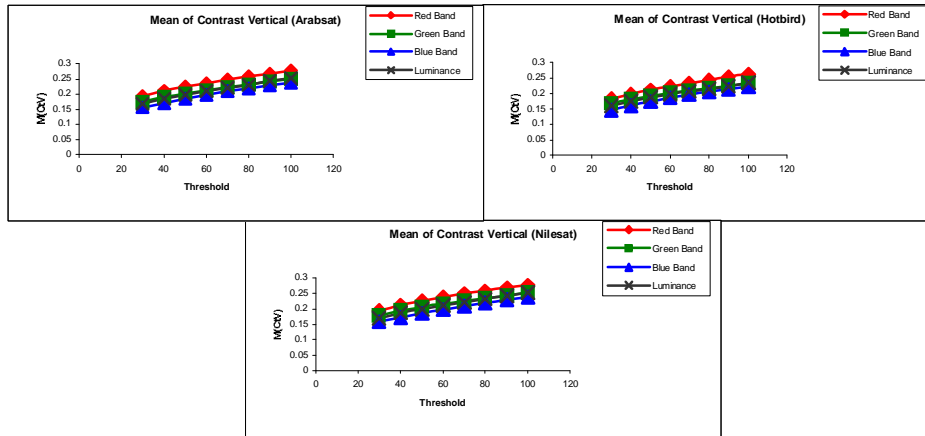Figure (4.41): The relationship between the Ct_H of edges and the threshold values

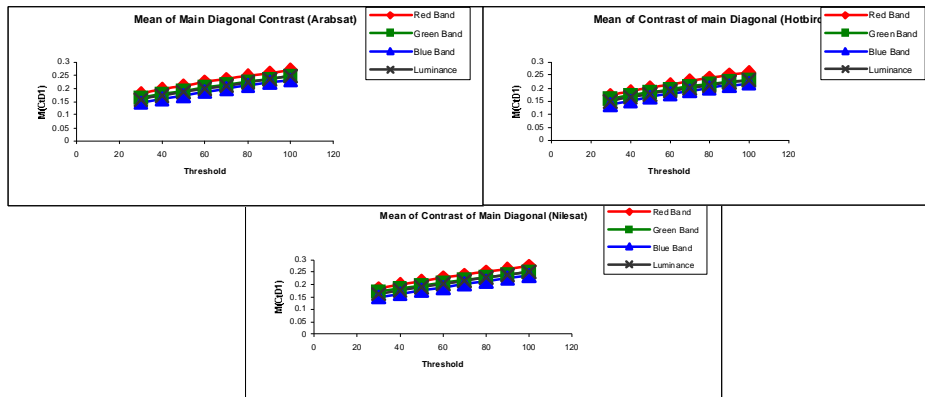Figure (4.42): The relationship between the Ct_V of edges and the threshold values.

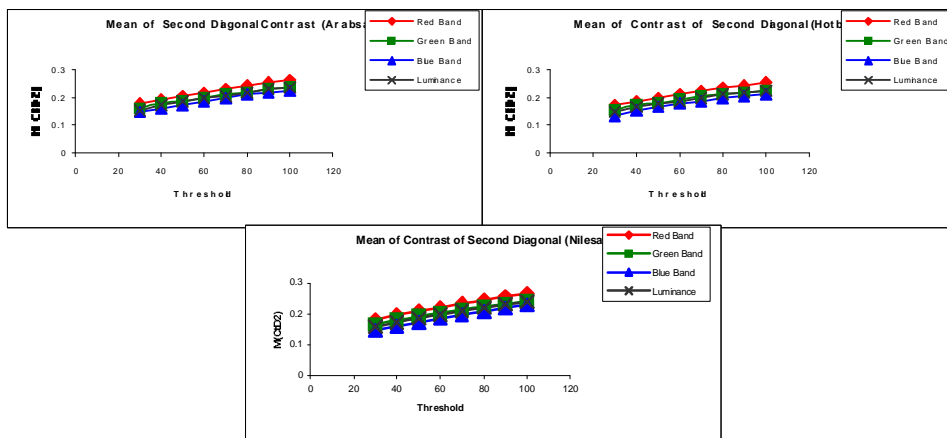Figure (4.43): The relationship between the Ct_{D1} of edges and the threshold values

Figure (4.44): The relationship between the Ct_{D2} and the threshold values

4.5 Correlation Results for TV-Satellite Images

Image correlation is one of the image quality measures that has been used in this study to estimate the image quality. The correlation method has been applied on the images by selecting (manually or automatically) homogeneous blocks from different places of the image, the correlation method is calculated for all RGB-L components for the satellites Arabsat, Hotbird, and Nilesat. Here are brief discussions for the most important obtained results.

4.5.1 The Correlation of the Manual Selected Regions

The manual selection of the regions has been applied on a single image and on the scene of the three satellites, and here are the discussion of the two methods results:

a) The Correlation of the Manual Selected Regions of the Image

In this method correlation has been calculated after selecting manually 40×40 homogeneous blocks of the images; which are shown in figure (4.45). This method is illustrated in section (3.8.1 a). Table (4.6) represents the image correlation results for manual selected homogeneous blocks. Two homogeneous blocks were selected from the image on the three satellites, (R1) which it is a region no.1 that its starting top left point is (140,12) in the black area of the image, and (R2) is a region no.2 that its starting top left point is (128, 81) in the blue area of the image. Both two regions are of size 40×40. The indicated table shows that the two blocks are highly correlated, whereas the correlation values reach to (1) for (R1) of the image in all three satellites (Arabsat, Hotbird and Nilesat) because it is homogeneous black region and there are few differences in intensity. Region (R2) shows correlation values almost equal to (0.99) for

all RGBL components of all satellites, because there are few differences in intensity of the blue block. It couldn't be found any differences among the three satellites, where the mentioned table approved that the three satellites have equal correlation values in this method.
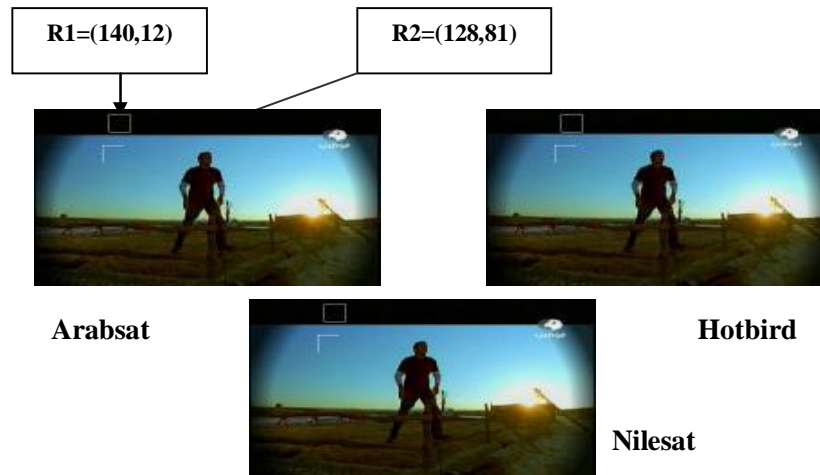
Figure (4.45): The images used to calculate correlation and their selected regions for the satellites (Arabsat, Hotbird and Nilesat)

Table (4.6): shows the image correlation results for the block of Size (40x40) the regions R1 = (140,12) and R2 = (128,81)of the satellites					
Satellite	Operation	Color Bands			
		Red	Green	Blue	Luminance
Arabsat	Cor(R1)	1	1	1	1
	Cor(R2)	0.99	0.99	0.99	0.99
Hotbird	Cor(R1)	1	1	1	1
	Cor(R2)	0.99	0.99	0.99	0.99
Nilesat	Cor(R1)	1	1	1	1
	Cor(R2)	0.99	0.99	0.99	0.99

b) The Correlation of the Manual Selected Regions of the Scene

The scene consisted of six image frames; from each image three different regions on different places in the image plane have been selected. The selected regions of the rest images of the scene should be on

the same locations of the first image (that applied on the three scenes of the three satellites). The correlation method applied on the selected homogenous regions for the RGBL components of each image. Figure (4.46) shows the first frame (F1) and the last frame (F6) from the scene with their extracted blocks and the starting points for each block of three satellites (Arabsat, Hotbird, and Nilesat). Figures [(4.47) to (4.49)] show the curves that presents the relationship between the correlation value for the selected block of each frame and the frame time in millisecond.

1. Figure (4.47) shows the curves of correlation of RGBL components for the beige homogeneous region that it is the region no.1 (R1) that its starting top left point is (511,164). The curves show that the correlation among the selected regions on the six frames for the three satellite are correlated constantly, that there are few differences in correlation from the first millisecond to the last millisecond of the scene on the three satellites, that indicate that there are a few variation of correlation in this region from the first to the last frame of the scene. The correlation of the region on the Hotbird indicated almost few variations during the time changing less than those on Arabsat and Nilesat.

2. The curves of the correlation for the white homogeneous region that its starting point is (180,100) are shown in figure (4.48). The curves of the RGBL components show that the selected region is correlated constantly for all frames with a high correlation value that equal to one of all satellites.

3. Figure (4.49) illustrates the curves of the correlation for the region that its starting point is (492,274). The curves show decreasing of correlation in comparison with the other regions. The B-band has a low correlation in comparison with the other bands. The Hotbird has

the worst correlated values among the considered satellites while the Arabsat shows the best values in this region.

According to the three selected regions, it has been found that the Nilesat and the Arabsat are highly correlated during the time changing of the scene more than Hotbird. Figure (4.46) shows the first and the last frame from each scene and their selected regions for the satellites (Arabsat, Hotbird, and Nilesat).

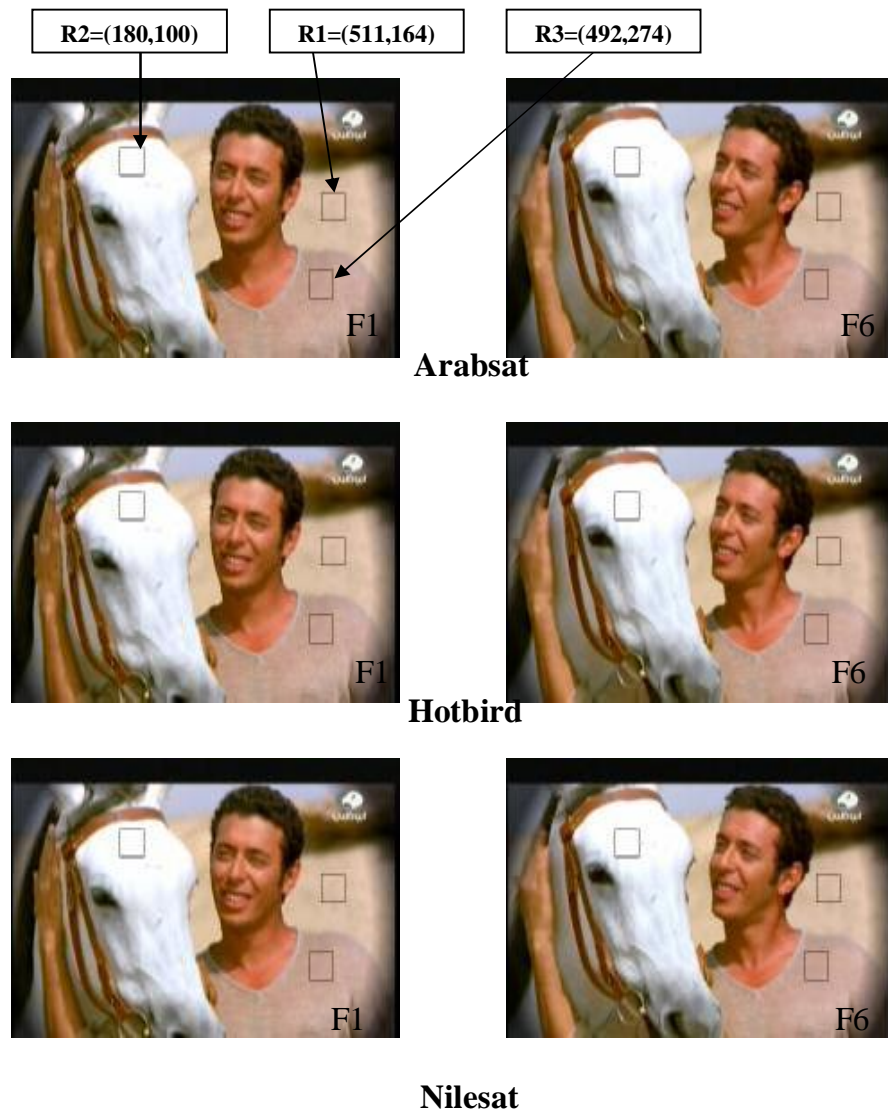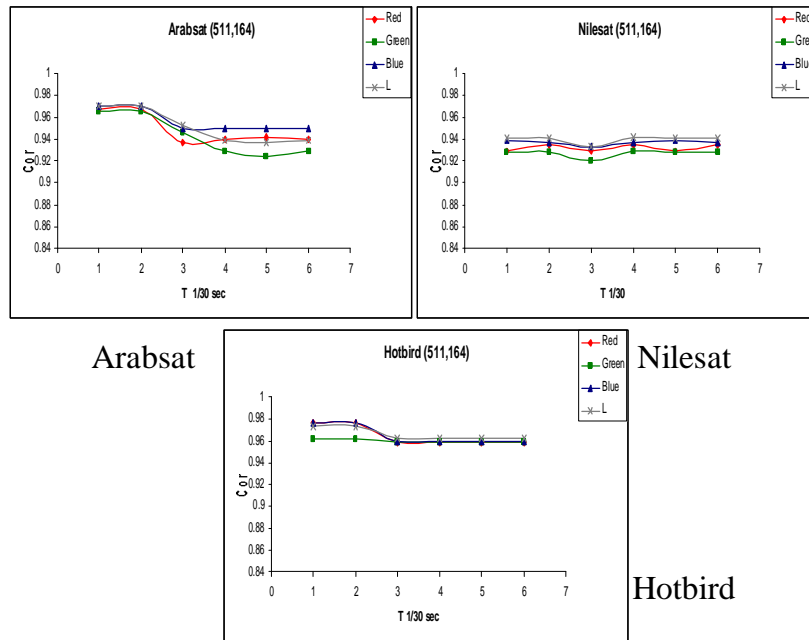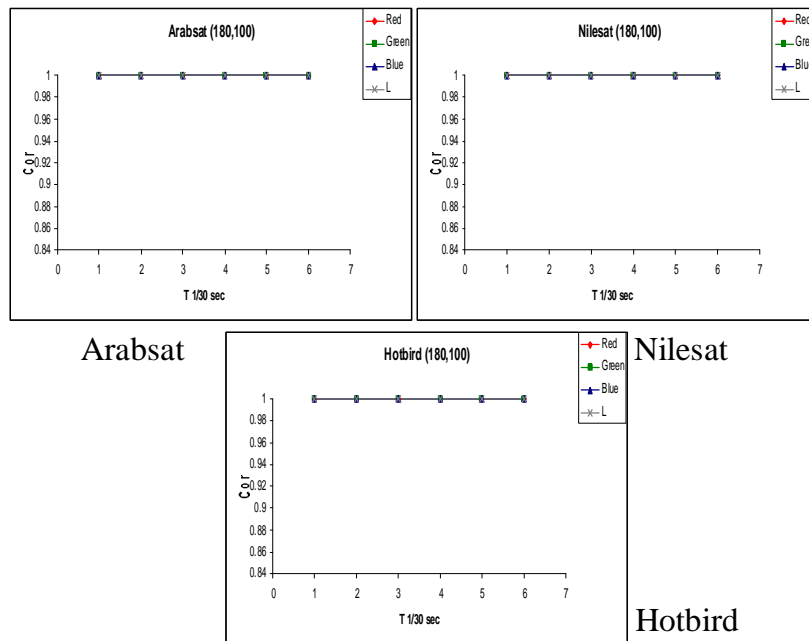**Arabsat**

Hotbird

Nilesat

Figure (4.46): Three scenes each of them contain six frames

Figure(4.47): The curves of the correlation as a function of frame time of the R1 (511,164) for three RGBL components

Figure(4.48): The curves of the correlation as a function of frame time of the R2 (180,100) for three RGBL components
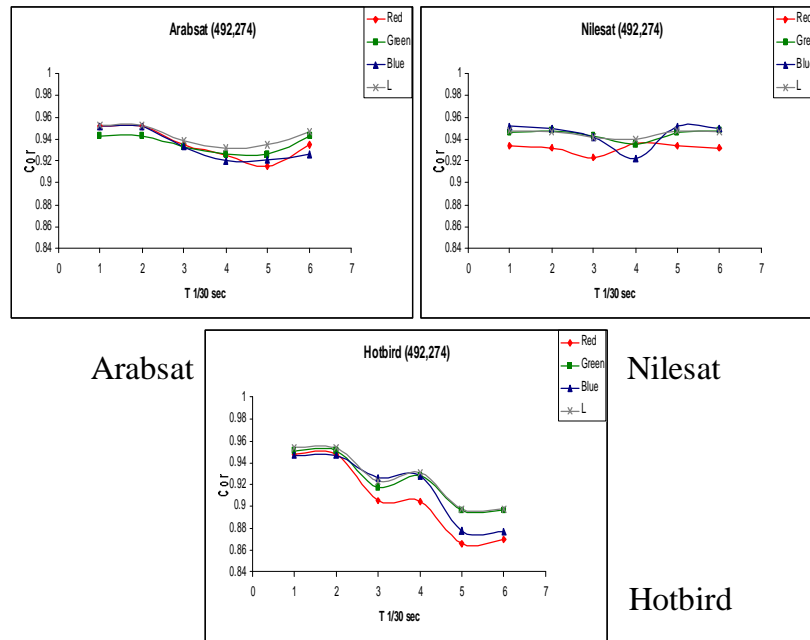
Figure (4.49): The curves of the correlation as a function of frame time of the R3 (492,274) for three RGBL components

4.5.2 The Correlation of the Automatic Selected Regions

In this method the correlation quality measure has been applied on an automatically selected homogeneous region of size 30×30. The selection made according to a procedure based on searching the σ_{Min} value of L in the image. Due to the number of blocks in the image have σ_{Min} values equal to zero, the procedure had chose the last block found has σ_{Min} value equal to zero of the image. After finding the block that has σ_{Min} value, the correlation has been calculated for all RGB-L component between the found block and the block next to it shifted to the right direction by one pixel. This method is illustrated in section (3.8.2 a). Figure (4.50) presents the images used in this method and their selected regions for three satellites (Arabsat, Hotbird, and Nilesat).

After the implementation method of this method, it has been found two different regions that have σ_{Min} for the three images of the three

satellites. The two regions are R1 which its starting top left point is (493,188) for images on Arabsat and Nilesat, and R2 which its starting point is (489,188) for the image on Hotbird. The two found σ_{Min} regions gave an indication for the different appearance of the images on the three satellites. Table (4.7) reveals that region R1 of the image on Nilesat has the higher correlation then Hotbird comes second, more than the region R2 of the images on Hotbird. In the second stage of this study, it has been selected the same location of region R1 from the image on Hotbird to compare the results with the results of the images on Arabsat and Nilesat for the same region. It has been found that the correlation values for the images on Nilesat are the highest then Arabsat comes second and the Hotbird comes last. Therefore, the Arabsat and Nilesat were the best for this region (R1) as shown in Table (4.8).

In the same way that has been discussed in the previous paragraph, the region R2 has been selected from both images on Arabsat and Nilesat. As shown in Table (4.9) the results indicate that the Nilesat and the Arabsat have the highest correlation values for all RGB-L components more than Hotbird.
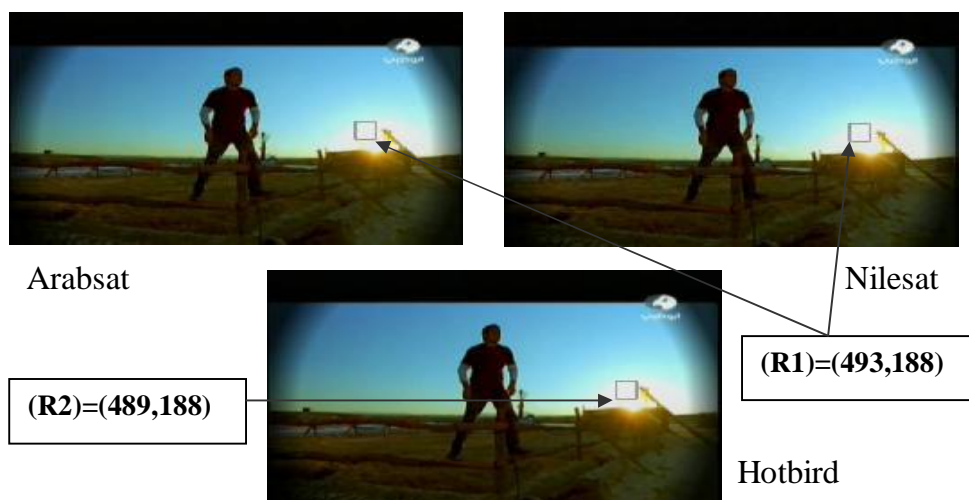

Figure (4.50): The images for three satellites used in the automatic selected block for the correlation and the block locations on each image for the Luminance.

Table (4.7): The correlation of the automatic selected region results of the (30x30) block Size for the regions R1 = (493,188) and R2 = (489,188) for all satellites.

Satellite	Operation	Color Bands			
		Red	Green	Blue	Luminance
Arabsat	μ	227	234	232	232
	σ	6.76	3.11	2.88	1.16
	Cor(R1)	0.98	0.96	1	1
Hotbird	μ	228	233	231	232
	σ	4.99	2.81	2.9	1.11
	Cor(R2)	0.98	0.97	1	1
Nilesat	μ	226	233	231	232
	σ	7.28	3.25	3.31	1.12
	Cor(R1)	0.99	0.96	1	1

Table (4.8): The correlation of the automatic selected region results of the (30x30) block Size For R1 = (493,188) of the three satellites.

Satellite	Operation	Color Bands			
		Red	Green	Blue	Luminance
Arabsat	μ	227	234	232	232
	σ	6.76	3.11	2.88	1.16
	Cor(R1)	0.98	0.96	1	1
Hotbird	μ	229	233	231	232
	σ	3.87	2.54	2.88	1.22
	Cor(R1)	0.94	0.95	1	1
Nilesat	μ	226	233	231	232
	σ	7.28	3.25	3.31	1.12
	Cor(R1)	0.99	0.96	1	1

Table (4.9): The correlation of the automatic selected region results of the (30x30) block Size For R2 = (489,188) of the three satellites.

Satellite	Operation	Color Bands			
		Red	Green	Blue	Luminance
Arabsat	μ	226	234	232	231
	σ	8.04	3.26	2.77	1.24
	Cor(R2)	0.99	0.97	1	1
Hotbird	μ	228	233	231	232
	σ	4.99	2.81	2.9	1.11
	Cor(R2)	0.98	0.97	1	1
Nilesat	μ	225	234	232	231
	σ	8.62	3.33	2.98	1.29
	Cor(R2)	0.99	0.97	1	1

4.5.3 The Maximum and Minimum Correlation

Maximum and minimum correlation is a newly suggested method for determining the correlation of the digital image; it is based on finding the block of size (40×40) that has the maximum correlation of L and the block that has the minimum correlation of L, whereas in the image there are more than one block has the same maximum and minimum correlation values, so that the correlation of the last block found has maximum correlation (or minimum correlation for the other image) for RGB-L components will be determined, this method is illustrated in section (3.8.2 b). Figures (4.52) and (4.53) show the images used in maximum and minimum correlation for three satellites (Arabsat, Hotbird, and Nilesat).

After the implementation method of the automatic search of the maximum correlation, it has been found a region (R1) that has maximum correlation values of L for the images on the three satellites. The starting top left point of the found region is (599, 341). The obtained results illustrated in table (4.10) for the correlation of RGB-L components indicate that the Arabsat has the high correlation values, Nilesat comes in the second place while Hotbird comes last.

While after the implementation method of the automatic search of the minimum correlation, it has been found two regions that have minimum correlation for the three images of the three satellites. The two regions are R1 which its starting point is (321,340) for images on Arabsat and Nilesat, and R2 which its starting point is (281,180) for the image on Hotbird. The two found minimum correlation regions gave an indication for the different appearance of the images on the three satellites. Table (4.11) reveals that region R2 of the image on Hotbird has the higher correlation, more than the region R1 of the images on Arabsat and Nilesat. In the second stage of this method, it has been selected the same

124

location of region R1 from the image on Hotbird to compare the results with the results of the images on Arabsat and Nilesat for the same region. It has been found that the correlation for the images on Arabsat and Nilesat is the lowest. Therefore, the Hotbird was the best for this region as shown in Table (4.12). In the same way that has been discussed earlier, the region R2 has been selected from both images on Arabsat and Nilesat. As shown in Table (4.13) the results didn't show big difference among the three images on the three satellites.

Arabsat   **Hotbird**

Nilesat   **R1=(599,341)**

Figure (4.51): The images used in the automatic selected block for the max correlation and the block locations on each image

Table (4.10): The maximum correlation results of (40x40) block size for region R1=(599, 341) for the three satellites.					
Satellite	Operation	Color Bands			
		Red	Green	Blue	Luminance
Arabsat	μ	12	16	5	14
	σ	6.02	6.49	5.09	6.21
	Cor(R1)	0.97	0.97	0.97	0.97
Hotbird	μ	11	14	3	12
	σ	5.74	6.33	3.98	5.83
	Cor(R1)	0.95	0.96	0.93	0.96
Nilesat	μ	13	17	5	14
	σ	6.08	6.55	5.58	6.30
	Cor(R1)	0.96	0.96	0.96	0.96

Arabsat

Nilesat
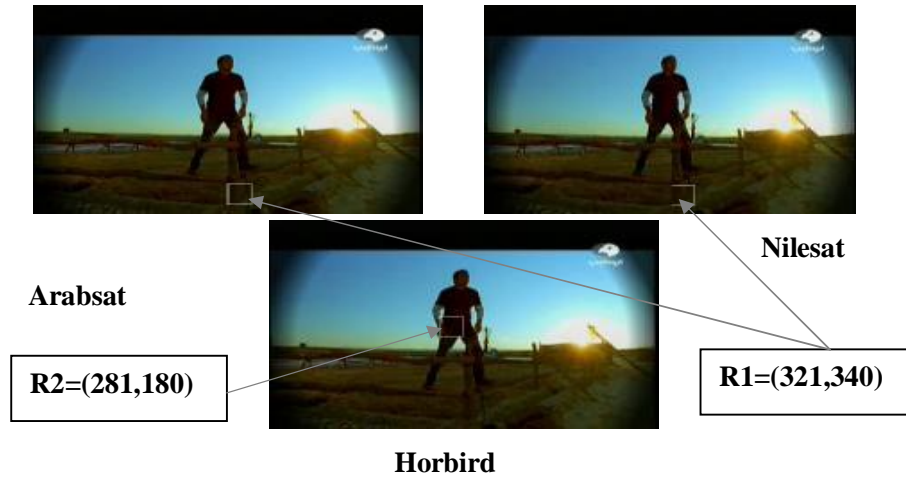
R2=(281,180)

R1=(321,340)

Horbird

Figure (4.52): The images used in the automatic selected block for the Min. correlation and the block locations on each image

Table (4.11): The maximum correlation results of (40x40) block size for regions R1=(321, 340) and R2=(281, 180) for the three satellites.					
Satellite	Operation	Color Bands			
		Red	Green	Blue	Luminance
Arabsat	μ	31	22	1	22
	σ	6.77	9.04	4.27	7.45
	Cor(R1)	0.79	0.88	0.82	0.85
Hotbird	μ	25	9	5	13
	σ	21.29	26.09	24.87	23.93
	Cor(R2)	0.84	0.89	0.88	0.87
Nilesat	μ	32	23	1	23
	σ	6.88	9.51	3.97	7.65
	Cor(R1)	0.77	0.87	0.86	0.85

Table (4.12): The maximum correlation results of (40x40) block size for region R1=(321, 340) for the three satellites.					
Satellite	Operation	Color Bands			
		Red	Green	Blue	Luminance
Arabsat	μ	31	22	1	22
	σ	6.77	9.04	4.27	7.45
	Cor(R1)	0.79	0.88	0.82	0.85
Hotbird	μ	31	23	1	23
	σ	6.72	9.10	4.25	7.48
	Cor(R1)	0.82	0.9	0.86	0.88
Nilesat	μ	32	23	1	23
	σ	6.88	9.51	3.97	7.65
	Cor(R1)	0.77	0.87	0.86	0.85

Table (4.13): The maximum correlation results of (40x40) block size for region R2=(281, 180) for the three satellites					
Block Size = 30 For all Regions **R2 = (281,180)**					
Satellite	**Operation**	**Color Bands**			
		Red	**Green**	**Blue**	**Luminance**
Arabsat	μ	28	12	8	16
	σ	25.33	34.17	33.30	30.87
	Cor(R2)	0.83	0.89	0.89	0.88
Hotbird	μ	25	9	5	13
	σ	21.29	26.09	24.87	23.93
	Cor(R2)	0.84	0.89	0.88	0.87
Nilesat	μ	27	12	8	16
	σ	26.03	33.87	33.14	30.85
	Cor(R2)	0.83	0.89	0.89	0.87

Chapter Five
Conclusions and Future Work

Chapter Five
Conclusions and Future Works

5.1 Conclusions

The results of the present study have revealed the following articles:

1. Threshold value (30) of the edge detector has proved to be more effective threshold than the other values. That gives the highest amount of image edges, contrast, and SNR values of the images on the three satellites.

2. The amount of edges has proved that the Nilesat has the highest amount of edges among the Hotbird and the Arabsat.

3. SNR, mean and σ of contrast of image edges also show that the Nilesat has the best results compared to Hotbird and Arabsat.

4. All the contrast methods of edges show the Nilesat has the higher contrast among the Hotbird and Arabsat.

5. The results of image correlation of the two manual selected homogeneous regions have proved that the correlation values are equal for all RGBL components of all satellites.

6. The manual image correlation for the scene shows that is highly correlated among the images of the scene on the Nilesat and Arabsat during time changing more than the Hotbird.

7. Using automatic searched correlation based on σ_{Min} of L shows that Nilesat has the best correlation results compared to the Arabsat and Hotbird.

8. Maximum and minimum correlation have proved that Arabsat has the highest maximum correlation values, while in the minimum correlation method, it has been concluded that the Nilesat has the best

results, because it has the least correlation values in non-homogeneous region.

9. Finally, from the above mentioned articles, it has been concluded that the TV-Satellite images on the Nilesat is better than those on Arabsat and Hotbird in all image quality measures that were used in this study.

5.2 Suggestion for the Future Work

The work performed during the period of this study could be improved in many directions. Among the important directions are:

1. Use the suggested approaches of calculating contrast as features of recognition methods.

2. Use other contrast methods to determine the quality of the images and comparing the results with the results of this research.

3. The automatic search correlation used to estimate the quality of the image can be improved by using it on all RGB-L color components.

4. The correlation can be calculated between the block and the block next to it to the left or down of the block by more than one pixel, then determine the relationship between the computed correlation values of the two blocks and the distance between them for all RGB-L components.

5. Use different edge detection filters to extract the edges of the TV images, and then determine the contrast of the image edges using each filter. The obtained results used to determine the best filter gives the best contrast of image edges values.

6. Study the resistance effects of the wire that transfer signal on the quality of the images that captured from the satellites channels.

References

References

- [Ach05] Acharya T. and Ray A. K., "Image Processing Principles and Applications", John Wiley & sons, Inc., 2005.

- [Ald01] Alder M., "An Introduction to Pattern Recognition", Mike Alder, 2001.

- [Ald08] Al-Dalawy A. J., "A Study of TV Images Quality for Channels Broadcast Television Satellite", Master of Science in Physics, Physics Department, Al-Mustansiriya University, 2008.

- [Alda08] Al-Dalawy N. M., "TV Image Quality Study of Broadcasting Television Terrestrial Channels", M.Sc. Thesis, Physics Department, Al Mustansiriya University, 2008.

- [Alj06] Al Jiboori A. H., "A Study of the Noise That Associated with TV images and the Reduction Methods of Its Effects", Ph.D. Thesis, Physics Department, Al Mustansiriya University, 2006.

- [Alt02] Al-Taay H. J., "Edge Detection in IR Image by Using Digital Filters', M.Sc. Thesis, Physics Department, Al-Mustansiriyah University, 2002.

- [Alt06] Al Taweel R. Sh., "Study of TV-Satellite Images and Analysis of their Associated Noise in Digital Receiver System", Ph.D. Thesis, Physics Department, Al Mustansiriya University, 2006.

- [Ava01] Avacibas I., "Image Quality Statistics and their Use in Steganalysis and compression", Ph.D. Thesis, Bogazici University, Turkey, 2001.

- [Bay97] Baylin F., "Digital Satellite TV", Balylin Publications, 1997.

- [Bex01] Bex P. J. and Walter Makous, "Spatial Frequency, Phase, and the Contrast Natural Images", Optical Society of America, A/Vol. 19, No. 6, 2002.

- [Bri05] Bringier B., N. Richard, M.-C. Larabi and C. Fernandez-Maliogue, "No-Reference Perceptual Quality Assessment of Colour Image", SIC Laboratory, University of Poitiers, France, 2005

- [Cat01] Catanzarite B., "Structure wiring", NASA Lewis Research Center, 2001.

- [Cra97] Crane R., "A Simplified Approach to Image Processing: Classified and Modern Techniques in C", Hewlett-Packard Company, Prentice Hall PTR, 1997.

- [Del98] Delaigle J.F., C. Devleeschouwer, B. Macq, and I. Langendijk, "Human Visual System Features Enabling Watermarking", Laboratoire de Telecommunications et Teledetection, Universite catholique Louvain, Belgium, 1998.

- [Dou02] Doug D., Anthoney S., "Stylization and Abstraction of Photographs", M.Sc. Thesis, Department of Computer Science and Center for Cognitive Science, Siggraph, 2002.

- [Dun07] Dunbar B., "World Book at NASA", World Book Online Reference Center, 2007.

- [Fly98] Flynn R. J., W. H. Tetzlaff, "Multimedia", International Business Machines Corporation, Vol. 42, No. 2, 1998.

- [For03] Forsythe D., and J. Ponce, "Computer Vision: A Modern Approach, Prentice-Hall, 2003.

- [Gon02] Gonzalez, R. C., "Digital Image Processing", 2, Prentice-Hall, Inc., 2002.

- [Gon87] Gonzalez, R. C., "Digital Image processing", 2, Wesley Publishing Company Addison, 1987.

- [Gup04] Gupta S., Dan P., "Bone Geometry and Medical Properties of the Human Scapula Using Computed Tomography Data", Department of Applied Mechanics, Bengal Engineering College, India, Vol. 17(2) PP 61-70, 2004.

- [Jah05] Jahne B., "Digital Image Processing", Springer-Verlag Berlin Heidelberg, 2005.

- [Kon02] Konak, E.S., "A Content-Based Image Retrieval System for Texture and Color Queries", M.Sc. Thesis, Institute of Engineering and Science, Bilkent Univertsity, Turkey, August, 2002.

- [Kro01] Kropatsch W. G. and Horst Bischof, "Digital Image Analysis Selected Techniques and Applications", Springer-Verlay NY, Inc., 2001.

- [Leo07] Leonard R., "Satellite Communications", NASA Lewis Research Center, 2007.

- [Loo04] Loo S. P., "System Design of All Integrated Terrestrial-Satellite Communications network for Disaster Recovery", Department of Electrical Engineering, Virginia Polytechnic Institute and State University, 2004.

- [Luk07] Lukac R., Konstantions N. Plataniotis, "Color Image Processing Methods and Application", Taylor & Francis Group, LLC, CRC Press, 2007.

- [Mag77] Magnant R. S., "Domestic Satellite DOMSAT", Westview Press Inc., Library of Congress Cataloging, U.S.,

1977.

- [Mat05] Matkovic K., L. Neumann, A. Neumann, T. Psik, and W. Purgathofer, "Global Contrast Factor –a New Approach to Image Contrast", Computational Aesthelics in Graphics, Visualization and Imaging, Vienna, Austria, 2005.

- [Nix02] Nixon M. S., Aguado A. S., "Feature Extraction and Image Processing", Newnes, 2002.

- [Pan02] Pan T., "Fine Aggregate Characterization Using Digital Image Analysis", The Department of Civil and Environment Engineering, Louisiana University, 2002.

- [Pel90] Peli E., "Contrast in Complex Images", Optical Society of America, A/Vol. 7, No. 10, 1990.

- [Pel96] Peli E., Lawrence Arend, and Angela T. Labiance, "Contrast Perception Across Changes in Luminance and Spatial Frequency", Optical Society of America, Vol. 13, No. 10, October 1996.

- [Pra01] Pratt W. K., "Digital Image Processing", PIKS Inside, Third Edition, John Wiley & Sons, Inc., 2001.

- [Rac02] Rachenmacher A. L. and Saab N. A., "Digital Image Correlation (DIC) to Evaluate Progression and Uniformity of Shear Bands in Dilative Sands", 5th ASCE Engineering Mechanics Conference, Columbia University, New York NY, 2002.

- [Rob77] Robinson G., "Color Edge Detection", Optical Engineering, 16(5):479–484, September 1977.

- [Rus07] Russ J. C., "The Image Processing Handbook Fifth Edition", Tylor & Francis Group, LLC, 2007.

- [Sac96] Sachs J., "Digital Image Basics", Technical Report,

Digital light and color, Cambridge Press, PP. 1-14, 1996.
www.dl-c.com/basics.pdf

- [See02] Seemann T., "Digital Image Processing Using Local Segmenattion", Ph.D. Thesis in School of Computer Science and Software Engineering, Faculty of Information Technology, Monash University, Australia, April, 2002.

- [Ser08] Sergey B., pavel B., Dmitry I., "Brightness Calculation in Digital Image Processing", KWE Int. Inc., San Francisco, CA, USA, 2008.

- [Sha03] Sharma G., "Digital Color Image HandBook", CRC Press, LLC, 2003.

- [Sri05] Srinivasan V., S. Radhakrishnan1, X. Zhang1, G. Subbarayan1, T. Baughn2, L., "High Resolution Characterization of Materials Used in Packages Through Digital Image Correlation", Nguyen Purdue University, Raytheon Systems Corporation, National Semiconductor Corporation, Santa Clara, CA 95052, 2005.

- [Top06] Topchev V. I. and Lidia T. Jordanova, "Analysis of Sensors for Limiting the Dynamic Range of the Signals in CATV Systems", Communications and Communications Technologies, Technical University, Kliment Ohridiski, Sofia Bulgaria, 2006.

- [Tou88] Touzi R., Armand L., and P. Bousquet, "A statistical and Geometrical Edge Detector for SAR Images", IEEE Transactions on Geoscience and Remote Sensing, Vol. 26, No. 6, Nov. 1988.

- [Umb98] Umbaugh S. E., "Computer Vision and Image Processing: a practice approach using CVIPtools", Prentice Hall PTR, A Simon & Schuster Company 1998.

- [Wad95] Wade P., "More on Parabolic Dish Antenna", Published by American Radio Relay League Inc., 1995.

- [Wah00] Wahiba A. A., Salim Idrees, "Tv Satellites Technology Troubleshooting and Scrambling, first Edition 2000.

- [Web02] Webb A. R., "Statistical Pattern Recognition", Second Edition, John Wiley & Sons, LTD, 2002.

- [Wes99] Wesolkowski S. B., "Color Image Edge Detection and Segmentation: A Comparison of the Vector Angle and the Euclidean Distance Color Similarity Measures", Master Degree of Science, Department of System Design and Engineering, Ontario, Canada, 1999.

- [You98] Young I. J., Jacob G. J., and Van Vliet L. J., "Fundamental of Image Processing", Printed in Netherlands, Delft University of Technology, 1998.

الخلاصة

ان تقنيات تحليل الصور التلفزيونية الفضائية تـأتي من الاهميـة الكبيـرة للمعلومـات المنقولـة خلال وسائل الاعلام في العالم. في هذا البحث تم دراسة جودة الصور التلفزيونية الفضائية على الاقمار الثلاث (العرب سات, الهوت بيرد و النايل سات) لتثمين افضل جودة صـورة علـى اي قمر. تم استخدام مجموعة من معايير قياس جودة الصورة وتطبيقها علـى الصـور التلفزيونيـة الفضائية. المعيار الاول المستخدم في هذه الدراسة هو طريقة التباين لحافات الصورة والمعيـار الثاني هو طريقة الترابط المتقاطع لمناطق متجانسة من الصورة. في الطريقة الاولى تم استخراج حافات الصورة من خـلال استخدام مؤثر سوبل للكشف الحافي لكل الحزم اللونية (الحمراء, الخضراء, الزرقاء) بالاضافة الى مركبة الاضاءة لقيم عتبات مختلفة. بالاضافة الى الطريقتين المـذكورتين لحساب جودة الصورة, تم حساب مقدار حافات الصـورة ونسـبة الاشـارة الـى الـضوضاء والمعـدل والانحـراف المعيـاري لحافـات الصـورة لكـل الحـزم اللونيـة (الحمـراء, الخضراء, الزرقاء) بالاضافة الى مركبة الاضاءة. ان نسبة التباين لحافات الصور تم حسابها لعتبات مختلفة بأستخدام معادلة مايكلسون التي حورت الى مجموعة طرق لتقديم اساليب جديدة لحساب مقدار التباين لحافات الصورة للجزم(الحمراء, الخضراء, الزرقاء) ومركبة الاضاءة. اما في طريقة الترابط المتقاطع, تم حساب الترابط للمناطق المتجانسة المستقطعة من الصورة لكل الحزم اللونية (الحمراء, الخضراء, الزرقاء) بالاضافة الى مركبة الاضاءة. حيث تم الاستقطاع للمناطق يدويا و اوتوماتيكيا من الصورة. لقد اشارت النتائج لكل الطرق المعتمدة لحساب الجودة الى ان الصور على النايل سات قد اعطت افضل جودة من بين الصور على العرب سات والهوت بيرد. حيث ان الصور على العرب سات قد احتلت المرتبة الثانية من حيث الجودة تليها الصور على الهوت بيرد في المرتبة الاخيرة.

جمهورية العراق
وزارة التعليم العالي و البحث العلمي
جامعة النهرين
كلية العلوم

تحليل الصور التلفزيونية الفضائية
وتخمين جودتها

رسالة مقدمة الى كلية العلوم, جامعة النهرين كجزء من متطلبات نيل شهادة
الماجستير في علوم الحاسوب

من قبل
اسراء حسين علي
(بكالوريوس جامعة النهرين 2005)

اشراف
د.علي عبد داود الزكي

جمادي الاول 1430   آيار 2009